ECHOGENIC LIPOSOMES FOR ULTRASOUND-TRIGGERED DRUG DELIVERY.

A thesis submitted in fulfillment of the requirements of the degree of

Master of science (chemistry)

At

By

Ezekiel Charles Izuchukwu

Supervised by Prof Rui Werner Maçedo Krause

January 2021

DEDICATION

To almighty God, my wife, and children.

ACKNOWLEDGEMENTS

My sincere appreciation goes to my supervisor Prof Rui Werner Maçedo Krause, first for accepting me as his student and his outstanding contributions and close supervision that made this research work possible.

I wish to immensely thank my wife, Mrs. Lebechi Izuchukwu, for all her sacrifices, prayers, and encouragement and for taking care of the children throughout the period I was away for this program. To my lovely children Chinecherem, Chinemerem, and Chidubem, for enduring my absence and fatherly love. You guys are amazing.

I sincerely appreciate Prof. R.B. Walker of the pharmacy department for introducing and giving me access to use the instruments in his laboratory. My gratitude also to Dr, Xavier Siwe Noundou for all his guidance during the duration of this research and for taking his time to read through the thesis with helpful corrections.

I also want to thank my colleagues in the F22 research group of the Chemistry Department, especially Mr. Alain Bapolisi, for his assistance in putting me through most of the processes during the research, Mrs. Bertha Chithambo, Baa Ebenezer, Lydia Kisula, and others for their advice and experimental assistance.

Lastly, I also wish to acknowledge the immense contributions of my mother, Mrs. Grace Ezekiel, and the entire family members of late Mr. Ezekiel Okereke for all their moral and spiritual supports during the program's duration.

ABSTRACT

Colorectal cancer is one of common cancers worldwide. It is the third most diagnosed cancer and the second leading cause of death. The use of 5-fluorouracil (5-FU) alone or in a chemotherapy regime has been the effective treatment of colorectal cancer patients. The efficacy of 5-FU in colorectal cancer treatment is significantly limited by drug resistance, gastrointestinal, and bone marrow toxicity through high-level expression of thymidylate synthase, justifying a need to improve its therapeutic index. Liposomes are colloidal membranes comprising of one or more lipid bilayers enclosing an aqueous core. They have been used to improve the therapeutic index of many anti-cancer drugs by changing drug absorption, elongating biological half-life, reducing metabolism, and reducing toxicity to healthy tissues. Echogenic liposomes are specifically designed to respond to external triggering like ultrasound stimulation by entrapping a gas or an emulsion that can vaporize. A liposome's unique property is that it can entrap both hydrophobic and hydrophilic substances simultaneously in the lipid bilayer and the aqueous core, respectively. These stimuli-responsive liposomes can be triggered externally with ultrasound, to release the chemotherapeutic cargo only at the required site. This research aims to formulate echogenic liposomes encapsulating 5-FU for potential ultrasound triggered release (echogenic). Liposome formulations were prepared with lipid composition of crude soybean lecithin and cholesterol by thin-film hydration method and the drug was passively loaded in the formulation. The 5-FU loaded liposomes were evaluated by dynamic light scattering (DLS) for particle size, polydispersity index, and zeta potential and transmission electron microscopy (TEM) for morphology. Encapsulated liposomal formulations were also evaluated using physicochemical techniques including thermogravimetric analysis (TGA), differential scanning calorimetry (DSC), Fourier-transform infrared spectroscopy (FTIR), and X-ray diffraction (XRD). The encapsulation efficiency and release kinetics were studied using a validated high-performance liquid chromatography (HPLC) method. Echogenic properties were explored by entrapping a biocompatible gas (argon) at the same time as the drug (5-FU) using a pressure/freeze methodology. The liposomal formulations were typically spherical with a size of about 150 nm and encapsulation efficiency of 62%. Low-frequency ultrasound (20 kHz) was used to trigger the drug release from the complete formulation at 10%, 15%, and 20% amplitude and exposure time of 5 min and 10 min. The rate of drug release from the nano-carrier was a function of the ultrasound amplitude and exposure time and reached a maximum of 65% release under the conditions investigated. The cumulative release was investigated, with and without the application of ultrasound. It was demonstrated that the application of ultrasound resulted in

complete release (99%) after 12 h while this dropped to 70% without ultrasound. These results are encouraging for optimizing ultrasound parameters for triggered and controlled release of the 5-FU, for conditions such as the management of cancer where low-power ultrasound can be applied.

GRAPHICAL ABSTRACT

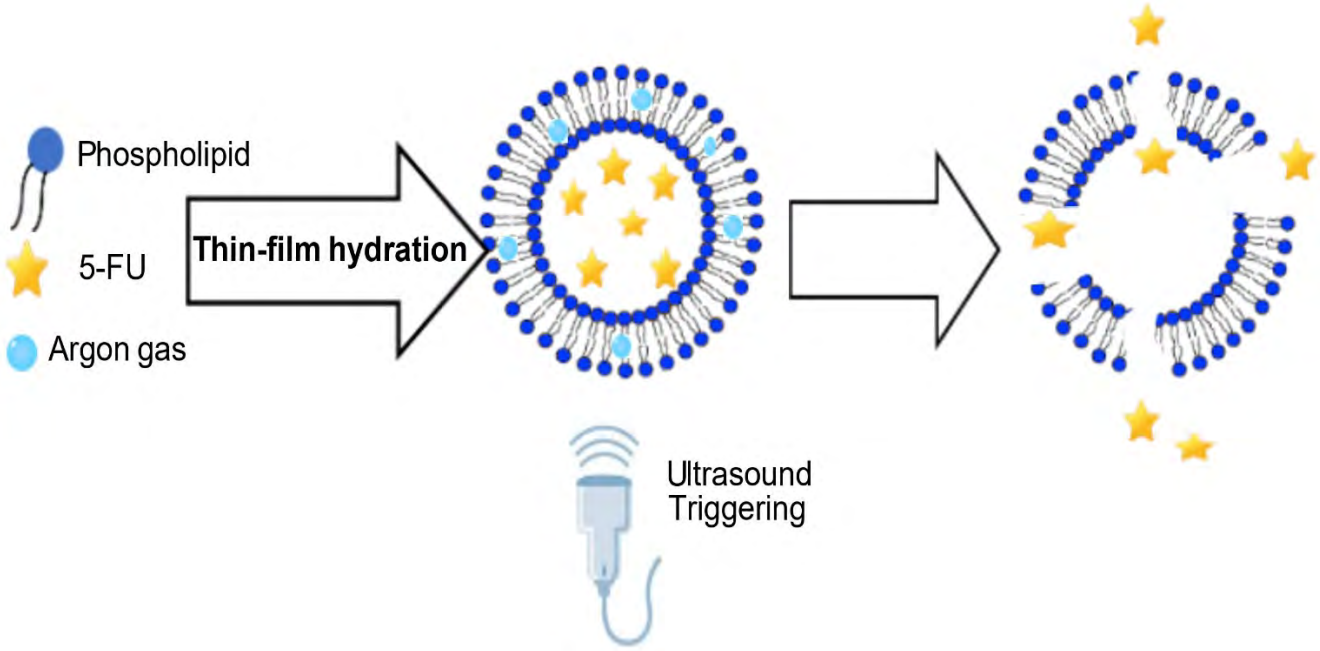

Ultrasound-Triggered release of 5-FU from Soy Lecithin Echogenic Liposome

TABLE OF CONTENTS

Contents

LIST OF FIGURES

LIST OF TABLES

CHAPTER ONE

GENERAL INTRODUCTION

1. **CANCER**

1.1. Definition and History

Cancer starts developing when cells in any part of the body begin to grow out of control. All types of cancer begin due to uncontrolled growth and spread of abnormal cells. Our oldest knowledge of cancer (although the word cancer was not used) came from Egypt and it can be traced to about 3000 BC (Hajdu 2011). The origin of the word 'cancer' was credited to the Greek physician Hippocrates (460-370 BC), known as "the father of medicine." He used the phrase *carcinos* and *carcinoma* to describe non-ulcer forming and ulcer forming tumors (Winer *et al.* 2009).

In Greek, the words referred to a crab and applied to the disease because of the finger-like spreading projections from cancer that resemble a crab's shape. Celsus (28-50 BC) a Roman physician translated the Greek term into cancer, the Latin word for crab (Hajdu 2011). There are many theories about the causes of cancer. Hippocrates postulated one of the earliest in what he called "humoral theory", where he believed that if the four humors in the body (blood, phlegm, yellow bile, and black bile) are not balanced, it causes disease. Later, Stahl and Hoffman theorized that cancer was composed of fermenting and degenerating lymph, changing density, acidity, and alkalinity. In 1838, German pathologist Johannes Muller showed that cancer comprises of cells and not lymphs. He also believed that cancer cells did not come from normal cells rather than budding elements (blastema) between normal tissues (Hajdu 2012).

Cancer was also believed to be contagious all through the 17th and 18th centuries; thus, the first cancer hospital in France was forced to relocate from the city in 1779 because people were afraid it would spread to the town. We now know that this is not the case, although some viruses, bacteria, and parasites can increase a person's risk of developing cancer (Hajdu 2012). For many decades there was little progress in cancer treatment since ancient physicians believed that cancer could not be cured. Although some people still consider cancer incurable, and therefore leave treatment until it is too late, we now have many options. Cancer treatment has gone through a long development process, including surgery, hormone therapy, radiation, chemotherapy, immunotherapy, targeted and triggered therapy (Sudhakar 2009). Since there are many types of cancer, some treatments are more useful than others, depending on the part of the body where the cancer is located (Sudhakar 2009).

1.2. Epidemiology

Cancer is a major public heath challenge and leading cause of dead globally. One in 5 men and one in 6 women worldwide are currently likely to develop cancer during their lifetime; one in 8 men and in 11 women currently die from the disease (Akaza 2019). Several factors lead to this increase in global cancer burden: including a growth in- and an aging population. However, lifestyles continue to change and especially in rapidly growing economies there has been a shift from poverty and infection-related diseases to cancers linked to industrialization and lifestyle. For example, almost half of the new cases and death from cancer in 2018 occurred in Asia because the region has about 60% of the world population. Europe, however, accounts for 23.4% of the global cancer cases and 20.3% of the cancer deaths, while it has only 9.0% of the world population. Similarly, America accounts for 13.3% of the world population, 21.0% of the cancer incidence, and 14.4% globally (**Figure 1.1**). The rate of cancer deaths in Asia and Africa (57.3% and 7.3%, respectively) are higher than the proportion of incident cases (48.4% and 5.8%, respectively); the reason being that Asia and Africa have a higher rate of specific cancer types linked with poorer prognosis and higher mortality rates coupled with limited access to early diagnosis and treatment in many countries (Bray *et al.* 2018)

Lung cancer, breast cancer, and colorectal cancer are the top three in incidence and are responsible for one-third of the cancer incidence and mortality burden globally. Lung and breast cancers are also among the leading types of cancer globally in terms of new cases (Akaza 2019). From these alarming statistics, the burden of cancer globally is far from over, and more needs to be done regarding prevention and early detection, as well as treatment.

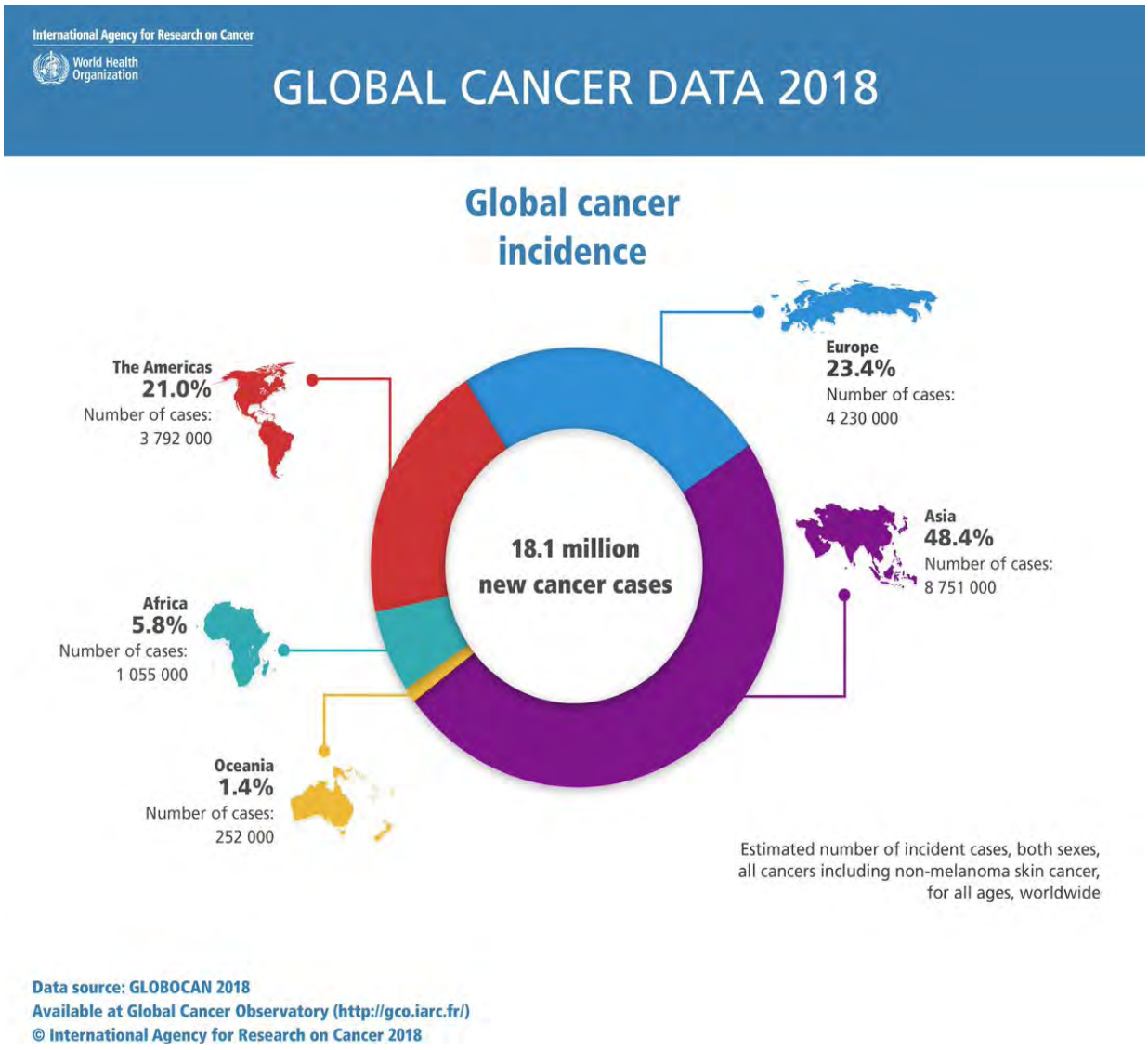

Figure 1.1 The estimated global number of incident cases for all cancer types in 2018 (WHO, 2018).

1.3. Pathogenesis and symptoms

Cancer pathogenesis entails the damage to cells' genetic devices through mutation, disturbance of gene expression, activation of genes that promote tumor, and deactivation of genes that suppress tumor (Halazonetis *et al.* 2008). There are three types of cancer-causing agents: chemical carcinogens like asbestos, benzopyrene and, about 900 chemicals, physical carcinogens such as exposure to ultraviolet and ionizing radiation and, biological carcinogens like viruses, bacteria, and fungi (Pitot and Dragan 1991).

Environmental factors such as air pollution and some lifestyles like excessive smoking and heavy alcohol consumption can also damage the DNA and cause cancer. The abnormal weight of cells is called a tumor, and it is divided into malignant (cancerous) and benign (non-cancerous). Benign tumor only grows at the primary site but do not spread and are not considered cancer, (**Figure 1.2**). A malignant tumor can spread and invade other cells in a process called metastasis (Bartsch and Nair 2006).

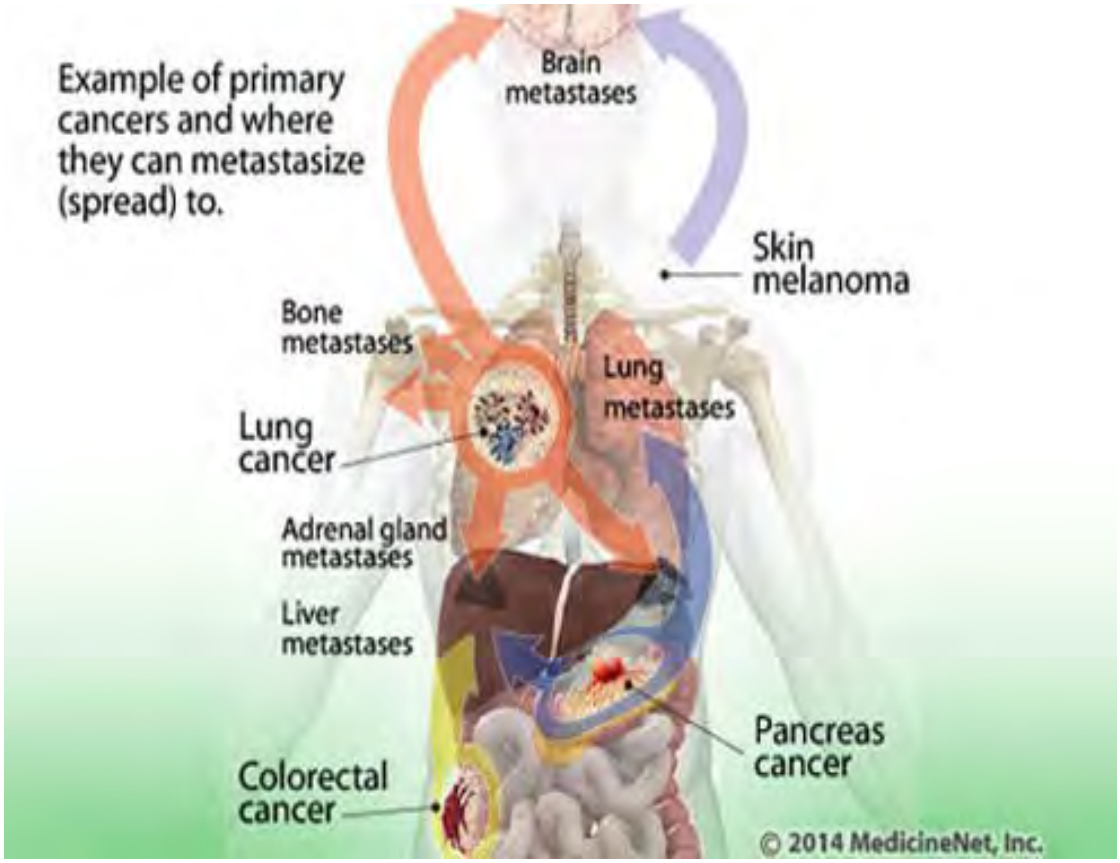

Figure 1.2 Examples of primary cancer and where they spread. Adapted from www.emedicinehealth.com/ 18common cancer symptoms and signs in men and women and accessed on 24/03/2020.

1.4. Diagnosis

Early diagnosis, detection, and treatment are a better approach to curing cancer. Some tumors like breast cancer and melanoma can easily be identified by self-examination and other screening procedures before they spread. Different types of cancer can only be detected and

diagnosed when disease progression and symptoms have already developed. The majority of the repetitive screening processes for cancer detection are based on cell morphology, tissue histology, and measurement of body fluid markers, which cannot give complete results for the early detection of cancer (Dermime 2013).

It is still predominant to detect cancer only when the symptoms have started showing. Nonetheless, tests have been developed in some cancer sites to see tissue changes that indicate either cancer precursor or early-stage tumors. When these precursors are recognizable, the abnormal tissue can be removed, and cancer development will be prevented; this process is called primary prevention. The target is an early-stage tumor; the diagnosis is called secondary prevention because it is designed to improve long-term outcomes by treating cancer when it has spread (Wardle *et al.* 2015). For colorectal cancer, a stool-based test called fecal immunochemical test helps in early detection. If blood is detected during this process, the patient will undergo endoscopic visualization of the whole colon to detect cancer or the precancer. Polyps can be removed during this screening, preventing the formation of colorectal cancer (Levin *et al.* 2008). For this research, emphasis will be on colorectal cancer henceforth.

1.5. Colorectal Cancer

Colorectal cancer (CRC), also known as bowel, colon, or rectal cancer, is any cancer that affects the colon and the rectum (**Figure 1.3**). It is the third most commonly diagnosed cancer and the second leading cause of death worldwide (Siegel *et al.* 2014). Almost all colorectal carcinomas are adenocarcinomas from the epithelial cells of the colorectal mucosa (Fleming *et al.* 2012).

Early detection of colorectal cancer is by colonoscopy, with biopsy and histological confirmation of the diagnosis. Computed tomography (CT) is immediately recommended if carcinoma is detected for initial evaluation, staging, and treatment planning (Nakayama *et al.* 2013).

Most colorectal cancer symptoms include alterations of bowel habit, constipation and diarrhea, black feces that contain blood, bright red blood coming from the rectum, painful and bloating abdomen, fatigue, weight loss, and so many more. Some of the risk factors of colorectal cancer include older age, high alcohol consumption, smoking, low fiber diets, lack of physical exercise, obesity, and eating red or processed meat.

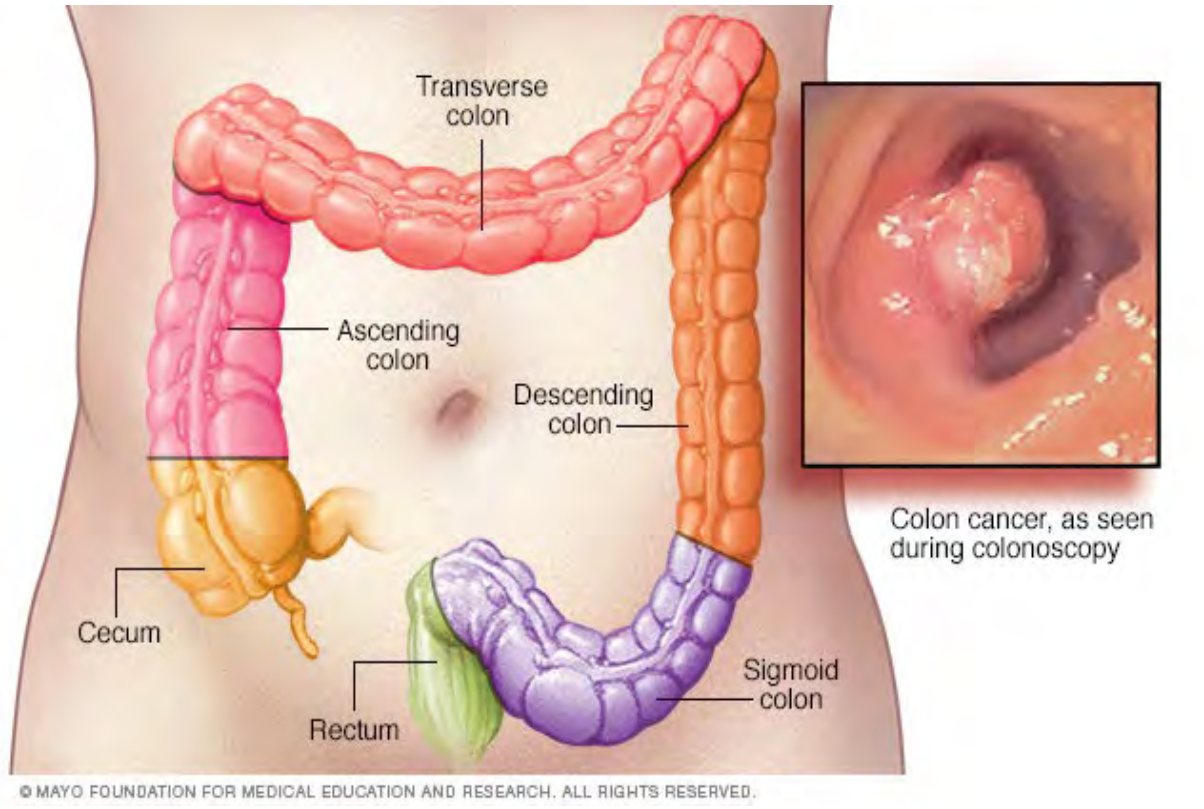

Figure 1.3. Different parts of colons and formation of colorectal cancer, as seen during colonoscopy, adapted from *Mayo foundation for medical education and research.*

1.6. Therapeutic Management

To predict patient outcomes and improve clinical management, colorectal cancer's heterogeneous nature and unique genetic and epigenetic background must be understood. This has led to the disease classification based on location, histology, etiological factors, and molecular mechanisms. Optimal surgical resection is still the mainstay of curative treatment, and this can maintain long-term survival, life quality, and cure in some patients. Treatment and management decisions are found on established guidelines like the National comprehensive cancer network (NCCN) and European society for medical oncology (ESMO), (Schmoll *et al.* 2012, Carlson *et al.* 2014). Patients whose tumors are not located in the rectum or transverse colon, and those without acute bowel damage can undergo laparoscopic colectomy. Surgery is the most common treatment as the affected malignant tumor, and lymph nearby will be removed to reduce it from spreading and stopping the symptoms.

Chemotherapy is another means of treatment for colorectal cancer. It entails using medicine or

chemical to destroy or shrink cancerous cells. 5-Fluorouracil, oxaliplatin, leucovorin (LV), and capecitabine are some of the drugs used in adjuvant chemotherapy as a standard cure for stage III colorectal cancer (André *et al.* 2015). In stage II colon cancer, adjuvant therapy alone cannot cure it but there is a reported 2-4% greater chance of survival than surgery alone. Management of metastatic CRC comprises many active drugs such as 5-FU/LV, capecitabine, irinotecan, bevacizumab, cetuximab, panitumumab, and regorafenib (Carlson *et al.* 2014). Some considerations, like the purpose of the treatment, tumor biology, patients, and drug-related factors, must be taken care of before selecting the drug. Most of these drugs can be used as single drugs or in combinations. A multi-dimensional approach, including standard surgery, moderate choice of chemotherapy, and radiotherapy routines according to the disease features and patients' aspects, could potentially cure colorectal cancer.

1.7. Colorectal cancer drug profiles

5-Fluorouracil (5-FU) was used as the drug for encapsulation study and release mechanism in this research because it is a first-line chemotherapeutic treatment for colorectal cancer (CRC) either as a single dose or in combination with other chemotherapeutic agents. More than 70 decades ago, treatment of CRC by chemotherapy has been revolving around using this fluoropyrimidine with various degrees of administration and scheduling routines, encompassing bolus injection to continuous infusion and oral pro-drug form (Ou *et al.* 2019).

1.7.1. 5-Fluorouracil (5-FU)

1.7.1.1. Description

5-Fluorouracil is an analogue of uracil (**Figure 1.4**), a natural pyrimidine that must be converted to the nucleotide to exert its efficacy. 5-FU is metabolized rapidly after administration to give cytotoxic fluoronucleotide with established antineoplastic properties (Maring *et al.* 2005).

1.7.1.2. Physicochemical properties

Molecular formula: $C_4H_3FN_2O_2$

Molecular weight: 130.08 g/mol

Chemical structure:

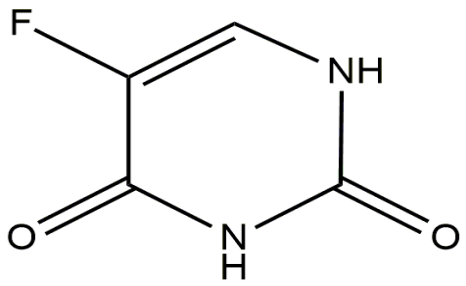

5-fluoro-1H-pyrimidine-2,4-dione

Figure 1.4 Chemical structure of 5-fluorouracil

Synonyms: 5-fluorouracil, Fluorouracil, 5-FU, 51-21-8, Efudex, Adrucil, Fluoroplex, Fluracil, Carac, Fluoroblastin, Kecimeton, 5-fluoracil, etc.

Organoleptic characters: 5-FU is a white to nearly white crystalline powder that is practically odorless, sparingly soluble in water, and slightly soluble in alcohol.

Melting point: 280 to 282°C

1.7.1.3. Pharmacological features

Drug Class: Antineoplastic agents used in cancer chemotherapy.

Dosage forms: Injectable solution (50 mg/mL). All dosage is dependent on the patient's body weight.

Mechanism of action: The mechanism of cytotoxicity is very complicated because it is activated through different pathways resulting in about three cytotoxic compounds; fluorodeoxyuridine monophosphate, that hinders thymidylate synthase and subsequent DNA synthesis, fluorouridine triphosphate that integrates directly to the RNA, and fluorodeoxyuridine triphosphate that its integration into DNA has been suggested (Pardini *et al.* 2011).

By binding the deoxyribonucleotide the drug and the folate cofactor *N*5,10-methylenetetrahydrofolate to thymidylate synthase, a covalently bound ternary complex is formed. This prevents thymidylate from uracil from being developed, leading to the inhibition of DNA and RNA synthesis and cell death (**Figure 1.5**). The drug requires enzymatic alteration to the nucleotide to exert its cytotoxic action, but this is an advantage, since fluorouridine

triphosphate (FUTP) can be merged into RNA in place of uridine trisphosphate (UTP) to produce a “false RNA” that interferes with RNA processing and synthesis of proteins. The rate-limiting enzyme in 5-FU catabolism is dihydropyrimidine dehydrogenase (DPD), which converts 5-FU to dihydrofluorouracil (DHFU). Above 70% of administered 5-FU is usually catabolized first in the liver, where DPD is expressed excessively (Longley *et al.* 2003).

Metabolism: Fluorodeoxyuridine monophosphate (FdUMP), a 5-FU metabolite, forms a ternary complex with thymidylate synthase (TS) and 5,10-methylenetetrahydrofolate (CH_2THF), inhibiting the synthesis of DNA in the process. The mechanism of 5-FU in cells is diverse, just like every other pyrimidine. The metabolism follows the following steps: 5-FU is first converted into the following metabolites: 1. Fluorouridine triphosphate (FUTP); this is fused into the RNA instead of uridine triphosphate (UTP), 2. Fluorodeoxyuridine triphosphate (FdUTP), incorporated into DNA instead of deoxythymidine triphosphate (dTTP), 3. FdUMP inhibits the activity of the TS at the ternary complex. FUTP results in changes in the RNA processing and function; FdUTP and FdUMP result in DNA damage. All these processes affect RNA and DNA and cause cell deaths as shown in **Figure 1.6** (Miura *et al.* 2010).

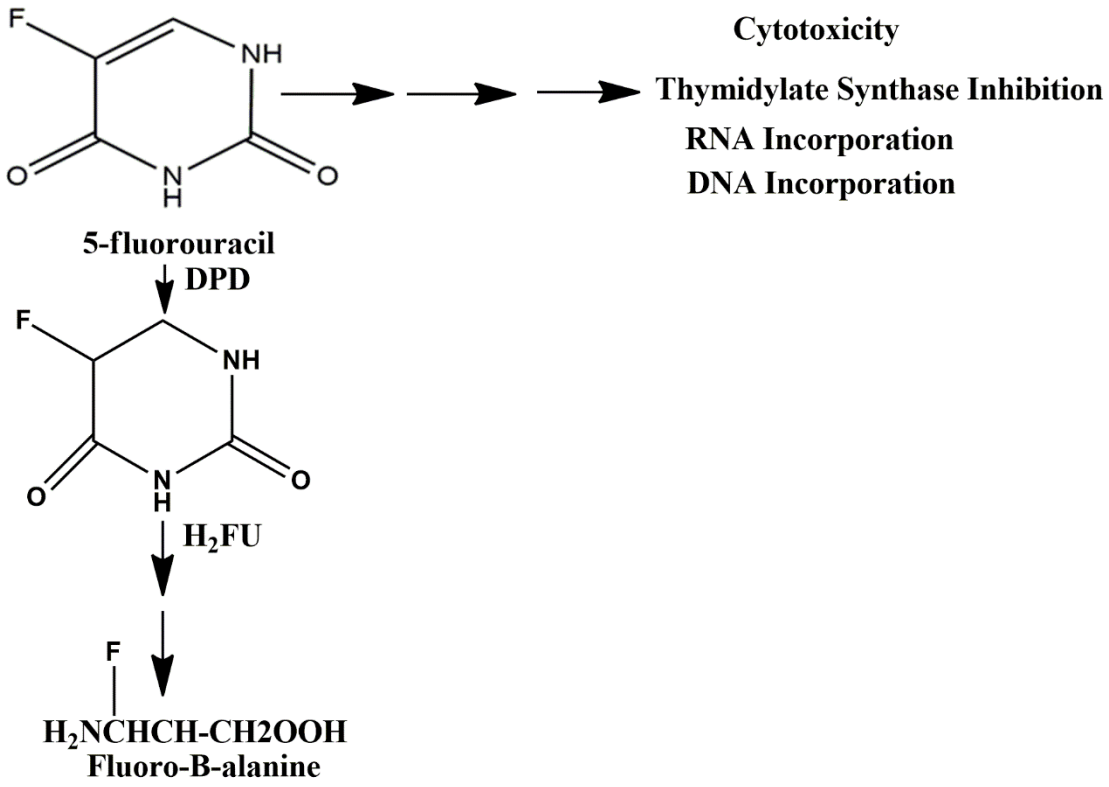

Figure 1.5. Metabolic pathway of 5-fluorouracil adapted from (Ken-ichi Fujita and Yasutsuna

Sasaki 2007)

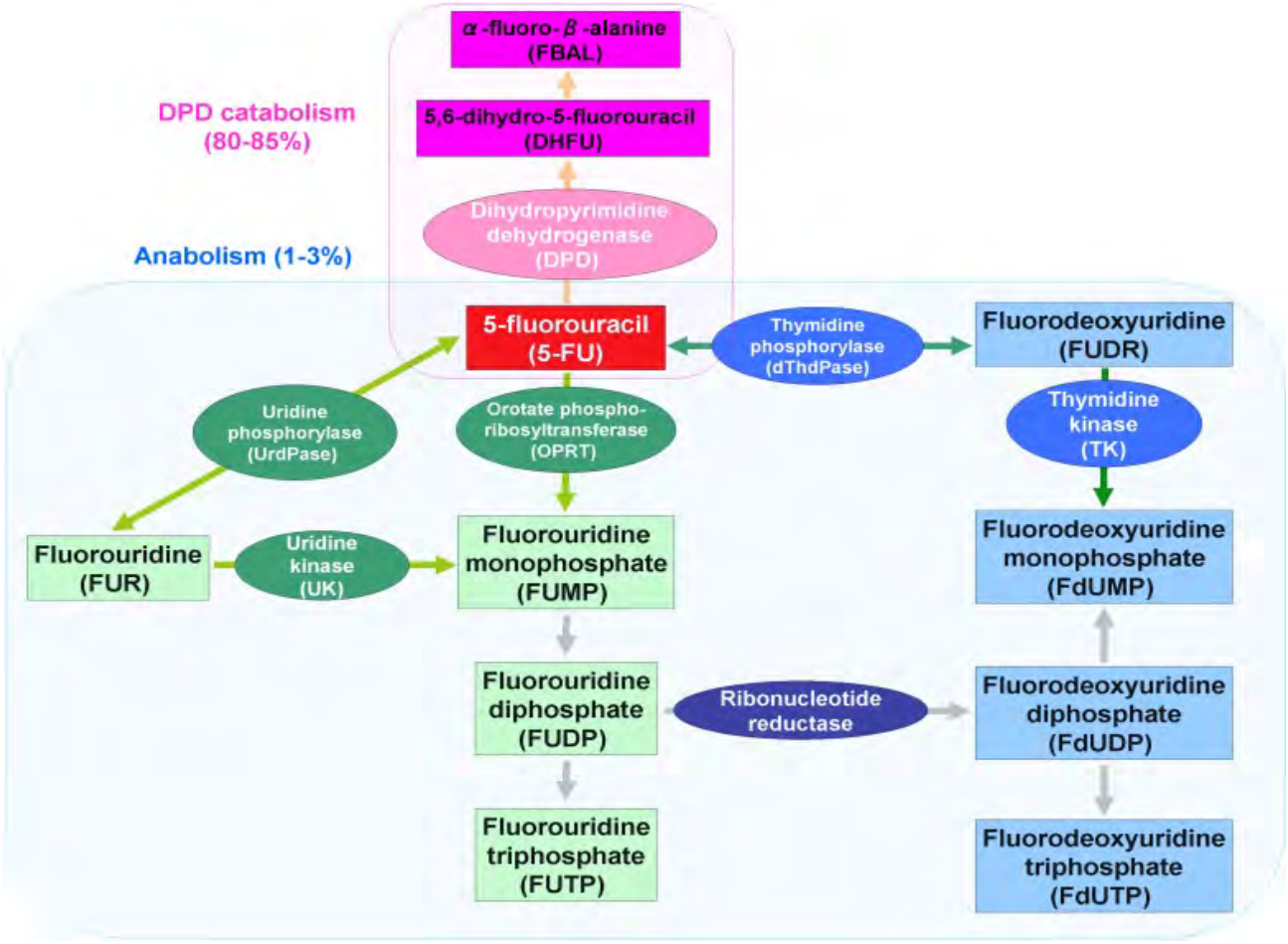

Figure 1.6. Summary of the current understanding of 5-FU metabolism. Adapted from (Miura *et al.* 2010).

Elimination: About 7-20% of the parent drug is excreted unchanged in the urine in 6 hours, and close to 90% of that is excreted in the first hour. The remaining dose administered is metabolized primarily in the liver.

Indications: 5-FU is used to treat metastatic colorectal cancer either alone or in combination with irinotecan, leucovorin, and oxaliplatin, with or without bevacizumab.

Contraindications: 5-FU is contraindicated for patients in a poor nutritional state, depressed bone marrow function, and those with potentially adverse infections, also those with known hypersensitivity to the drug and pregnant women.

Adverse effects: Anorexia, nausea, and vomiting are frequently reported as common side effects of 5-FU. Stomatitis is also a sign of early toxicity. Diarrhea, esophagitis, proctitis, and gastrointestinal ulceration and bleeding have been reported during therapy. Leukopenia and anemia, pancytopenia, and agranulocytosis have also occurred. Hair loss frequently occurs also, and the pruritic maculopapular rash, which is the most common skin adverse effect, has been reported (Diasio and Harris 1989).

2.1 Stimuli-responsive nano-carriers

Since there is a greater need to prevent early release of therapeutics, control, and target drug delivery only to the diseased cells, stimuli-responsive nanoparticles are dedicated active delivery vesicles within the nano or micro-sized range that are designed to include some "load and release" modalities. This is because some intrinsic or externally applied stimulus causes a change in properties of the vesicles such that they release the cargo.

The principle of stimuli-responsive nanoparticles encompasses the fact that an inherent cellular or extracellular stimulus of chemical, biochemical or physical nature can alter the nanoparticles' structural arrangements and/or compositions, promoting the release of their cargo to some biological regions as illustrated in **Figure 1.7** (Hu *et al.* 2017). The changes are varied, including decomposition, isomerization, polymerization, supramolecular combination, and many more. This stimuli-responsive characteristic, whether inherent or chemically modified, is an added advantage to these systems.

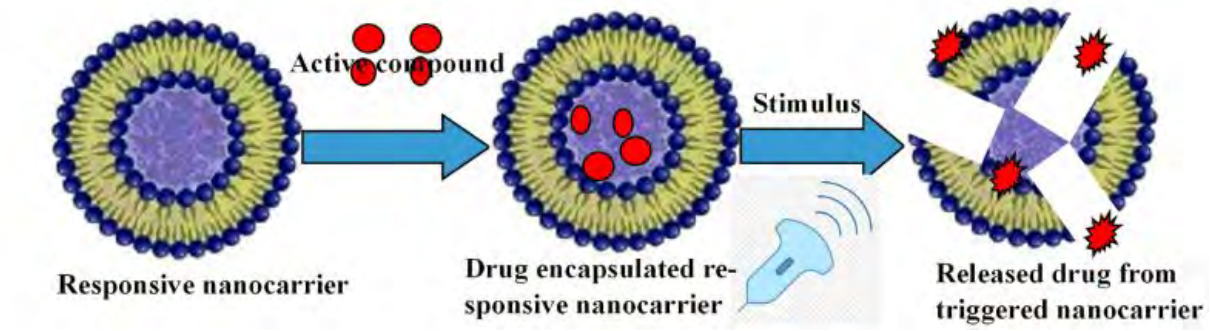

Figure 1.7. A general illustration of stimuli-responsive nanoparticles for the carriage of an active compound. Adapted from (Fleige *et al.* 2012).

2.1.1. Triggered drug delivery

Drug delivery systems that are externally triggered to release their payloads hold significant

aptitude for improving the treatment of many diseases by reducing off-target toxicity and increasing therapeutic efficacy. Stimuli-responsive nanomaterials that respond to endogenous stimuli rely on the differences between diseased and healthy tissues, including chemical variations like pH, redox, hypoxia, enzymes, and physical discrepancies like mechanical triggers and temperature changes. Exogenously triggered nanocarriers on the other hand react to changes in stimuli such as light, magnetic field, ultrasound, and mechanical triggers (Kauscher *et al.* 2019).

2.1.2. Ultrasound (US)

Ultrasound is made up of pressure waves with frequencies higher than the human audible range (20 kHz) (Ahmed *et al.* 2014). It is among the broadest area of application of exogenously triggered physical release from nanoparticles. It is a non-invasive, well-established, not expensive, and readily available medical imaging and drug delivery tool. Ultrasonic waves can be reflected, refracted, focused, or absorbed – as with most sound waves. However, unlike most other sound, US is very physical, that is US waves are actually molecules in movement, as the medium is repeatedly compressed at high pressure and expanded at low pressure. This results in substantial effects on biomolecules and cells (Pitt *et al.* 2004). Unlike visible light waves, ultrasonic waves can be absorbed a little by water, flesh, and most tissue, which makes it possible for the ultrasound to be used as a tool for both diagnosis and transmission of energy into the body at a targeted area for treatment. There are high and low-intensity US waves based on the employed power densities. The US devices used in medicine comprise a generator that produces a high frequency alternating current and a transducer that converts the energy into US vibrations.

2.1.3. Mechanisms of ultrasound triggered drug delivery

The US used as a trigger can be focused on the drug carriers when they have reached the target sites so that the therapeutics are released and diffuse into the anticipated cells. When interacting with the biological system, the effects of the US could either be thermal or non-thermal. Hyperthermia is a thermal effect that results in the adsorption of acoustic energy by fluids or cells, which occurs due to increased power density when the US beam is focused on the target tissue. Hyperthermia has the therapeutic effects of heating the drug carriers, the drug, and the treated cells. Hyperthermia initiated by US application can be used in medicine as adjuvant chemotherapy, causing cancer cells to die faster and for heating tissues in physical therapy

(Draper *et al.* 1995).

Oscillating and cavitating bubbles and non-cavitating bubble-like radiation are products of non-thermal effects of ultrasound. This interaction of acoustic waves with gas bubbles or other fluids is called acoustic cavitation (Leighton 2007). Cavitation is the formation or activity of gas-filled bubbles when exposed to ultrasound. Depending on the nature of oscillation, there is stable or non-inertial cavitation, which creates a circulating fluid flow called microstreaming around the bubble with velocities and shear rates proportional to the amplitude of the oscillation. This shear force can tear a synthetic nanocarrier like liposome (Pitt *et al.* 2004).

Inertia or collapse cavitation is when the amplitude of oscillation under high ultrasonic intensity increases to a spot; thereby, the movement of fluids in the walls have enough inertial that it cannot reverse itself even when the acoustic pressure reverses; instead, it continues to compress the gas in the bubble into a very small volume, resulting in very high pressure and temperature (Mitragotri 2005).

2.1.4. Ultrasound-induced mechanism in drug delivery

There are three ways through which the effects of ultrasound application in a medium can be manifested.

2.1.4.1 Enhanced movement of drug carriers

A fluid under ultrasound oscillation results in higher molecular diffusivity, thereby increasing the transport of drugs, whether free or bound to a carrier, either within the blood or the cells. Drug transport increases by several orders of magnitude in the presence of oscillating bubbles, and the circulating eddies created during microstreaming transport drugs at a very high velocities. Acoustic pressure, which is the net force acting on other suspended bodies in the region of the oscillating bubble, also increases drug carriers (Stratmeyer and Christman 1983).

2.1.4.2 Disruption of the drug carrier

Ultrasound can perturb the drug carrier, thereby releasing the therapeutics. This can happen when a carrier undergoes shear stress and ruptures, thereby releasing the contents. Some carriers like liposomes or micelles will reform (albeit usually at smaller sizes) after rupture, and in the process, the encapsulated drugs are released by stable cavitation. Shock waves generated from ultrasound exposure can also perturb drug carriers leading to the release of the drug by

collapse cavitation.

2.1.4.3 Cell permeabilization and capillary rupture

The stresses exacted on the cells due to collapse cavitation can also lead to drug release. In the presence of these nanocarriers, tissues under cavitation events are subjected to shear from microstreaming, shock wave, and sonic jet which happens when the collapse is close to a solid surface. This results to asymmetrical collapse ejecting a liquid jet at sonic speed towards the surface , all these results to capillary rupture and delivery of payloads (Pitt *et al.* 2004).

Ultrasound is regarded as safe and cost-effective in biomedical areas because it does not require surgery to penetrate the body. US also increases the efficacy of thrombolytic drugs and improves the anti-tumor activity of anti-neoplastic medications; it also enhances transdermal drug delivery and gene therapy (Ahmed *et al.* 2014).

2.1.5. Applications of ultrasound in drug delivery

Transdermal drug delivery is the highest area of US-enhanced drug delivery because of the approval of Sontra Medical system for transdermal drug delivery of topical therapeutics in 2004 (Ahmed *et al.* 2014). Ultrasound has been in use for many years in delivering small hydrophobic substances such as steroids into or through the skin (Barry 2001). Cavitation processes opens reversible pores in the lipids layers of the stratum corneum, opening path of delivery for proteins like insulin (Mitragotri and Kost 2004).

Ultrasound has been used to deliver therapeutics to tight endothelial junctions like the blood-brain barrier, one of the few approaches to improving the transport of many molecules. In conjunction with microbubbles, movement of magnetic resonance contrast agents is enhanced by 260 kHz ultrasound frequency (Hynynen *et al.* 2006). US also enhances delivery to solid tumors, which can be very limited; liposomes, micelles, and microbubbles can all be used to deliver drugs to solid tumors in combination with US-technology. Ultrasound, combined with thrombolytic agents also enhances thrombolysis; microbubble oscillation improves a blood clot's breakup combined with ultrasound, as proved by Unger (Unger *et al.* 2004).

3. Liposomes

Liposomes are small artificial spherical lipid bilayers made from natural, non-toxic phospholipids and cholesterol when dispersed in an aqueous medium (Huang *et al.* 2014). Liposomes have been attracting prompt attention as carriers of therapeutics for drug delivery system because they can carry both hydrophilic and lipophilic compounds. The lipid-soluble drugs are usually entrapped in the bilayer membrane, while the water-soluble compounds are entrapped in the vesicles' aqueous core (Karami *et al.* 2018). Bangham *et al.* in 1963 were the first to synthesize liposomes by showing that when phospholipids are hydrated in an aqueous medium, they form spherical structures as illustrated in **Figure 1.8** (Bangham *et al.* 1965).

Phospholipids and cholesterol are the major components of liposomes. Phospholipids are amphiphilic substances with a water-soluble hydrophilic heads group and a lipophilic hydrophobic tail. Many factors influence the properties of liposomes, including the lipid composition, preparation method, size, and surface charge. Liposomes have been established as a very good nanocarrier for therapeutics in drug delivery because they are biocompatible, biodegradable, non-toxic, flexible, and non-immunogenic for systemic and non-systemic administration (Karami *et al.* 2018). Liposomes also improve the solubility of lipophilic and amphiphilic drugs, offer selective targeting to tumor cells, and enhance drug potency and efficacy (Huwyler *et al.* 2008). Liposomes can also be coupled with targeting ligands because of this flexibility; they can be used to prevent enzymatic degradation and therefore makes drugs more stable and helps decrease the toxicity of the drugs (Gregoriadis 1983).

Some of the limitations of liposomes as therapeutics nanocarriers for drug delivery are as follows; the cost of production of liposomes is usually very high, most times there is some leakage or aggregation of the encapsulated drugs, phospholipids do undergo oxidation or hydrolysis reactions which affects their stability, and most liposomes have a short half-life and low solubility. The long-term storage stability of most liposomes is also not encouraging (Anwekar *et al.* 2011). Despite these shortcomings, the utility of liposomes has improved after many decades of research. This includes research on their stability and mode of actions within the system, resulting in many of the formulations being in a clinical trial or already in the market to treat various diseases (**Table 1**) (Sharma Vijay *et al.* 2010).

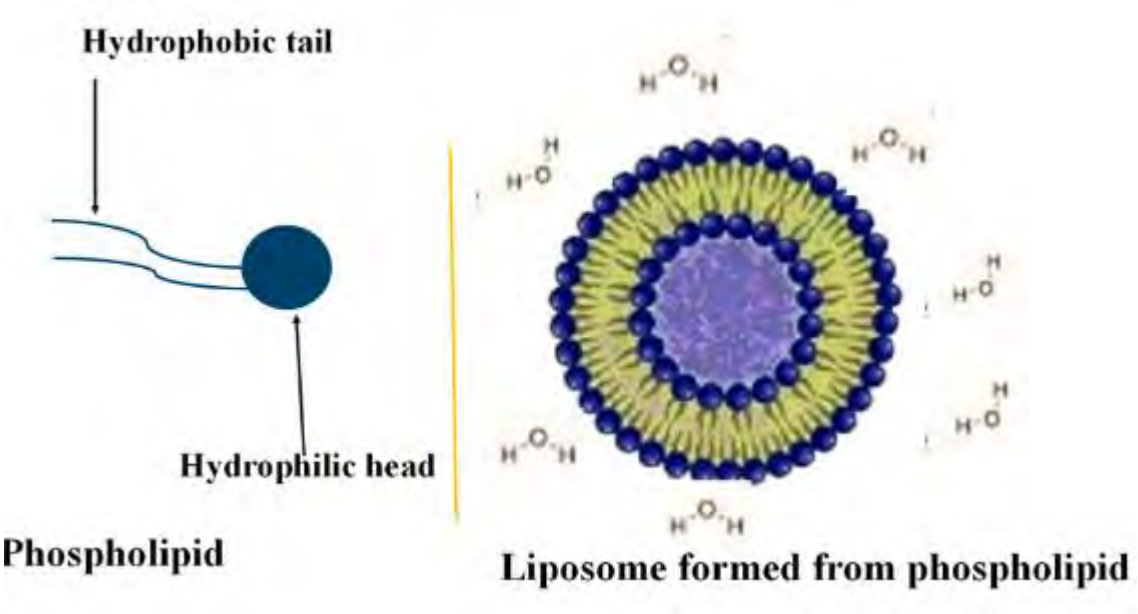

Figure 1.8. Structure of liposomes formed from phospholipids in an aqueous medium. Adapted from (Karami et al. 2018).

Table 1.3. *Various formulations of liposomes in the market, including their drug name and indications, adapted from (Sharma Vijay et al. 2010).*

Market product	Liposomal drug name	Target/ indications
Amphocil™	Amphotericin B	Serious fungal infections
Ambisome™	Amphotericin B	Severe fungal infections
Abelcet™	Amphotericin B	Severe fungal infections
Doxil™	Doxorubicin	Kaposi sarcoma in AIDS
DC99™	Doxorubicin	Metastatic breast cancer
DaunoXome™	Daunorubicin	Kaposi sarcoma in AIDS
Ventus™	Prostaglandin E1	Acute Respiratory Distress Syndrome
Nyotran ™	Nystatin	Candidemia
DC99™	Annamycin	Kaposi sarcoma in AIDS

3.1. Classifications of Liposomes

3.1.1 Classification based on composition and functionality

Liposomes are comprised of natural and or synthetic lipids and other bilayer compositions like cholesterol. The physical and chemical properties of the lipids that make up the liposomes (membrane fluidity, charge density permeability, and steric hindrance) not only influence the properties of the liposome but determine its interactions with biological components after administration. Liposomes can therefore be classified according to the composition and processes of intracellular delivery into six classes.

1. Conventional liposomes; these are made from neutral or negatively charged phospholipid and cholesterol and are typically used for the reticuloendothelial system (RES), for targeting and for rapid saturable uptake. These types of liposomes almost always have short circulation half-life and are dose dependent.

2. Immunoliposomes; these are long- or short-circulating liposomes with antibodies attached and a sequence of recognition. These are characterized by receptor-mediated endocytosis but can be used to release content extracellularly close to the target cell.

3. pH-Sensitive liposomes; these are liposomes composed of phospholipids like phosphatidylethanolamine (PE) and dioleoyl phosphatidylethanolamine (DOPE) with pH-sensitive materials like oleic acid. They often fuse with cells or the endosome membrane at low pH and release contents in the cytoplasm where the pH is often different to either the extracellular pH or that of healthy tissue.

4. Cationic liposomes; the active components here are cationic lipids like dimethyl-dioctadecyl ammonium bromide (DDAB) with DOPE. They are used to deliver negatively charged macromolecules like DNA, RNA. They are easy to produce but structurally unstable.

5. Fusogenic liposomes; these are composed of liposomes with ultraviolet inactivated Sendai virus on the surface. They are used to effectively deliver content into animal cells through membrane fusion (Watabe *et al.* 1999).

6. Long-circulating liposomes; these have a hydrophilic surface coating, low opsonization, low rate of uptake by RES, and long circulation half-life of about 40 hours in the body (Sharma and Sharma 1997).

3.1.2 Classifications based on size and lamellarity.

Apart from the above classification on type, two further classification categories are important, namely the size and number of layers. The size of the liposome is a crucial factor in determining the circulation half-life, while the number of layers affect the amount of therapeutics that can be entrapped (Mozafari *et al.* 2017). The table below shows the classification base on their sizes and number of lipid bilayers.

***Table 1.4**. Classification of liposomes base on size and lamellarity. Adapted from (Samad* et al. *2007).*

Vesicle Type	**Abbreviation**	**Size**	**No of Bilayer**
Unilamellar vesicle	UV	All size range	One
Small Unilamellar vesicle	SUV	20-100 nm	One
Medium Unilamellar vesicle	MUV	Above 100 nm	One
Large Unilamellar vesicle	LUV	Above 100 nm	One
Giant Unilamellar vesicle	GUV	Above 1 µm	One
Oligolamellar vesicle	OLV	0.1-1 µm	Approx. 5
Multilamellar vesicle	MLV	Above 0.5 µm	5 to 25
Multi vesicular vesicle	MV	Above 1 µm	Multi compartmental

3.2. Liposomes formation

Phospholipids are naturally amphipathic, showing attraction for both aqueous and polar molecules because they have a hydrophobic tail and a hydrophilic head. Their thermodynamic phase properties and self-assembly features lead to entropically driven sequestration of hydrophobic regions into spherical bilayers (Sharma Vijay *et al.* 2010). The hydrophobic tail of most phospholipids comprises two fatty acid chains containing 10 to 26 carbon atoms and 0 to 6 double bonds in each chain. The macroscopic structures that form lamellar, hexagonal, or cubic phases, spread, resulting in colloidal nanoparticles called liposomes, hexosomes, or cubosomes. The most common natural polar phospholipid is phosphatidylcholine.

Liposomes are produced when lipid films or lipid cakes are hydrated in an aqueous medium, and stacks of lipid crystal-like bilayers become watery and swell (Anwekar *et al.* 2011). To gain stable states, these bilayers start folding or curl-in on themselves to form closed sealed bi-layered vesicles enclosing a central aqueous core, as shown in Figure **1.9.**

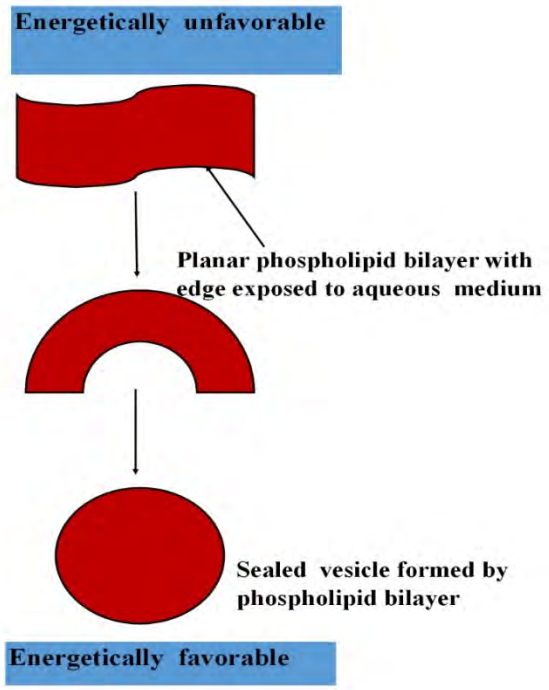

Figure 1.9. Liposomes formation mechanisms. Adapted from (Sharma Vijay *et al.* 2010).

3.3. Compositions of liposomes

The main components of liposomes are lipids (either natural or synthetic phospholipids, cholesterol, additives, and water). Phospholipids are lipids that contain phosphorus, polar and non-polar portions in their structures (Li *et al.* 2016). Phospholipids are compounds in which hydrophilic head group and hydrophobic acyl chains are joined to the alcohol functional group. The glycerol containing phospholipids are the most common components of liposomes formulation. Most of the phospholipids used in liposomes formulations are phosphatidylcholine (PC), also known as lecithin, phosphatidylethanolamine (PE), phosphatidylserine (PS), phosphatidylinositol (PI), phosphatidylglycerol (PG) (Anwekar *et al.* 2011). **Figure 1.10** shows most of the glycerol-phospholipids and their X-moieties.

Phospholipid name	**X-moiety**
Ester glycerol-phospholipids with R_1 & R_2 representing different acyl chains of fatty acids	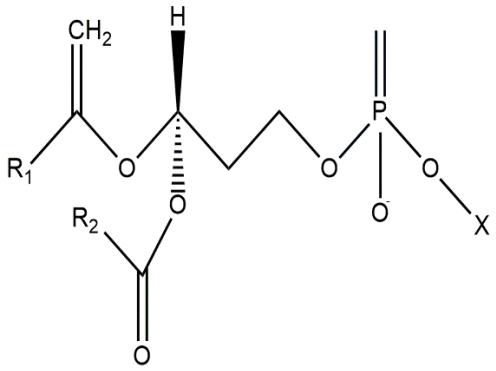
PC	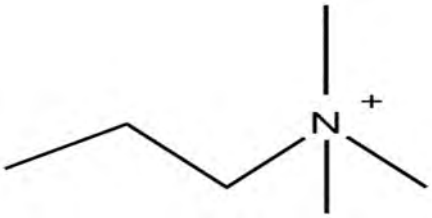
PE	
PS	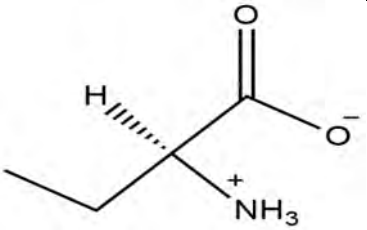
PG	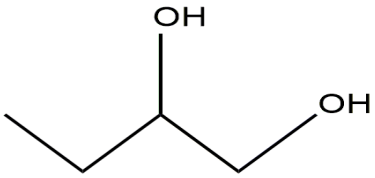

Figure 1.10. Schematic illustration of different types of X-Moieties. Adapted from (Li *et al.* 2016)

Phosphatidylcholine (lecithin) and phosphatidylethanolamine are the two most important structural components of most liposomes. A significant parameter of all these phospholipids is the phase transition temperature (T_M), described as the temperature above which phospholipids exist in a liquid crystalline state. Lipids can either exist in a fluid or gel state depending on T_M. Phospholipids with a gel state above the body's physiological temperature of 37 °C are typically chosen to stabilize liposomes in other to avoid leakage of the encapsulated drugs by the liposomes becoming fluid in the body (Pattni *et al.* 2015).

However, since most phospholipids used in liposomal formulations have phase transition temperatures below 37 °C cholesterol is added to increase the phase transition temperature. This prevents leakage of the entrapped therapeutics and helps to improve the membrane fluidity and bilayer stability and reduces the permeability of water-soluble molecules through the membrane. Cholesterol sometimes increases the size of the vesicles depending on the amount used (López-Pinto *et al.* 2005). The liposome's charge is another critical parameter in determining its behavior during drug delivery; they can be positively or negatively charged, or neutral depending on lipids and additives included. Some examples of positively charged phospholipids are 1,2-dihexadecyl-*N N*-dimethyl-*N*-trimethylamine, methyl ethanolamine. Some negatively charged phospholipids are dipalmitoyl phosphatidylcholine, dipalmitoyl phosphatidyl acid (DDPA), distearoyl phosphatidylcholine (DSPC), dioleoyl phosphatidylcholine (DOPC), while neutral phospholipids are sphingomyelin, phosphatidylethanolamine, and phosphatidylcholine (Sharma Vijay *et al.* 2010). Liposomes that are charged show electrostatic repulsion preventing them from aggregating during storage. This can positively affect their long-term storage and transportation but can also affect the drug release profile.

3.3.1. Lipid profile

Crude soybean lecithin and cholesterol in varying compositions were used to prepare liposomes in this research because of their availability and low cost. They also fall within the physiological lipids with no known toxicity to biological membranes. Modifications were made based on functionality by entrapment of argon, a biocompatible gas to produce echogenic liposomes that are responsive to external ultrasound triggering.

3.3.2. Lecithin

Lecithin refers to mixtures of different triglycerides, phospholipids, and glycolipids. In some fields, lecithin only refers to pure phosphatidylcholine, a phospholipid derived from phosphate segment taken out from vegetables like soybeans, rice beans, sunflower, and rapeseed. Natural phospholipids are also

obtained from animal sources like egg yolk, milk, and marine sources (Le *et al.* 2019). Soybean lecithin is the most used in liposomes formulations because it contains less polyunsaturated fatty acids making it more stable. Animal-based derived lecithin like egg yolk and milk are faced with protein and pathological contamination such as viruses. They require more testing to ensure contamination-free liposomes when used.

From a production point of view, soybean lecithin is considered economical, safe, and stable. It's also readily available in purified and unpurified forms for both laboratory and industrial production of liposomes (Adriana *et al.* 2014). Lecithin is used as emulsifiers and lubricants in foods and pharmaceutical industries. They are non-toxic surfactants, well tolerated by biological membranes, and are quickly metabolized. Soy lecithin can also be used as a vitamin preservative against oxidation and a source of growth, promoting choline and inositol (Adriana *et al.* 2014). Soybean lecithin is produced by hydration and separation from the crude soybean oil, as shown in the flowchart below in **Figure 1.11**

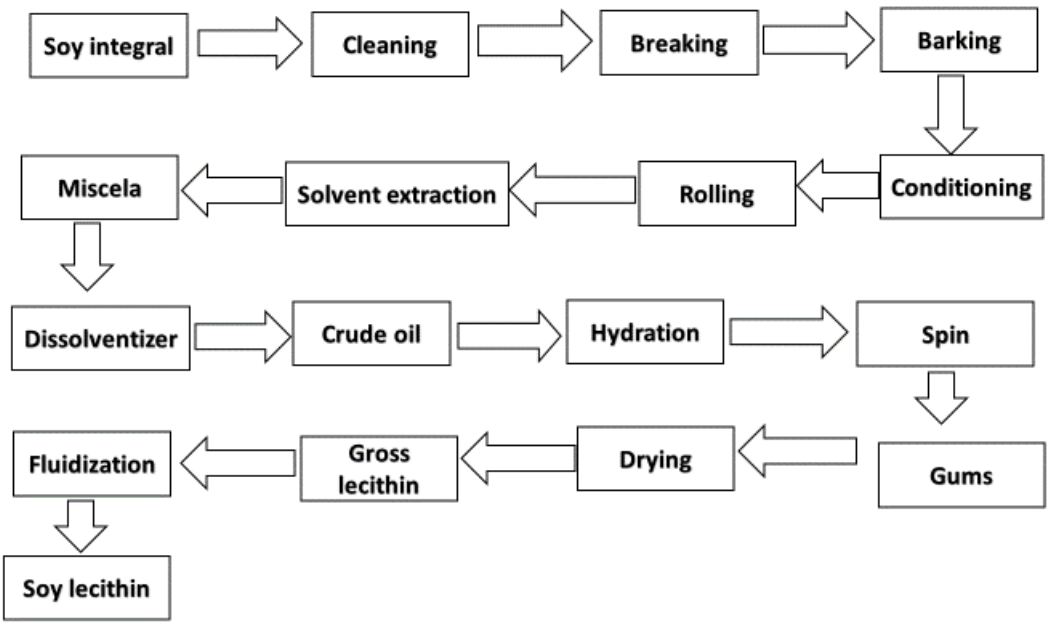

Figure 1.11. Flowchart showing the production of soy lecithin from crude soybean. Adapted from (Adriana *et al.* 2014)

3.3.3. Cholesterol

Molecular formula: $C_{27}H_{46}O$

Molar mass: 386.654 g/mol

Melting point: 148 - 150°C

Density: 1.052 g/cm^3

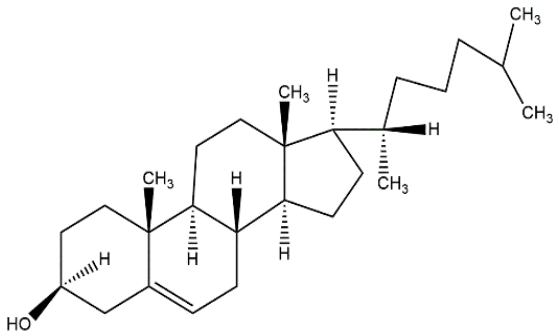

Figure 1.12. Molecular structure of cholesterol

Cholesterol is a white or faintly yellow, almost odorless powder. It is used in pharmaceutical and cosmetic formulations as an emulsifier, often at concentrations of 0.3-5% w/w. It is practically insoluble in water but soluble in some organic solvents like acetone and ethanol. All higher animals have this as the principal sterol, found in all body tissues, especially in the spinal cord and brain (Dinh *et al.* 2011). It is non-toxic and non-irritant when used as excipient. It has shown teratogenic and reproductive characteristics experimentally. Cholesterol can be derived naturally from animal sources. Cholesterol is produced commercially from the spinal cords of cattle extracted with petroleum ether and from wool fats and is purified by repeated bromination (Domańska *et al.* 1994). The molecular structure of cholesterol is shown in **Figure 1.12.**

3.4. Methods of liposomes preparation

There are several methods for liposomes preparations, some of which have advantages for large scale production. All these methods have to do with the dispersing the lipids in an aqueous environment. The size, encapsulation efficiency and lamellarity are all affected by the method of preparation.

3.4.1. Thin-film hydration method

One of the most common and simplest methods essentially involves storing a thin film of lipid under

water. The lipid components are first dissolved in a round bottom flask in an organic solvent like chloroform, ethanol, or dichloromethane to form a clear lipid solution and completely mix the lipids. The organic solvent is then removed using a rotary evaporator to create a thin and homogenous lipid film on the sides of the round bottom flask. This can be stored overnight in a desiccator or under nitrogen gas for complete drying (Achim *et al.* 2009). The lipid film is then hydrated in aqueous media under continuous agitation to separate the forming bilayers from the glassware and make sure sealed vesicles are formed. The hydration period lasts between 1 to 2 hours at a temperature above the lipid transition temperature. Multilamellar vesicles (MLVs) are majorly formed by this easy and widespread method. Drugs can also be added during the process by passive loading. Size reduction procedure like sonication is employed to reduce the sizes to small unilamellar vesicles (SUVs). This method produces liposomes with low encapsulation efficiency and heterogeneous size distribution (Karami *et al.* 2018).

3.4.2 Dehydration-rehydration method

In this method, SUVs are first prepared and then converted to MLV. The thin-film hydration method with sonication is used to prepare the SUV, then frozen and freeze-dried, and the obtained powder rehydrated in small volumes of aqueous media to form a large MLV. This method is used to obtain vesicles with a higher loading, especially of sensitive biological molecules like nucleic acid and proteins (Gregoriadis *et al.* 1990).

3.4.3. Reverse phase evaporation method

This method is centered on forming inverted micelles shaped by sonication of a mixture of aqueous phase that contains the water-soluble molecules to be entrapped into the liposomes and the organic phase in which the lipid components are dissolved. The gradual removal of the organic solvent converts these inverted micelles into a sticky state and gel form. It gets to a stage where the gel state collapses and most of the inverted micelles are perturbed during the process. Excess lipid components in the surrounding contributes to forming a complete bilayer around the micelles, leading to the production of liposomes with enormous aqueous volume-to-lipid ratios making this method an advancement in liposome production. Liposomes produced by this method can entrap a large amount of therapeutics in the aqueous core. It has been used to produce liposomes used to encapsulate small, large, and macromolecules. The only drawback of this method is the contact of the therapeutics to be encapsulated with the organic solvent. It can result in breakage of DNA or protein denaturation (Szoka and Papahadjopoulos 1978).

3.4.4 Solvent injection method

This method comprises the dissolution of the lipid components in an organic solvent such as ethanol or diethyl ether, and then the lipid solution is injected into aqueous media to form liposomes. The lipids first form a monolayer at the interface between the organic and aqueous phase, leading to the formation of liposomes. This method is comfortable and has a low risk of degradation of sensitive lipids, but its major disadvantage is that not all lipids are soluble in ethanol or ether (Szebeni *et al.* 1984).

3.4.4. Detergent removal method

In this method, lipid components are solubilized in detergents to yield defined mixed micelles. The detergents are removed by controlled dialysis, the lipid components form homogenous unilamellar liposomes within the size range of 40 to 180 nm, with large, encapsulated volumes. The major drawback is that large amounts of organic solvent are required in this method, which is harmful to both the environment and human health. Also, it requires a large amount of energy to produce, which isn’t ideal for large scale production (Laouini *et al.* 2012).

3.4.5. Heating method

This method involves the hydration of lipid components in an aqueous medium, then heating in the presence of 3% v/v glycerol to about 120°C. It is a swift method that does not require the use of hazardous chemicals or processes. Glycerol helps increase the lipid components' stability and does not need to be removed after forming the liposomes. Heat and mechanical agitation are the energy required to produce the liposomes here. The nature of the lipid components, the nature of agitation, and the shape of the reaction vessel help control the formed liposomes' size. No further sterilization is needed because the heat used in the production has taken care of that, thereby reducing the time and production cost (Laouini *et al.* 2012).

3.4.6. Microfluidic method

Microfluidics is a technology that allows exact control and manipulations of fluids and fluid interface at the micrometer level. Confinement and well-defined mixing in microfluidics make it attractive to produce liposomes from nanometer to micrometer range. The aggregation in this method can be controlled by changing liquid flow rates, ratios of crossflow, and composition of lipid components resulting in tunable sizes and narrower distributions (Yu *et al.* 2009). The lipids are first dissolved in an organic solvent and the solution channeled perpendicularly or in the position opposite the aqueous medium in the micro-

channels. Diffusion of various molecular species (such as alcohol and water, and also lipids) at the liquid interface between the solvent and non-solvent phase is what control the formation of liposomes by microfluidic method (Carugo *et al.* 2016)

3.4.7. Supercritical reverse-phase evaporation method (SRPE)

The SRPE is a new method that has been developed for the preparation of liposomes using supercritical carbon dioxide. An aqueous dispersion of liposomes is obtained by emulsion formation by introducing an amount of water into a homogenous mixture of supercritical carbon dioxide /LR-dipalmitoylphosphatidylcholine/ethanol under constant stirring and reduction of pressure. The liposomes formed here are in size range of 0.1 to 1.2 μm with a high encapsulation efficiency of about five times higher of hydrophilic and lipophilic substances than liposomes made from the film hydration method. SRPE is an excellent technique that allows the one-step formulation of large unilamellar vesicles with a high encapsulation efficiency for both water and oil-soluble compounds (Laouini *et al.* 2012).

3.5. Post-preparation treatments

3.5.1 Drug loading

There are two ways to load drugs into liposomes; passive loading is when the drug is entrapped during the formulation of liposomes, and active loading occurs when the drug is entrapped after formation. Most hydrophobic drugs are loaded passively during liposome formation, and the amount of the drug intake and retentions governed by the drug interactions and the properties of the lipids. The solubility of the drug will determine the trapping effectiveness that will be achieved (Akbarzadeh *et al.* 2013). The physicochemical properties of the drugs and the lipids and method of preparing the liposomes must be considered for the significant loading of therapeutics in liposomes.

Active loading method results in higher efficiency of encapsulation than passive loading procedures. The active loading mechanism is by diffusion properties when a gradient is established across the lipid bilayers (Pattni *et al.* 2015).

3.5.2 Freeze-thawing

Freeze-thawing is a process used after liposome preparation to increase the encapsulation efficiency. It is performed by freezing the liposome in liquid nitrogen at -196°C and thawing at a temperature above the

lipids' phase transition temperature. It is performed to reduce liposome lamellarity, form less polydisperse vesicles, and disrupt the bilayers to allow the drug molecules to diffuse into the vesicles, thus enhancing encapsulation. Multiple freeze-thaw cycles are performed to reach equilibrium drug concentration conditions. The physical perturbation of the lipid- bilayer because of the ice formation results in liposomes fusion leading to higher encapsulation of the loaded drugs (Costa *et al.* 2014).

3.5.3. Freeze-drying

Freeze-drying, also known as lyophilization in liposomes preparation, removes water from vesicles that are frozen under tremendously low pressure. It is used to dry products that are thermo-labile or can be destroyed by heat. It is used to increase the long-term stability of liposomes during storage. Leakage of entrapped materials may take place during freeze-drying, and this is prevented by the addition of cryo-protectants like trehalose and mannitol to help retain its original contents (Anwekar *et al.* 2011).

3.6. Characterization of liposomes

After preparation and before the application of liposomes, they must be characterized to ensure the *in vitro* and *in vivo* performances can be matched to certain characteristics. The characterization helps to assess the quality and to get quantitative measures that can be used to compare different batches of formulated liposomes. The parameters that are mostly monitored are lamellarity, diameter and size distribution, lipid composition and charge. Drug encapsulation efficiency is also important (Laouini *et al.* 2012).

3.6.1. Determination of lamellarity

The number of lipid bilayers determines the encapsulation efficiency and release kinetics of liposomes. Lamellarity also affects intracellular behavior when vesicles are taken up in the cell. Lipid composition and methods of preparations determine the lamellarity of liposome (Laouini *et al.* 2012). Liposome lamellarity is measured by electron spectroscopy or by electroscopic techniques. Nuclear magnetic resonance has been employed to observe the outside-inside distribution of phospholipids within bilayers. NMR is used to determine the size and lamellarity of liposomes as the dispersion of MLVs results in a clear powder ^{31}P-NMR spectra because of the restricted anisotropic motion SUVs are characterized by small line spectra (Laouini *et al.* 2012). Other methods used in lamellarity characterization include small-angle x-ray scattering. The liposome dispersions are dropped in glass capillaries, and curves are noted with a camera equipped with a dimensional position sensitive detector, and the data are analyzed using indirect Fourier transformation. This method evaluates liposome lamellarity with high accuracy. All the ways serve to determine the structure of formulated liposomes, which is an important parameter to assess

liposomes' success in therapy (Laouini *et al.* 2012).

3.6.2. Size and size distribution

Determination of average size and size distribution of liposomes is crucial when they are intended for use in drug delivery through the parenteral route or by inhalation. Batch and quality differentiation during formulations are also determine through size monitoring. There are many techniques to measure the size of liposomes like dynamic light scattering (DLS), size exclusion chromatography (SEC), Transmission electron microscopy (TEM), cryogenic-TEM, and nuclear magnetic resonance (NMR). DLS is a widely used and easiest method of size determination. It evaluates the Brownian motion of the colliding particles, resulting in the scattering of the incident light. The dispersion of light depends on the refractive index between the suspended particle and the solvent. The scattered light is then calculated and analyzed to give the average particle size of the suspended liposome (Pattni *et al.* 2015). DLS is easy to operate, and it has an extensive range of measurement intensity (20-1000 nm), and the liposomes are analyzed in their natural environment. Moreover, the system cannot resolve the variation between a single and an aggregated liposome. DLS is also sensitive to small amounts of impurities (Provder 1997).

The electron microscopy methods such as TEM and cryo TEM provides a view of morphology and sizes of liposomes. The liposomes dispersions are removed from their native environment and stained in a copper grid and allowed to dry before characterization. It most times generates artifacts, shrinkage, and shape distortions. It requires a long time to obtain a representative size distribution of the dispersions, and it’s difficult to program them as routine characterization techniques. Atomic force microscopy (AFM) has recently been developed to measure liposomes size, morphology, and stability. AFM has a dimensional resolution of close to 0.1 nm and can visualize small liposomes in their natural environment without manipulating the sample. The technique is rapid, robust, and non-invasive and gives information on a possible fusion of liposomes during storage (Laouini *et al.* 2012).

HPLC-SEC is another technique for determining the size and morphology of liposomes. It can be used to separate and analyze liposomes dispersions as per a time-based resolution of hydrodynamic size. The mechanism leads to separations based on large particle elution before smaller ones. HPLC-SEC gives a high resolution of liposome populations and reduced sample size and reproducibility. It can be used to measure size distribution, stability, and permeability of liposome formulation. The accuracy of the results depends on the liposome's chemistry and the HPLC column packing (Pattni *et al.* 2015).

The latest liposome size distribution measurement technique is nanoparticle tracking analysis (NTA), which detects the liposomes by the light scattered when irradiated by laser lights. The dispersed liposomes

in their natural setting are transferred into a new transparent cell irradiated by a laser beam. A digital camera captures the liposomes' motion as they move in the medium and trace them from frame to frame. The particle movement rate is then related to the square equivalent hydrodynamic radius computed using the Stokes-Einstein equation. The instrument's software then calculates the liposome's size on an individual particle basis (Ohlsson *et al.* 2012).

3.6.3. Zeta Potential

The zeta potential of a liposome is the overall charge it acquires in a medium. It is a physical property that any particle in a medium exhibits. Liposomes can be positively charged, negatively charged, or neutral based on their compositions and attached ligands. Characterization of zeta potential is used to determine the stability of the liposome in a medium. Liposomes with neutral or low charges will fuse with time, but those with a higher negative or positive charge do not flocculate because of higher repulsive forces existing between them. In zeta potential measurement, a laser provides a source of light illuminating particles within the samples. Fluctuations in the scattered light then measure it as the liposomes moved due to the electric field's application. The movement of the liposomes corresponds to the type of charge the liposomes carry (Laouini *et al.* 2012).

3.6.4. Encapsulation efficiency

Encapsulation efficiency (EE) is defined as the total amount of encapsulant found in liposome solution versus the total initial input of encapsulant in the solution. The encapsulated drug is first separated from the carrier either by ultracentrifugation, dialysis, or column separation. The lipid membrane is then destroyed with organic phases like acetonitrile, methanol, or Triton X-100, and the released therapeutics is then measured. Depending on the drug's nature, techniques such as UV or fluorescence spectroscopy, gel electrophoresis, HPLC, UPLC, and LC-MS can be used (Pattni *et al.* 2015).

3.6.5. Phase behaviour

Thermal analysis is a group of techniques in which a property of the sample is measured against time or temperature. In contrast, the sample temperature in a specified atmosphere is heated or cooled at a fixed temperature change rate or held at a constant temperature. Thermal analysis procedures such as Thermogravimetric Analysis (TGA), differential scanning calorimetry (DSC), and X-ray diffraction (XRD) are the most frequently used methods of characterizing the phase behavior of liposomes. They both measure the thermal behavior and crystallinity of the liposomes (Singh *et al.* 2015). Since a change

of temperature and moisture occur by processing and storage, changes of the solid-state may have a considerable effect on activity, toxicity, and stability of liposomes.

DSC is used to determine the nature and speciation of crystallinity within liposomes by measuring glass and melting point temperatures and their corresponding enthalpies. It contains a sample cell and a reference cell that is maintained at the same temperature. They are raised at the same temperature in a controlled style that they are kept at the same temperature, and the power supplied to heat the cell is monitored by this process. Once the sample cell undergoes a phase transition, the energy needed to heat the two cells differs. The power required to keep both cells at the same temperature is measured and converted to give an output of heat capacity versus temperature, which is analyzed to determine the transition temperature, Tm, and the calorimetric enthalpy of transition, ΔHcal. DSC is the most commonly used thermal analysis technique in characterizing lipid-based materials in terms of polymorphism, glass transition, melting and crystallization behavior, amorphous and crystalline states (Durowoju *et al.* 2017).

TGA is a technique used to measure a sample's weight against temperature or time while under controlled heating or cooling environment. It is calibrated for a linear rise in temperature against time. TGA's experimental outcome corresponds to a mass loss curve showing the profile of the weight loss versus temperature. This is followed by a derivative curve known as DGT that shows the decomposition process of the sample been analyzed (Giron 2002).

XRD is used to determine the necessary structural information of material by showing its crystalline nature. The XRD measurement of crystalline compounds gives a diffraction pattern consisting of a well-defined, narrow, sharp, and substantial peak. Amorphous materials do not provide clear peaks; instead, the pattern has noise signals, unclear peak, or some short order bump. It takes advantage of X-rays to see through the material and allows for collecting information under the atomic structure level. The peak intensities are determined by the distribution of atoms within the lattice. XRD instrument is easy to operate, reliable, and cost-effective because of its accessible data collection, processing, interpretation, and maintenance. It is useful in characterizing polymorph, monitoring nanoparticles' stability, and method development and validation in pharmaceutical industries (Chauhan 2014).

3.6.6. *In vitro* drug release

In vitro release study is performed using the dialysis tube diffusion technique to evaluate the release profile of the therapeutic from the carrier. This method involves enclosing the formulation into a cut off dialysis bag of known molecular weight. Some aliquots of liposomes are put into dialysis bag, tied, and dropped in the receptor with the dissolution medium maintained at 37°C closed system under continuous magnetic

stirring to mimic an *in vivo* environment. Sink condition must be maintained throughout the experiment. Samples are taken at various time intervals and analyzed using HPLC or UV/fluorescence spectroscopy. The release profile is plotted to estimate the drug released by the liposome carrier (Laouini *et al.* 2012).

3.7. Applications of liposomes

The field of liposomes research has expanded tremendously in the past decades. It is now easy to formulate a wide range of liposomes of varying sizes, lipid compositions, surface morphology, and charges to suit the specific applications for which they are projected. The surface of the liposomes can be modified by choosing lipid components or binding and covalent linkage of glycoproteins and synthetic polymers to suit varying applications (Banerjee 2001). Liposomes can carry different drugs and substances, and this has made their applications very widely. It can encapsulate antimicrobial medicines, anti-cancer drugs, anti-fungal agents, vaccines, peptides, genetic materials, and enzymes. Most of its applications are discussed below.

3.7.1. Applications in drug delivery

The encapsulation of a wide range of drugs in liposomes has resulted in remarkable increases in therapeutic indices, both in preclinical models and in clinical applications, compared to their non-liposomal forms (Sharma Vijay *et al.* 2010). Some specific uses of liposomes in drug delivery are briefly described below.

3.7.1.1. Applications in anti-cancer therapy

Anti-cancer drugs have been encapsulated in liposomes for systemic delivery to reduce its toxicity when administered alone or to increase its circulation time and efficacy. The accumulation of liposomes into solid tumors is possible due to contrasts between healthy and cancerous tissue. Tumors are generally dependent on an increased blood supply over normal tissue because of the high turnover of neoplastic cells. Furthermore, the endothelium is often more permeable than standard endothelial linings. This means that can liposomes diffuse into the interstitium of solid tumors. At the same time, the liposomes are retained in the tumor tissue due to reduced lymphatic drainage. This increased accumulation is often referred to as the “enhanced permeability and retention effect” (EPR). Small liposomes, slightly below 100 nm in diameter, can circulate in the blood, reaching specific targets such as a solid tumor. Anthracycline is anti-cancer drug that intercalate into the DNA and kill rapidly dividing cells found in tumors, hair, gastrointestinal mucosa, and blood cells, making them very toxic. When these drugs are

encapsulated in liposomal formulations, their acute and chronic toxicities have been reduced to about 50% compared to the free drugs (Muggia 2001). However, the efficacy was reduced in some formulations because of the reduced bioavailability of the drug when the tumor was not located in the mononuclear phagocytic system's organs. The continued release effects of some drugs when encapsulated in liposomes also enhanced the drugs' efficacy because of the prolonged presence of the therapeutic concentrations in the circulation. Still, sequestrations of the drugs into the mononuclear phagocytic tissue system reduce the effectiveness of some drugs (Akbarzadeh *et al.* 2013). Liposome-based chemotherapeutics used in cancer treatment, such as breast cancer, can improve an entrapped drug's pharmacokinetics and pharmacodynamics. It can deliver the drug to the target tissue in the body, reducing off-target toxicity, and increasing therapeutic efficacy.

3.7.1.2. Applications in anti-microbial therapy

Liposomal formulations have been used to deliver therapeutics in infective conditions like malaria, leishmaniasis, and several fungal infections (Banerjee 2001). Glucose or galactose entrapped in liposomes on intravenous injection has been shown to prevent the presence of erythrocytic forms of *Plasmodium berghei* in mice injected with sporozoites (Alving *et al.* 1979). One of the best results reported in human therapy are liposomes encapsulating amphotericin B in antifungal therapy. This drug is used to treat fungal infections, which often work in parallel with chemotherapy, the immune system, and AIDS, which is usually fatal and toxic. Still, its encapsulation in liposomes has reduced the toxicity (Akbarzadeh *et al.* 2013). Many liposome encapsulating antivirals have also been shown to reduce toxicity.

3.7.1.3. Application in diagnosis

Liposomes are also used in therapeutic imaging as a diagnostic tool and for monitoring of disease treatment. Echogenic liposomes that entrap contrast agents have been used in diagnostic X-rays and nuclear magnetic resonance imaging (NMR). Theranostics is an area of diagnostic that employs liposomes co-loaded with drug and imaging agents for drug delivery and imaging measurements of the effectiveness of the drug release and the therapeutic effects (Pattni *et al.* 2015). Liposomal formulation encapsulating both gases and therapeutic agents would therefore be responsive to ultrasound and exhibit ultrasound-triggered release. It has been demonstrated that gases such as nitric oxide (NO) can be encapsulated into echogenic liposomes thereby producing a ‘theranostic’ agent with both echogenic and bioactive gas-delivery characteristics (Huang *et al.* 2009).

3.7.2. Application in analysis.

Liposome formulations have been used in various analytical processes like liquid chromatography, immunoassays, and biosensors. Liposomes have a large surface area and larger encapsulation volume than some analytes; this is advantageous in broadening the signal intensity by entrapping large amounts of signaling molecules in the bilayer. Liposomes also behave like a biological membrane; used in analyzing the drug/ biomolecule/ microbe interactions with the membrane to be reproduced. Furthermore, liposomes have been used as models to examine the partitioning of drugs within phospholipid bilayers and the effects of free ions, membrane-bound detergents, and fatty acids on the partitioning. The applications of liposomes have stretched to many analytical areas like detection of analytes in samples, high-throughput screening of lead candidates, and clinical diagnosis (Pattni *et al.* 2015).

3.7.3 Applications in cosmetics

Liposomal formulations have been exploited in the delivery of ingredients in cosmetics. Liposomes are used in dermatology because they can enclose many different biological materials and deliver them to the epidermal cells. Hydrated lipids help in reducing skin dryness, thereby stopping early aging of the skin. Liposomes can also supply and replenish lipids and linolenic acid to the skin. Liposomes have also been used in hair loss treatment. Many liposomal formulations have been available since 1987, ranging from pastes used as a replacement for creams, gels, and ointments to products containing various extracts, antibiotics, and moisturizers. Sunscreens, long-lasting perfumes, aftershaves, lipsticks, make-up, and similar products are liposomal formulations in cosmetics, gaining market attention (Laouini *et al.* 2012). Anti-inflammatory agents, immunostimulants, and enhancers of molecular and cellular detoxification within liposomes could also prevent age spots, dark circles, wrinkles, and other clinical aspects of skin. The use of liposomes in nano cosmetology also has many advantages, including improved penetration and diffusion of active ingredients, selective transport of active ingredients, longer release time, more excellent stability of active ingredients, reduced unwanted side effects, and high biocompatibility (Karami *et al.* 2018).

3.7.4. Food application

Many liposomes applications in the food industry include controlling the release of flavor, developing new taste, improving food coloration, and enhancing its taste. Liposomes can encapsulate antimicrobials, flavors, antioxidants, and bioactive elements, protecting them from chemical and environmental degradations like enzymatic chemical changes and temperature and ionic differences and only release the entrapped particle at the required site. In the food production industry, liposomes have been used to

encapsulate enzymes to stabilize the enzymes against food manufacture processes and preserve them for a long time and maintain their beneficial effects in foods (Karami *et al.* 2018).

The sustained release process can be used in various fermentation processes in which the encapsulated enzymes can significantly shorten fermentation times and enhance the product quality. Liposomes are also used to preserve some food components like cheese and antioxidants like vitamins C and E. In other areas of agriculture and food production, biocides encapsulated into liposomes have shown superior action due to the elongated presence of fungicides, herbicides, or pesticides at minimal damage to other forms of life (Laouini *et al.* 2012).

3.8. Echogenic liposomes (ELIP)

Echogenic liposomes (ELIP) are lipid bilayer vesicles that encapsulate a gas within the lipid monolayer and entraps a therapeutic in the aqueous core. They have a broad size distribution range of 40 nm to 6 µm (Radhakrishnan *et al.* 2012). ELIPs are designed to release their payloads on exposure to ultrasound (US) (**Figure 1.13**). A unique property of liposomes for drug delivery allows both hydrophilic and hydrophobic substances to be entrapped together at the aqueous core and the lipid bilayers, respectively. When gas is entrapped into liposome to make it echogenic, it is presumed to behave like a hydrophobic drug because air settles at the bilayer of liposomal formulations. When this gas-carrying liposome also carries a therapeutic at the aqueous core, they are triggerable by ultrasound stimuli (Huang *et al.* 2008).

The mechanisms of US-mediated permeabilization of phospholipid membranes and drug release from liposomes have not been clearly explained in the literature. Still, the hypothesis is that the actions leading to drug release are that the rarefaction phase causes the expansion of the gas in the bilayer perturbing the monolayers bounding, including those in the adjacent bilayer (Huang *et al.* 2008). As the pressure continues to drop, the perturbation will surpass the elastic limit of the weakest surface. Along the line, the bilayer will tear, leading to the loss of some or all the loaded drugs depending on how fast it takes to reseal. An ultrasound stimulus transfers energy to the encapsulated gas bilayer in the ELIPs, leading to bilayer expansion and collapse, causing disruptions to the liposome bilayer membrane and release of the encapsulated materials (Huang *et al.* 2008).

In imaging, a contrast in ultrasound depends on the variation in acoustic impedance between the contrast agent and the nearby tissues. One of the vital properties of a contrast agent is the improvement of backscatter or echogenicity, and this happens because of the difference in density and sound velocity. A vascular ultrasound contrast agent (UCA) must have a solid, liquid, and gas dispersion in an aqueous medium compatible with the blood (Huang *et al.* 2002). All three dispersions have been utilized in varying

contexts. The enormous acoustic impedance difference comes from the diffusion of gases in an aqueous medium showing precise promise for generating high echogenicity (Huang *et al.* 2002). Echogenic liposomes may be prepared to target a particular disease tissue, especially the difficult to access cardiovascular system extending the diagnostic potential and pharmaceutical possibilities (Anwekar *et al.* 2011).

Optison™, for example, are particles containing air bubbles stabilized by albumin that have been used as contrast agents for echocardiographic imaging (Podell *et al.* 1999). A gas-filled lipid formulation has also been used, but a significant setback to some of the previously formulated UACs is that they are larger (above 2 µm), thus not allowing passage through the pulmonary tubes. To take care of this, novel formulations have been made using biocompatible perfluorocarbon emulsions with sizes ranging from 150-200 nm after extrusion. The diffusion of gas in the UCAs depends on the concentration and the type of gas in the surrounding fluid and the permeability of the UCA shell (Radhakrishnan *et al.* 2012).

Air (being a mixture of gases), perfluorocarbon gases (perfluoropentane, perfluorocyclobutane), nitrogen, oxygen, and argon, has all been entrapped in liposomes making it echogenic. According to a report by Huang *et al*. (Huang *et al.* 2008), the echogenic properties of air, perfluorocarbons gases, and argon were investigated, and it was discovered that argon gave higher or similar echogenicity as perflurocyclobutane. Argon been a less expensive, biocompatible, and highly available gas, was used to prepare echogenic liposomes in this research.

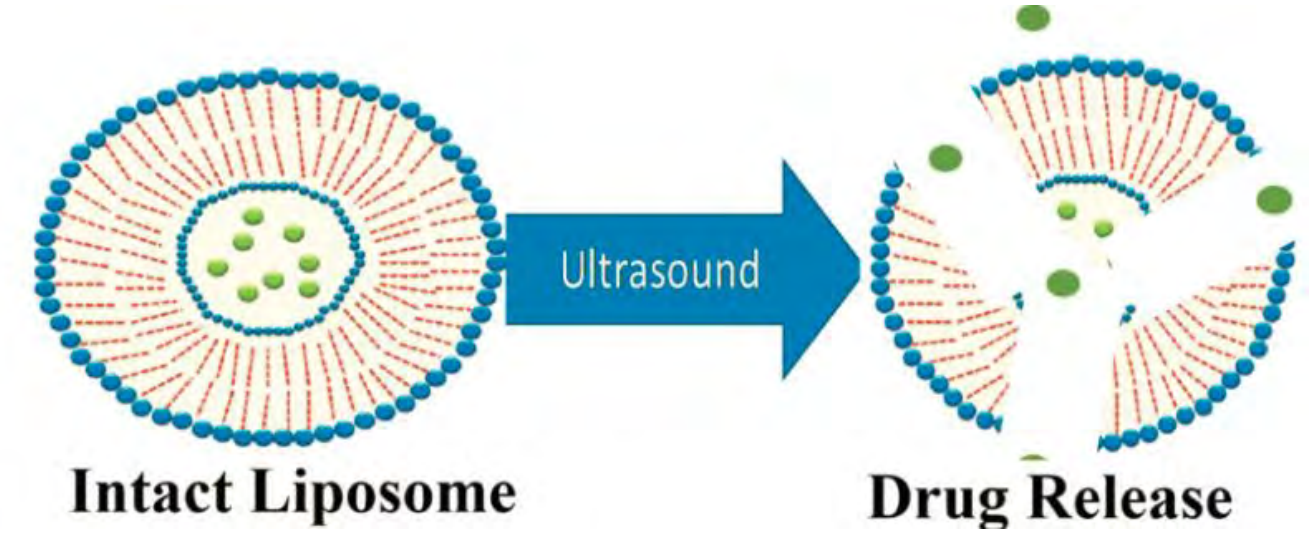

Figure 1.13. Illustration of echogenic liposomes releasing its payload when triggered with ultrasound.

3.8.1. Argon

Argon (Ar) is a noble gas element with atomic mass of 39.948 amu. It has demonstrated narcotic and

protective features that have proved useful in the medical field. It is a nonreactive gas that does not contain any biologically functional characteristics (Nowrangi *et al.* 2014). Argon has exhibited some features such as narcosis at hyperbaric pressures, including neuroprotective and organoprotective properties (Balon *et al.* 2002).

Argon has been used as a medical gas both as a narcotic agent during the study of high-pressure effects of naturally occurring gases during sea diving, which shows that argon produced a potent narcotic effect at high pressure (> 10 atm) when compared to helium and nitrogen. This narcotic property was more physical than chemical since argon is nonreactive in the body (Nowrangi *et al.* 2014). Argon has been used as an ischemic neuroprotective agent. It has helped increase the recovery of patients who have experienced neurological damage in cases like physical trauma. Argon has been used as protectants for essential organs like kidney, liver, heart preserving their functions and quality before transplant. It has also been used in medicine as a surgical tool. Argon plasma coagulation (APC) is a non-contact procedure that uses high-frequency stimulation of argon plasma to seal nearby tissues and stop bleeding by coagulation within surgery sites (Reich *et al.* 2004).

All the above-stated functionalities of argon gas in medicine, coupled with its high availability and cost-effectiveness, resulted in its use in the formulation of echogenic liposome for the US triggered drug delivery in this research.

4. Reports on ultrasound triggered anti-cancer drug delivery and liposomes.

Ning *et al*. in 1994 showed that ultrasound-mediated hyperthermia increased doxorubicin (Dox) release from long-circulating liposomes while enhancing its anti-tumor activity. They reported that by increasing the temperature from physiological temperature to 41°C, the rate of Dox release increased by six times after an hour of ultrasound exposure at 2 W/cm^2. The accumulation of Dox in RIF-1 cancer cells increased ten times higher when encapsulated in liposomes at 42°C than when introduced as a free drug at a physiological temperature (Ning *et al.* 1994).

Schroeder *et al.* in 2009 investigated the efficiency of low-frequency ultrasound (LFUS) (20 kHz) and high-frequency ultrasound (HFUS) (1 and 3 MHz) mediated release of PEGylated liposomes (Doxil®/ Caelyx™). They found out that after half an hour of exposure to LFUS, 85% of the Dox was released in saline solution, while 61% was released in human plasma. They observed a decrease in 58% and 5%, respectively, when exposed to 1 MHz HFUS and more decrease when 3 MHz was applied. These difference in the rate of release was hypothesized to happen because of cavitation. In contrast, the

differences between the release in saline and human-plasma were explained by the fact that plasma proteins absorb some acoustic energy, thus reducing the number of cavitation events (Schroeder *et al.* 2009).

Huang and MacDonald in 2004 monitored the release of calcein from echogenic liposomes composed of phosphatidylcholine, phosphatidylethanolamine, and phosphatidylglycerol through the application of 1 MHz US, at the intensity of 2 W/cm^2 for 10 seconds. The echogenic liposomes were prepared in the presence of mannitol, a cryo-protectant by freeze-drying method. This condition increased the encapsulation efficiency by 15%, and they observed that the addition of diheptanolyphosphatidylcholine in liposomes made it sensitive to ultrasound triggering with significant drug release (Huang and MacDonald 2004).

Frenkel (2008) investigated the ability to release drugs from thermo-sensitive liposomes by applying high intensity focused ultrasound (HIFU), a non-invasive technique that allows targeted treatment of a broad range of diseases by focusing high-frequency ultrasonic beams to form a high energy focal point at a particular tissue. The membranes of these thermo-sensitive liposomes are composed of lipids with phase transition temperature T_m within the range of 40-45°C. The liposomal permeability increases during the phase transition, disrupt the closed and ordered packing of the lipid bilayer, and creates extra volume allowing the drugs to move within the bilayers from the aqueous core to the liposomal membrane (Frenkel 2008).

Tata and Dunn in 1992 studied the relaxation kinetics of membranes of single and multilamellar liposomes comprising of DMPC or DPPC by determining the absorption of ultrasound and the velocity in the formulations, using 1.42 MHz US for DMPC and 2.11 MHz for DPPC at T_m of 23.2 and 41.4°C respectively. They discovered that the primary ultrasonic absorbance at the solid ordered to liquid disordered (SO to LD) lipid transition phase and the US does not absorb below the phase transition. That the US was hardly absorbed by the membrane implies that the drug release below the phase transition temperature may be attributed to mechanical or thermal effects and not ultrasonic absorbance by the lipid bilayer (Tata and Dunn 1992).

Schroeder *et al.* in 2007 examined the potential of low-frequency ultrasound (LFUS) to control the release of ions and drugs exhibiting varying physical and chemical properties like molecular weight, solubility, and pH, from liposomes. This result showed that release follows first-order kinetics, depending on the actual irradiation time including the concentration gradient of the drug between the intra-liposomal aqueous compartment and the bilayer membrane. They hypothesized that LFUS induces the formation of transient pore-like disruption to the vesicle membrane that reseals on withdrawal of LFUS exposure

(Schroeder *et al.* 2007)

Papahadjopoulos *et al* in 1991 examined the use of stealth (PEGylated) liposomes. They investigated the pharmacokinetics and therapeutic efficiency of encapsulated doxorubicin and epirubicin in mice models with lymphomas and colon cancers. There was a significant increase in the therapeutic efficacy of both drugs from their results. There was a reduction in the size of the tumor in the laboratory mice placed on the treatment of the new formulation compared to the tumor size of non-treated mice or those treated with the free form of the drugs. They also observed a lower uptake in other organs like the liver and spleen, with drugs accumulating preferentially in the targeted tumor tissue (Papahadjopoulos *et al.* 1991).

Lentacker *et al.* in 2010 compared the US-induced delivery of Dox entrapped in liposomes and Dox-liposomes-containing microbubbles. The latter was formulated by attaching biotinylated Dox-containing liposomes to the surface of a biotinylated lipid microbubble containing perfluorobutane by using an avidin molecule. The *in vitro* investigation using a cancer BLM cell line reviewed that as 1 MHz was triggered this microbubble-liposome formulation, there was a two-fold cell death compared to the regular liposome formulation. This was attributed to an improved cellular uptake of the Dox released from the system by the action of the US, followed by an accumulation of Dox in the nuclei of the cancer cell. There was a distribution in the cytoplasm, and the cell's nucleus when regular liposome entrapped Dox was used. They hypothesized that the cells' enhanced uptake resulted from the permeability of the cell membrane by ultrasound due to the collapse of the cell membrane by the microbubbles under the US action. The microbubble-liposome-US formulation appears to be promising in improving the *in vivo* efficacy of Doxil® and simultaneously causing fewer side effects (Lentacker *et al.* 2010).

Thomas and Lin in 2003 did calcein release studies to check the susceptibility of PEGylated liposomes to 20 kHz LFUS US. They noticed that these liposomes, like phosphatidylcholine (PC) liposomes used as a control, were not sensitive to ultrasound below an intensity threshold of 2 W/cm^2. Still, above this threshold, the stealth liposomes exhibited 10-fold responsiveness to the US, resulting in higher permeabilization of the vesicle membrane. They arrived at the conclusion that PEG-lipids and those of its kind aids the power of LFUS to permeabilize 100 nm unilamellar liposomes as a result of the development of pores in the vesicle membranes called nanoporation, destabilization of membranes, or both (Lin and Thomas 2003).

Ueno *et al.* in 2011 studied the *in vivo* effects of a mixture of Dox, acoustically active liposomes and ultrasound, in a mice model infected with osteosarcoma (C3H female mice with LM8 tumor). They separated the mice into eight groups, (i) untreated mice; (ii) free Dox (1 mg/kg); (iii) Dox (1 mg/kg) +AAL+US; (iv) free Dox (5 mg/kg); (v) free Dox (1 mg/kg) +US; (vi) AAL alone; (vii) US alone; and

(viii) AAL+US. Ultrasound was used three times in nonconsecutive days, in groups (iii), (v), (vii), and (viii) with a frequency of 2 MHz, a power density of 2 W/cm2, a 50% duty cycle, a burst rate of 2 Hz, and a cycle duration of the 60 S. They observed in the result that the mice treated with the mixture of Doxil® and US [group (iii)] exhibited the highest survival, uptake of drugs, and tumor regression rate, notwithstanding that the lowest concentration of Dox, (1 mg/kg) being five times lower the concentration used in the group (iv). There was no variation in the hepatic Dox concentrations in groups (iii) and (v), showing a decrease in the reticuloendothelial system's drug uptake. The researchers attributed it to the formulation of Dox-AAL liposomes, and concluded that Dox was mixed instead of sealed inside the liposomal formulations (Ueno *et al.* 2011).

Rizzitelli and co-workers in 2014 encapsulated paramagnetic drugs in liposomes. They used pulsed low-intensity non-focused ultrasound to release the drug from the vesicle and increase its accumulation *in vivo* on mice infected with syngeneic B16 melanoma. They also used magnetic resonance imaging (MRI) to investigate the location of these magnetically sensitive molecules. They observed a 35% rise in magnetic responsiveness when exposed to 1.5 MHz of ultrasound for 2 mins (Rizzitelli *et al.* 2014).

In a recent work by Aryal *et al*. in 2013 on glioma-bearing mice that they separated into four groups, the first group were treated with Doxil® and triggered with 700 kHz focused ultrasound, group 2 was only treated with Doxil® alone, the third group was treated without Doxil® or liposome but triggered by ultrasound, and the final group served as the control, without treatment. Their main obstacle in the investigation was to design a drug delivery system that can cross the blood-brain-barrier (BBB). They discovered a considerable increase in the survival rate and a significant statistical regression in the size of the tumor in group one compared to others, proving progress in BBB's temporal disruption by the exposure to multiple focused US. Many adverse side effects were observed in the treatment like damage to the adjacent brain tissue, toxicity to the skin, and intratumoral hemorrhage in one of the rats treated with a combination of Doxil® and ultrasound and these were the limitations of the study(Aryal *et al.* 2013).

Afadzi *et al*. in 2013 examined the effects of 300 kHz ultrasound and microbubbles on the cellular uptake of Dox entrapped in dierucoyl-phosphatidylcholine (DEPC) liposomes and fluorescein-isothiocyanate (FITC)- dextran by HeLa cells. They tried to understand the mechanism leading to the uptake, whether it was ultrasound stimulation or endocytosis. They observed an increase in the cellular uptake by liposomes and dextran under the combination of microbubble and ultrasound, signifying an extracellular disruption of liposomes and drug uptake. On further analysis, they found out that endocytosis and sonoporation were part of the uptake mechanism (Afadzi *et al.* 2013).

In all these reports, none has used crude soy lecithin, a readily available and inexpensive phospholipid to

produce echogenic liposomes neither has there been any report where they co-encapsulate argon gas, also inexpensive and readily available gas in these liposomes. The use of these two components may lead to large scale industrial production of these nanocarriers and this is the gap this research is trying to address.

5. PROJECT JUSTIFICATIONS AND OBJECTIVES

5.1. Project justification

Most anti-cancer drug agents available today affect both diseased and healthy tissues resulting in many unwanted side effects. Their uncontrolled release has led to prolonged and higher consumption of the therapeutics causing higher drug resistance and economic waste. This reason and more has increased the demand for the development of new drug delivery systems such as the “new smart” DDS that can be targeted directly to diseased tissues and organs and triggered to release the therapeutics at the required site using internal and external stimuli (Ahmed *et al.* 2014).

An outstanding challenge to the improved tumor delivery of liposomes showing high drug retention is that the availability of drugs to tumor tissues may be limited. Encapsulated drugs must be released as soon as possible after the carrier has accumulated in the interstitial tumor space in other for the drugs to be absorbed by the nearby neoplastic cells. A fast-growing tumor also requires a fast drug release mechanism to match up with tumor cell division rates. Triggered release of the liposomal drug formulations within cancer might significantly improve drug availability and improved therapeutic efficacy (Moosavian *et al.* 2018).

Colorectal cancer is still the third most diagnosed cancer, and the second leading cause of death in the world. 5-Fluorouracil, either alone or in combination with liposomal formations, is a primary chemotherapeutic agent in treating the disease. An improvement in its delivery mode to the tumor tissues for enhanced therapeutic efficacy and reduced toxicity is required. This justifies its entrapment in a stimuli-responsive vesicle and triggering its release with ultrasound.

A significant drawback to the use of liposomal formulations has been its high economic cost due to the expensive nature of the synthetic or purified natural phospholipids used in its production (Huang *et al.* 2014). Most of the gases entrapped in liposomes to make them responsive to ultrasound stimulation are either expensive or not readily available, limiting the formulations of echogenic liposomes that can be used for triggerable release (Sierra *et al.* 2015). Using argon gas as an alternative has proved successful because of its biocompatibility, bioavailability, and inexpensive nature.

5.2. Project objectives

The aim of the research was to develop a smart stimuli-responsive echogenic liposome for ultrasound triggered drug delivery of 5-fluorouracil using crude soybean lecithin and argon gas.

The specific objectives of the research were to:

i. Develop and formulate liposomes for encapsulation of 5-fluorouracil (5-FU)
ii. Validate the HPLC method for the quantification of 5-fluorouracil (5-FU)
iii. Prepare and characterize 5-FU loaded liposomes.
iv. Prepare and characterize 5-FU loaded echogenic liposomes.
v. Investigate the release of the 5-FU loaded echogenic liposomes with ultrasound (US).
vi. Evaluate the short-term stability of the formulation.

CHAPTER TWO

FORMULATION OF 5-FLUOROURACIL LOADED LIPOSOMES

Ezekiel Charles Izuchukwu, Alain Murhimalika Bapolisi, Roderick Bryan Walker, Rui Werner Maçedo Krause (2020). "Ultrasound-Triggered Release of 5-fluorouracil from Soy Lecithin Echogenic Liposomes"

(A manuscript with the above title has been accepted for publication in the Journal of Pharmaceutics, based largely on the results from this Chapter and chapter three. Professors Walker and Krause were the study supervisors, and Mr Bapolisi is a former MSc student who also did some previous studies on the development of liposomes from soy-based lipids.)

1.INTRODUCTION

Liposomes formulations are rated among the best nanocarriers. They are one of the best drug delivery systems (DDS) because they are biodegradable, non-toxic, and non-immunogenic. Their varying compositions, method of preparations, surface charge and colloidal characteristics can be utilized in various applications (Ahmed *et al.* 2014). Liposomes can also be prepared to be responsive to external stimuli. By entrapping a gas and having an aqueous solute they are sensitive to ultrasound irradiation and the solute that is a water soluble drug can be released by this slight exposure (Huang and MacDonald 2004).

Colorectal cancer is one of the major dreaded and life threatening disease in the world today and the second leading cause of cancer related death (Karan *et al.* 2019). 5-Fluorouracil (5-FU) is among the first line cytotoxic drug used in treatment of colorectal cancer but as a result of lack of site specificity, the drug does not get to the target site in therapeutic concentrations. This results to increase in dose size leading to several toxicities. Entrapping the drug in echogenic liposomes can deliver it to the colon on a higher concentration when externally triggered by ultrasound (Ahmed *et al.* 2014).

The specific objective of this chapter was to formulate a 5-FU loaded liposomes with high encapsulation efficiency and required features for its responsiveness to ultrasound triggering. Crude soybean lecithin, a natural phospholipid was used because it is readily available and cost-effective. The encapsulation of 5-FU in liposomes was shown in the graphical illustration in **Figure 2.1.**

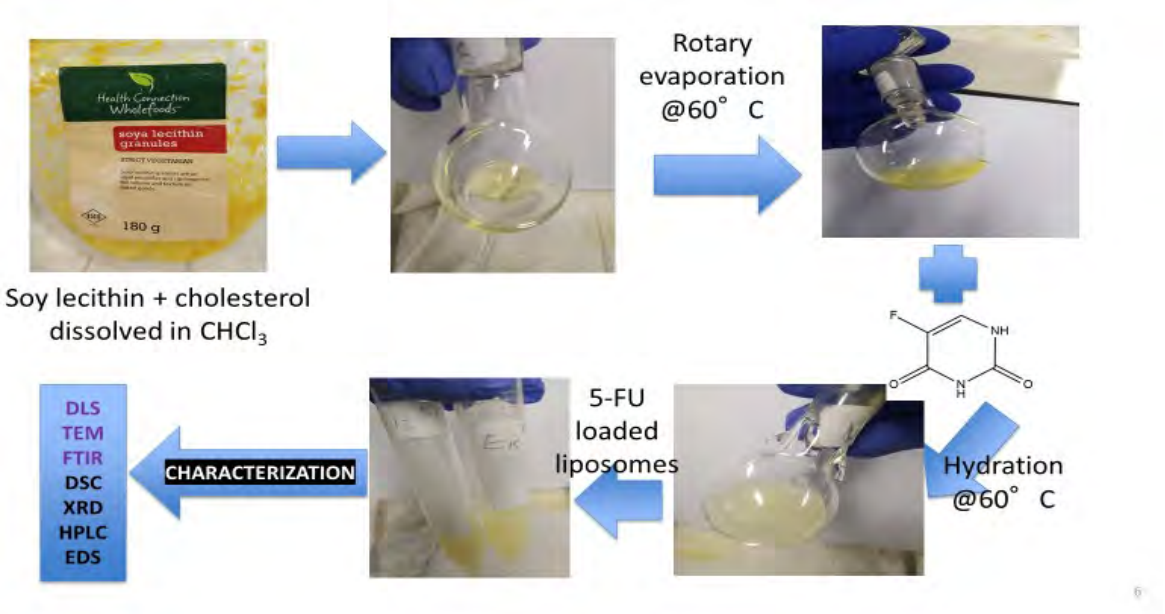

Figure 2.1. Flowchart showing the formulation of 5-FU loaded liposomes using soybean lecithin.

2. EXPERIMENTAL SECTION

2.1 Materials and Equipment

The crude soybean lecithin granules used in this work were purchased from Health Connection Wholefoods (USA). From the manufacturer's information, the 100 g of this granule comprises 23 g of phosphatidylcholines, 14 g of phosphatidylinositol, 35 g of unsaturated fats, 13 g of saturated fats, 8 g of glycaemic carbohydrates, 0.11 g of sodium, and about 2940 KJ of energy. Cholesterol was from Carlo Erba / Divisione Chimica (Italy). 5-Fluorouracil, mono and dibasic sodium phosphate, methanol, acetonitrile (HPLC grade), and chloroform were purchased from Sigma Aldrich (Germany) and were used as procured without any purification.

The following equipment was used in the research; Rotary evaporator (Buchi R-205 Switzerland), Bath sonicator (909-digital spellbound), Dynamic light scattering (Zetasizer nanoZEN Malvern instrument), Centrifuge (MSE – Mistral 1000), HP1100 Agilent LC-MSD high-performance liquid chromatography (HPLC), A Zeiss Libra-120 KV Transmission electron microscopy (TEM), PerkinElmer Spectrum 100 Fourier transform infrared spectroscopy (FTIR), A PerkinElmer TGA-4000 instrument and Differential scanning calorimeter (DSC- 6000, Perkin Elmer), XRD D8 Discover instrument (Bruker, USA), Bruker

AMX 600 MHz Spectrometer (Switzerland), Energy dispersive spectroscopy (VEGA TESCAN), LABCONCO FreeZone® 6 Liter Benchtop Freeze Dry System (USA).

2.2. Methods

2.2.1. Preformulation assessments

2.2.1.1. Drug-excipients compatibility study

The successful formulation of an effective and stable drug-encapsulated liposome depends on the careful selection of excipients. This results in more comfortable or proper administration, improve patient compliance, promote release and bioavailability of the drug, and shield it from degradation (Mura *et al.* 1998).

5-FU was physically mixed with the lipid components in the ration of 1:1 to make up a total mass of about 30 mg. Most of the techniques used in the thermal and solid-state analysis of pharmaceutical components like TGA, DSC, and FTIR were employed to evaluate the physicochemical stability of the physical mixture (Giron 2002).

DSC. The physicochemical interactions of the mixture of 5-FU and lipid components were evaluated and compared with pure 5-FU. The physical mixture (3 mg) was placed in an aluminum pan and heated from 30-300°C in a nitrogen-filled atmosphere using empty aluminum as reference. The heat flow rate was 10°C/min, and the nitrogen gas flow rate was set at 20 mL/min. The obtained data were analyzed using the DSC Pyris manager series software.

TGA. The physical mixture's thermal behavior was examined and compared with pure 5-FU using thermogravimetric analysis (TGA). About 2 mg of each sample was heated in a nitrogen-filled environment. The heat range was from 30 - 600 °C at a flow rate of 10 °C/min. The inert nitrogen gas flow was set at 20 ml/min. The data were obtained and analyzed using the software TGA Pyris series.

FTIR. The drug and excipients' characteristic features, the functional groups present, and any possible interaction in the physical mixture were evaluated. Eight scans were performed in each of the samples in the frequency band of 650-4000 $cm^{-1,}$ and the data obtained were analyzed using the FTIR spectrum software.

2.2.1.2. Preparation and evaluation of empty liposomes

2.2.1.2.1. Preparation of empty liposomes

Empty liposomes were prepared and evaluated in other to arrive at the best parameters and processes for encapsulation of 5-FU by thin-film hydration method. The empty liposomal formulations were prepared in two batches and characterized for particle size distribution, polydispersity index, and zeta potential. Two factors that could enhance the encapsulation of 5-FU in the formulations were selected in each of the batches. Minitab 17, the general statistical software, was used for the experiment's full factorial design to generate 27 possible preparations equating each to a liposomal formulation. Each set of the liposomal formulations characterized allowed considerations for factors to use in formulating the next batch. The best-characterized formulation was used to encapsulate 5-FU. **Table 2.1** illustrates the factors considered in the formulation of empty liposomes.

Table 2.1. Factors considered on preparations of the two batches of liposomal formulations C1 & C2.

Series	**Factors**	**Levels**		
		1	**2**	**3**
C1	Lecithin-cholesterol mass ratio	1:0	3:1	1:1
	Lipids-aqueous phase ratio	1:5	1:10	1:20
	Hydration time (min)	30	60	90

C2	Sonication time	10	20	30
	Voltex time (min)	5	10	15
	Hydration time	30	45	60

The thin-film hydration method was described by Nkanga *et al*. (Nkanga *et al.* 2017) with slight modifications according to the factors in considerations.

In summary, a total mass of 100 mg of crude soybean lecithin and cholesterol was dissolved in 1 ml of chloroform in a clean 25 ml round bottom flask. The dissolved organic mixture was dried at 60 °C using a rotary evaporator (Buchi Rotavapor R-205, Switzerland) set at 200 rotations per minute (rpm), under pressure of 30 mm Hg for 10 minutes. The dried thin film formed was removed and stored overnight in a desiccator at room temperature. HPLC grade water was added to the various formulations according to the experimental designs' ratios and hydrated at 60 °C under magnetic stirring at 400 rpm and the respective times in the design. The formulation was then vortexed according to the time indicated and sonicated using bath sonicator set at 60 °C. The obtained liposomal formulation was stored in a refrigerator at 4 °C for further analysis.

2.2.1.2.2 Characterization of empty liposomal formulations

The empty liposomal formulations were characterized by dynamic light scattering (DLS) to evaluate the particle size, polydispersity index, and zeta potential. The morphology of the particles and their interaction was examined using transmission electron microscopy (TEM).

Particle size, PDI, and Zeta Potential. HPLC grade water was used to dilute an aliquot of the liposomal formulation to make it more transparent. ZEN-3600 MAL1043132 (Malvern Instruments) was used at a scattering angle of 173° and a temperature of 25°C. For higher accuracy, it was measured in triplicate using the ordinary cuvette for particle size and polydispersity index and the capillary cuvette to measure Zeta Potential.

Transmission electron microscopy. A drop of the diluted liposomal dispersion was dropped

in a copper grid, and the excess liquid was absorbed using filter paper. It was allowed to dry all for 24 hours and then characterized using the Zeiss Libra-120 KV TEM instrument.

2.2.1.3. Validation of 5-fluorouracil quantification

Validation studies were done to arrive at the most suitable HPLC quantification for 5-FU under the most favorable analytical procedures. The validation was done according to the International Conference on Harmonization (ICH) guidelines. The validation parameters investigated were linearity, accuracy, inter- and intra-day precision.

The chromatographic system used was an Agilent HP1100. A reverse-phase HPLC analysis was adopted using Luna LC Column 5µ C18, 100 Å, 250 × 4.6 mm. The mobile phase consisted of a mixture of HPLC grade methanol and water (in the volume ratio of 80:20) in an isocratic elution mode at a flow rate of 0.5 mL/min, the temperature of 30°C, UV wavelength of 266 nm, and the injection volume was 20 µL. A 2000 µg/mL stock solution of 5-fluorouracil was prepared by dissolving it in HPLC grade water. A serial dilution of seven different concentrations (1.25, 2.50, 5.0, 10.0, 12.5, 25.0, and 50 µg/mL) was made from the stock solution and filtered with 0.22 µm Millipore syringe filters before injection into the HPLC system.

The validation study lasted for five days, with three times injection for each concentration except the standard solution 10 µg/mL injected six times daily. Fresh solutions were prepared daily. Each elution lasted for 4 minutes, with the retention time for 5-FU observed at 1.5 minutes. The peak areas were recorded, and its average plotted against their respective concentrations to obtain a calibration curve used to determine the linearity range, regression equation, and correlation coefficient. The accuracy, repeatability, and intermediate precision were calculated by evaluating the percentage recovery and relative standard deviation (RSD) (Masato *et al.* 2012).

2.2.2. Preparations of 5-FU loaded liposomes.

To limit the level of exposure to 5-fluorouracil and the side effects associated with it, uracil, a pyrimidine nucleobase, and a pyrimidone was first encapsulated in the liposomal formulation as a prodrug. Uracil is a naturally occurring pyrimidine present in RNA, its base pairs with adenine, and is replaced by thymine in DNA. The statistical software (Minitab 17) was used to generate a full factorial design of the experiment for 9 levels of parameters for considerations.

This resulted in 27 different uracil encapsulated liposomal formulations. The experiment was done in triplicate, and the best formulation with the highest encapsulation efficiency was selected for 5-FU encapsulation.

2.2.2.1. Encapsulation of uracil

The methods used in preparing the empty liposomes during the pre-formulation investigations were replicated in formulating drug-free liposomes for uracil encapsulation. In summary, crude soybean lecithin and cholesterol mass ratio of 3:1, comprising 75 mg soybean lecithin and 25 mg cholesterol, were weighted, and dissolved in 1 mL of chloroform in a clean 25 mL round bottom flask. The dissolved lipids were dried in a rotary evaporator set at 60 °C under reduced pressure of 30 mm Hg and 200 rpm for 5 minutes. The dried liposomal film was stored in a desiccator overnight at room temperature for the complete drying. The following quantities (25 mg, 50 mg, and 100 mg) of the white powdered uracil were dissolved in 2 mL of phosphate buffer (pH 7.4) and added into the dried thin film lipids by passive loading. HPLC grade water was added to make up the volume according to the lipids-aqueous mass ratio and hydrated under continuous heat and stirring for 60 minutes at 60 °C and 400 rpm. The dispersion passed through 2, 4, and 6 freeze-thawing circles by dipping them in liquid nitrogen at -196° C for 5 minutes and allowing them to thaw at room temperature for 15 minutes. After that, they were allowed to incubate for 1 hour each at room temperature and placed in a bath sonicator for 30 minutes for homogenization, and uracil loaded liposomal formulation was produced. The colloidal dispersion was transferred into a 50 mL centrifuge tube, and HPLC grade water was used to make up the volume to 20 mL for centrifugation. For comparison, pure uracil without lipids was treated in the same manner and used as a positive control, while empty liposomal formulation without uracil was used as a negative control.

Uracil was passively loaded in all the 27 liposomal formulations, including their replicates. The optimal formulations with the best encapsulation efficiency were selected and its method of formulations replicated for the encapsulation of 5-FU.

2.2.2.2. Determination of encapsulation efficiency

The liposomal formulation entrapping uracil was centrifuged for 20 minutes using MSE Mistral-1000 low-speed centrifuge set at a relative centrifugal force (RCF) of 1020 g. The pellets (unencapsulated uracil) were separated, and the supernatants were further transferred into 1.5 mL Eppendorf tubes and centrifuged using Eppendorf 5414 micro high-speed

centrifuge set at RCF of 15600 g for 20 minutes at room temperature of 25 °C. The supernatant was decanted off, and the pellets containing the liposomes were rinsed three times with 1mL HPLC grade water to separate the remaining uracil molecules. The separated liposomes were freeze-dried for further analysis using the Labconco Benchtop freeze dry system. The supernatant and the positive control were analyzed for uracil content using the already established HPLC method. After sonication for 20 minutes for homogenization, a 1/100 dilution was made of the various formulations and filtered using 0.22 μm Millipore filter, and 20 μl of each was injected in triplicate into the HPLC system following the already established validation method in **section 2.2.1.3**. According to the method described by Nkanga *et al.* (Nkanga *et al.* 2017), The amount of 5-FU incorporated into the nanocarrier was determined indirectly by gravimetric analysis after subtracting the amount of 5-FU not incorporated from the total known amount of drug added to the liposomes. The percentage encapsulation efficiency (%EE) was obtained using **equation 2.1** as used by Costa *et al.* (Costa *et al.* 2014)**.**

$$\%EE = \frac{mass\ of\ encapsulated\ uracil}{total\ mass\ of\ uracil\ used} \times 100 \qquad (2.1)$$

2.2.3. Characterization of uracil loaded liposomes.

2.2.3.1. Evaluation of particle size and zeta potential

The freeze-dried liposomal formulations (2 mg each) o were dissolved in HPLC grade water at room temperature, and a homogenous mixture was formed. The mixture was analyzed for particle size, PDI, and zeta potential according to the method described in **section 2.2.1.2.2.**

2.2.3.2. Morphology

The TEM analysis used to evaluate the morphology of empty liposomes in **section 2.2.1.2.2** was used to characterize the freeze-dried liposomal formulation encapsulating uracil.

2.2.3.3. Differential scanning calorimetry

Pure uracil, uracil encapsulated liposomal formulation with the best %EE, and empty liposomes were analyzed to investigate their thermal behavior. The same procedure used in the drugs-

excipient compatibility study in **section 2.2.1.1** was followed here.

2.2.3.4. Fourier transform infrared

The functional groups present and their interaction in the freeze-dried uracil loaded liposomal formulation, the free uracil, and empty liposomes were evaluated. The procedure was as described in **section 2.2.1.1.**

2.2.4. Encapsulation of 5-FU

After evaluating the uracil encapsulated liposomes, the formulation with the best encapsulation efficiency was selected. The parameters used in its formulation were employed to formulate and evaluate liposomes that encapsulate 5-fluorouracil. The chosen parameters are as follows; crude soybean lecithin and cholesterol mass ratio of 3:1 (75 mg and 25 mg), lipids and drug mass ratio of 1:2 (100 mg of lipids and 50 mg of 5-FU), the aqueous volume of 20 mL HPLC grade water, and sonication time of 30 minutes. The procedures used in **section 2.2.2.1** for uracil encapsulation were also used to encapsulate 5-FU in liposomes. A positive control, pure 5-FU without lipids, and negative control, empty liposome, were also formulated for comparison.

2.2.4.1. Determination of encapsulation efficiency of 5-FU

The methods used in **section 2.2.2.2** to determine the encapsulation efficiency of uracil loaded liposomes were repeated in determining the encapsulation efficiency of 5-FU loaded liposomes, and the percentage encapsulation efficiency (%EE) of 5-FU was calculated from equation **2.2.**

$$\%EE = \frac{Mass\ of\ Encapsulated\ 5\text{-}FU}{Total\ mass\ of\ 5\text{-}FU\ used} \times 100 \qquad (2.2)$$

2.2.5. Characterization of 5-FU loaded liposomes.

2.2.5.1. Size, PDI, and Zeta Potential evaluation

As stated in **section 2.2.3.1**, 5-FU encapsulated liposomal formulations were analyzed for size,

polydispersity index, and zeta potential replicating the same procedure. The particle size distribution was confirmed by analyzing TEM images with ImageJ software.

2.2.5.2. Morphology

The 5-FU encapsulated liposomes were also evaluated for morphology and aggregation according to the methods described in **section 2.2.3.2**.

2.2.5.3. Thermogravimetric analysis

The thermal behavior of the 5-FU encapsulated liposomes, free 5-FU, and empty liposomal formulations were investigated using thermogravimetric analysis (TGA). About 3 mg of each formulation was heated in a nitrogen-saturated environment and the heat range was from 30 - 600 °C at a flow rate of 10 °C/min. The inert nitrogen gas flow was set at 20 ml/min. The data were obtained and analyzed using the software TGA Pyris series.

2.2.5.4. Differential scanning calorimetry

The methods described in **section 2.2.3.3** was repeated in DSC analysis of 5-FU encapsulated liposomes, free 5-FU, and blank liposomes.

2.2.5.5. X-ray diffraction (XRD)

The crystalline nature of the liposomal 5-FU, empty liposomes, and free 5-FU was assessed using XRD. The evaluation was done with a nickel filter and Cu-Kα radiation set at 1.5404 Å while running the scan at 2-Ɵ range 10° to 60°, the scanning speed was 1°/min, and the slit width was 6.0 mm.

2.2.5.6. Fourier transform infrared

Fourier transform infrared (FTIR) spectroscopy was used to evaluate the functional groups and the interactions in the 5-FU loaded liposomes, free 5-FU, and empty liposomes according to the procedures described in **section 2.2.3.4.**

2.2.5.7. Energy-dispersive X-ray spectroscopy

The surface elemental analysis of the freeze-dried 5-FU encapsulated liposomal formulation was carried out and compared with the free 5-FU and blank liposome using the Energy-dispersive X-ray spectroscopy (EDX).

2.2.5.8. Proton nuclear magnetic resonance (^{1}H NMR)

^{1}H NMR spectroscopic characterization of the liposomal 5-FU was done and compared to the proton spectrum of the empty liposomes and the free 5-FU. The freeze-dried 5-FU liposomes (20 mg) was dissolved in 1 mL deuterated water and transferred in dedicated NMR tubes for the experiment. The data were recorded and analyzed using either Bruker Topspin 3.6 or MestReNova LITE software.

2.2.5.9. Drug release study

Following the method described by Nkanga *et al.* (Nkanga *et al.* 2019), the freeze-dried 5-FU encapsulated liposomal formulation was first analyzed for drug content. A 5 mg sample was weighed and placed in a 25 mL volumetric flask containing 10 mL acetonitrile to rupture the liposome bilayers to allow for 5-FU dissolution. The volume was made up to mark using HPLC grade water. The volumetric flask was placed in a bath sonicator set at 60 °C for 30 minutes for the complete dissolution of the 5-FU, and the validated HPLC method was applied to analyze the solution. The injection into the HPLC system was done in triplicate, and the 5-FU drug content (%DC) was determined with **equation 2.3.**

$$\%DC = \frac{\boldsymbol{Amount\ of\ recovered\ drug}}{\boldsymbol{Amount\ of\ fomulation\ used}} \times 100 \qquad \text{Equation 2.3}$$

The *in vitro* release profile of 5-FU was investigated by the dialysis method according to the process described in (Nkanga *et al.* 2017), with some modifications in aliquots and concentrations considered. A sample of freeze-dried liposomal 5-FU (20 mg) or free 5-FU (2 mg) was dissolved in 2 mL HPLC grade water and allowed to incubate for 60 min while the suspension was occasionally gently shaken by hand for homogenization. An aliquot of the suspension (0.5 mL) was placed in a 5 mL volumetric flask, and acetonitrile was added to make up the mark. The mixture was sonicated for 30 min at 60 °C to destroy the liposome structure

and filtered with 0.45 μm Millipore filter, and the solution was analyzed using the validated HPLC method to determine the total available concentration of 5-FU.

Another 0.5 mL of the liposomal suspension and free 5-FU was transferred into the dialysis tubing membrane (Membra-Cell MD10 14X100 CLR, Sigma-Aldrich) for the release studies. The dialysis bags were sealed and placed in a glass vial containing 20 mL of pH 7.4 phosphate buffer and maintained at 37 °C under continuous stirring at 100 rpm all through the duration of the study. An aliquot of 5 mL of the sample was withdrawn after 0.5, 1, 1.5, 2, 3, 4, 5, 7, 9, and 12 hours for the quantification of the 5-FU according to the HPLC validated method. For the renewal of the release medium, an equivalent volume of the fresh buffer was added after every sampling.

2.2.5.10. Statistical analysis

All the experiments were performed in replicates (n=3), and the data reported as mean ± standard deviation (SD). Minitab 17 (Minitab, Ltd, UK) was used for the statistical analysis, and one-way ANOVA was applied for the comparative data analysis. The data were considered statistically significant when the p-value was < 0.05. ImageJ software was used to process the TEM image and OriginPro 9 software to plot the graphs.

3.RESULTS AND DISCUSSIONS

3.1. Drug-excipients compatibility study

DSC. Figure 2.2 presents the DSC thermogram of the physical mixtures of 5-FU with soybean lecithin and cholesterol. Pure 5-FU exhibited a sharp melting endothermic peak at 285.5 °C, corresponding to the melting point and to what has been reported in the literature (Li *et al.* 2010). The physical mixtures exhibited a decrease in the endothermic peaks, but the presence of the peaks in them suggests that there is no significant physical change in the structure of the 5-FU.

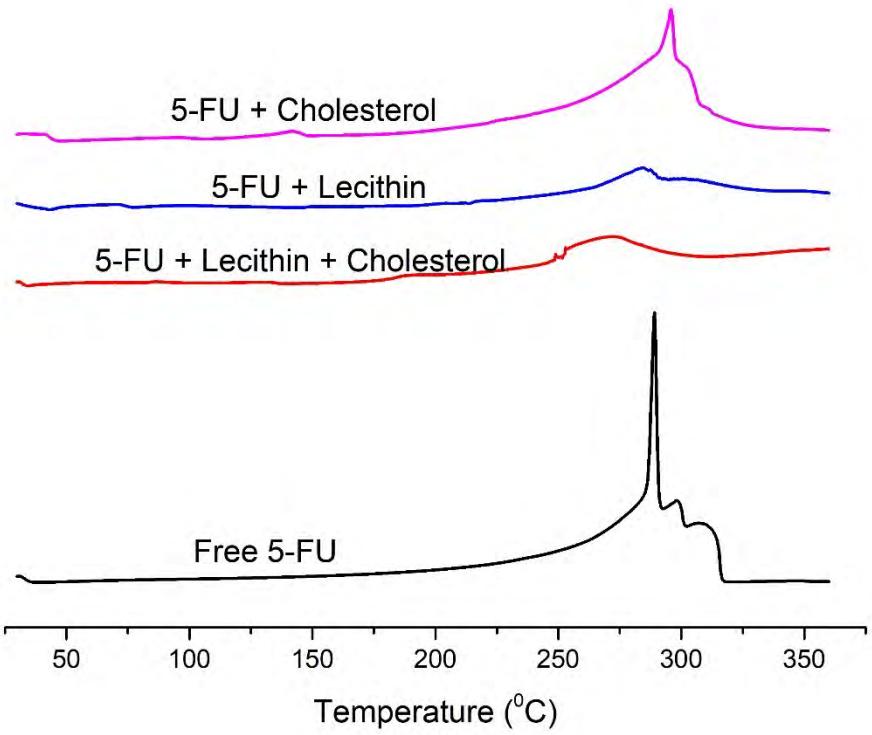

Figure 2.2. DSC thermogram of free 5-FU, physical mixture of 5-FU+soybean lecithin+ cholesterol, physical mixture of 5-FU+ soybean lecithin, and physical mixture of 5-FU+cholesterol

TGA. The TGA thermograms of physical mixtures of 5-FU with soybean lecithin and cholesterol are shown in **figure 2.3.** The extrapolated onset temperature in thermograms shows the temperature at which the weight loss begins. The pure 5-FU showed that the extrapolated onset temperature began at 286.5°C, which corresponds to the melting point and what has been reported in the literature (Gupta *et al.* 2015) and in correlation with DSC data. The extrapolated onset temperatures of the physical mixtures showed a slight decrease from 286.5°C. The presence of the extrapolated onset temperatures in all the mixtures also suggests that there were no significant changes in the physical structure of the 5-FU.

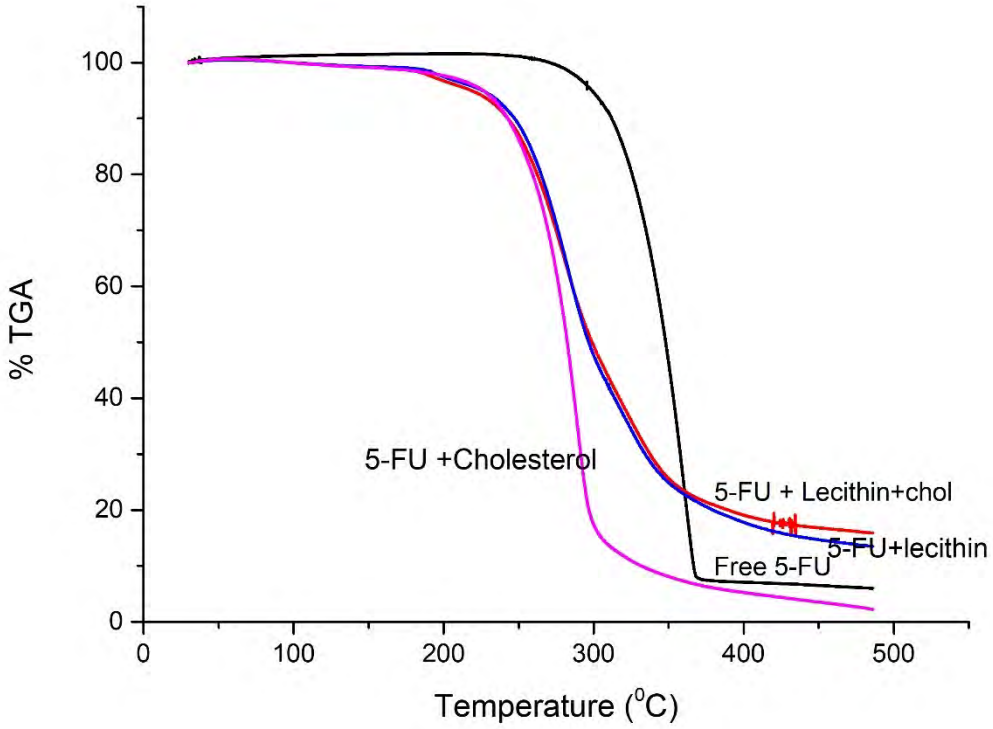

Figure 2.3. TGA thermograms of free 5-FU, physical mixtures of 5-FU+ soybean lecithin +cholesterol, physical mixtures of 5-FU + soybean lecithin, and physical mixtures of 5-FU +cholesterol.

FTIR. The FTIR spectra of the physical mixtures of 5-FU, crude soybean lecithin, and cholesterol were recorded and compared to the spectra of that of free 5-FU and showed in **figure 2.4.** The characteristic absorption band at 1661 cm^{-1} in the FTIR spectrum of free 5-FU is the vibration of C=O functional group, the band at 3160 cm^{-1} corresponds to N-H free stretching, the band at 1400 cm^{-1} is that of C-N stretch, the vibration band at 1250 cm^{-1} is that of C-H in-plane while the band at 1100 cm^{-1} is that of C-O single bond, as also reported in (Li *et al.* 2010). It was observed that there was no difference or shift in band position of functional groups in the spectrum of 5-fluorouracil alone and with excipients, which proved that 5-fluorouracil and excipients were compatible.

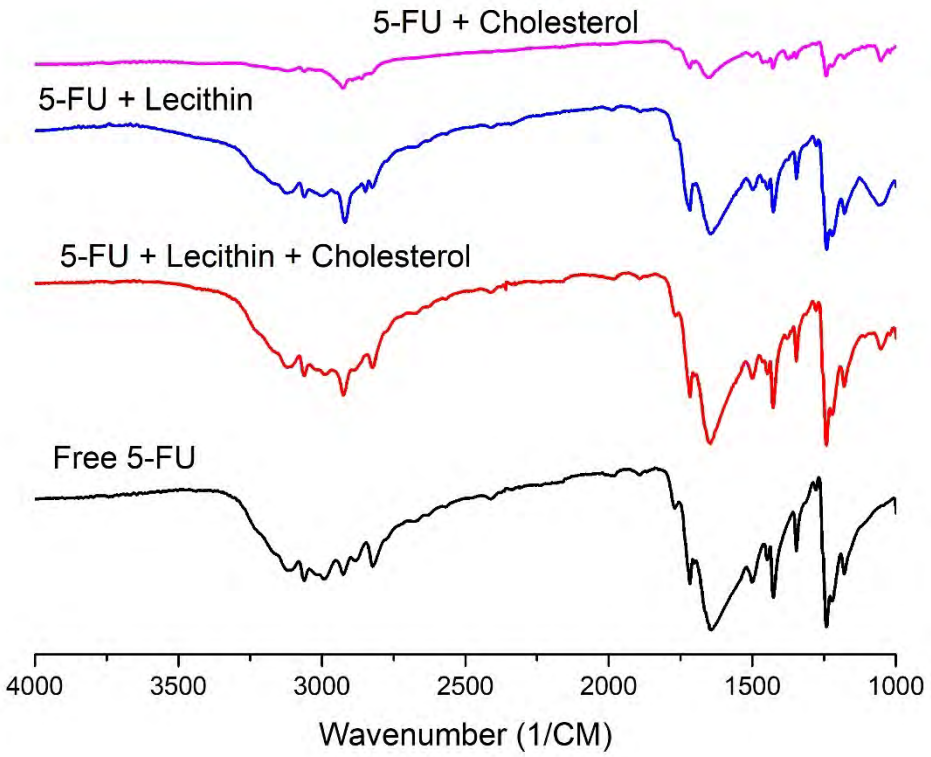

Figure 2.4. FTIR spectra of free 5-FU, physical mixture of 5-FU + lecithin +cholesterol, physical mixture of 5-FU + cholesterol, and physical mixture of 5-FU+ lecithin.

3.1.2. Evaluation of empty liposomes

3.1.2.1. Particle size and Zeta Potential

The empty liposomal formulations (E1-E27) with their polydispersity index (PDI), sizes, and zeta potential (ZP) are presented in **table 2.2**. considering the effects of negative zeta potential on the membrane bilayers' stability, circulation, and absorption into the body membrane (Honary and Zahir 2013), all the formulations were characterized for zeta potential and the formulations with the highest negative zeta potential were selected for the encapsulation of uracil. The preferred formulations were E8 and E27 with negative zeta potential (-ZP) of -54 mV and -55 mV and polydispersity index values of 0.305 and 0.286, respectively. The formulations' average sizes are 403 ± 7 for E8 and 164 ± 1 for E27 and were within the acceptable range for the encapsulation.

Other parameters selected are lecithin and cholesterol mass ratio of 3:1, hydration time of 60

min, sonication time of 30 min, and Voltex time of 10 min each based on the formulations with higher negative zeta potentials and acceptable sizes and polydispersity index.

Table 2.2. Average particle sizes, polydispersity index (PDI), and Zeta potentials of the empty liposomal formulations.

Formulation Code	**Lecithin-Chol mass ratio**	**Lipids-Water ratio**	**Hydration time (min)**	**Voltex time (min)**	**Sonication time (min)**	**Average size (nm)**	**PDI**	**ZP (mV)**
E1	1:0	1:5	30	5	10	475 ± 5	0.424 ± 0.02	-45 ± 1
E2	1:0	1:5	60	10	20	392 ± 2	0.520 ± 0.01	-23 ± 1
E3	1:0	1:5	90	15	30	368 ± 10	0.492 ± 0.02	-42 ± 2
E4	1:0	1:10	30	5	10	419 ± 11	0.481 ± 0.04	-51 ± 1
E5	1:0	1:10	60	10	20	196 ± 0.2	0.389 ± 0.01	-39 ± 1
E6	1:0	1:10	90	15	30	344 ± 7	0.505 ± 0.01	-47 ± 1
E7	1:0	1:20	30	5	10	444 ± 5	0.325 ± 0.02	-51 ± 2
E8	**1:0**	**1:20**	**60**	**10**	**20**	**403 ± 7**	**0.305 ± 0.06**	**-54 ± 2**
E9	1:0	1:20	90	15	30	104 ± 1	0.208 ± 0.01	-52 ± 1
E10	3:1	1:5	30	5	10	1435 ± 90	0.683 ± 0.17	-16 ± 1
E11	3:1	1:5	60	10	20	471 ± 4	0.540 ± 0.01	-25 ± 1
E12	3:1	1:5	90	15	30	458 ± 5	0.208 ±	-34 ±

							0.02	3
E13	3:1	1:10	30	5	10	660 ± 6	0.520 ± 0.01	-34 ± 1
E14	3:1	1:10	60	10	20	103 ± 9	0.270 ± 0.03	-50 ± 1
E15	3:1	1:10	90	15	30	729 ± 67	0.899 ± 0.17	-20 ± 1
E16	3:1	1:20	30	5	10	706 ± 22	0.330 ± 0.06	-40 ± 1
E17	3:1	1:20	60	10	20	740 ± 14	0.503 ± 0.04	-46 ± 1
E18	3:1	1:20	90	15	30	172 ± 2	0.256 ± 0.01	-41 ± 4
E19	1:1	1:5	30	5	10	626 ± 3	0.487 ± 0.01	-27 ± 2
E20	1:1	1:5	60	10	20	1470 ± 142	0.858 ± 0.13	-39 ± 1
E21	1:1	1:5	90	15	30	1375 ± 148	0.337 ± 0.02	-13 ± 2
E22	1:1	1:10	30	5	10	1052 ± 79	0.604 ± 0.14	-17 ± 1
E13	1:1	1:10	60	10	20	109 ± 1	0.297 ± 0.01	-51 ± 3
E24	1:1	1:10	90	15	30	1605 ± 67	0.677 ± 0.16	-23 ± 2
E25	1:1	1:20	30	5	10	256 ± 1	0.427 ± 0.01	-53 ± 2
E26	1:1	1:20	60	10	20	544 ± 9	0.548 ± 0.04	-40 ± 2
E27	**1:1**	**1:20**	**90**	**15**	**30**	**165 ± 1**	**0.286 ± 0.01**	**-55 ± 2**

3.1.2.2. Analysis of particle shape

The TEM image of the selected empty liposomal formulations chosen for analysis (E1, E7) is presented in **figures 2.5**. The observed shapes were spherical as characteristic to liposomes and with no sign of aggregation due to higher negative Zeta potentials observed.

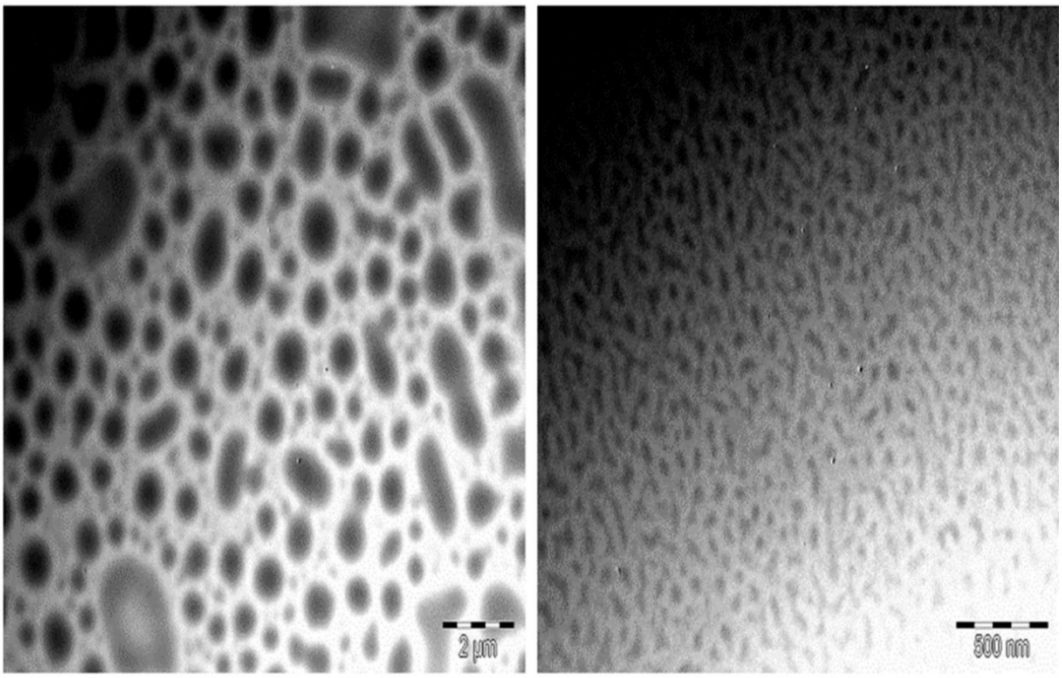

Figure 2.5. TEM image of empty liposomes

3.1.3. Validation analysis

The standard calibration curve obtained by plotting the average peak areas and corresponding concentrations of 5-FU is presented in **figure 2.6**. A good linearity was achieved over the concentration range of 1.25-50 µg/mL with a correlation coefficient of 0.9996. The repeatability was good with < 2% RSD for intra-day analyses and < 5% RSD for intermediate precision for the five days analyses as shown in **table 2.3,** (Ayyappan *et al.* 2011)(Gujral and Haque 2009). The percentage recoveries gotten were within the range of 95%-105% and it fell within the acceptable range of 90%-110% (Ayyappan *et al.* 2011).

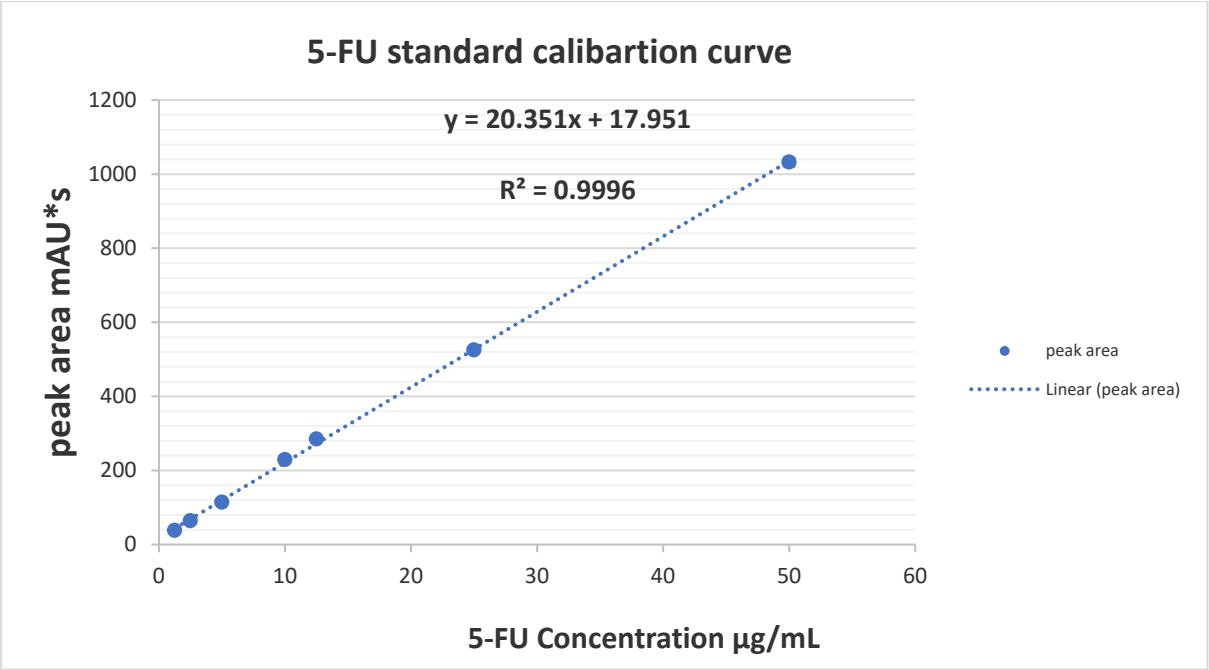

Figure 2.6. Standard calibration plot of 5-FU within the concentration range of 1.25-50 µg/mL.

Table 2.5. RSD and percentage recovery for the five days of analysis.

Concentration (µg/mL)	Intraday precision (%RSD)	Interday precision (%RSD)	Accuracy (% Recovery)
1.25	1.28	0.98	96.22
2.5	1.33	1.63	94.51
5	0.84	1.62	96.29
10	0.52	3.22	104.36
12.5	1.25	1.15	104.98
25	1.22	1.04	99.52
50	1.21	0.94	99.14

3.2. Characterization of uracil loaded liposomes

3.2.1. Encapsulation efficiency

Table 2.4 shows the mean encapsulation efficiency (%EE) of uracil loaded liposomes. The highest value of 61 ± 5 was obtained from drug to lipid mass ratio of 2:1 and two freeze-thawing circles. This obtained %EE is relatively high compared to what has been reported in the literature for hydrophilic drugs prepared by thin-film hydration methods (Nkanga *et al.* 2019). The presence of carbohydrates, a hydrophilic compound in the crude soybean lecithin, which entraps the uracil molecules, could have also contributed to the higher %EE observed (Pattni *et al.* 2015).

It was observed from **figures 2.7** that lower freeze-thaw circles of 1 and 2 resulted in higher encapsulation efficiency while the highest number of freeze-thaw circles resulted in smaller %EE. A reverse diffusion of the uracil molecules from the liposomes to the dispersing medium resulting from more freeze-thaw circles may be responsible for that, as explained by Costa *et al.* in (Costa *et al.* 2014). The highest sonication time of 15 minutes resulted in the highest %EE; thus, it can be concluded that the higher the sonication time, the greater the %EE.

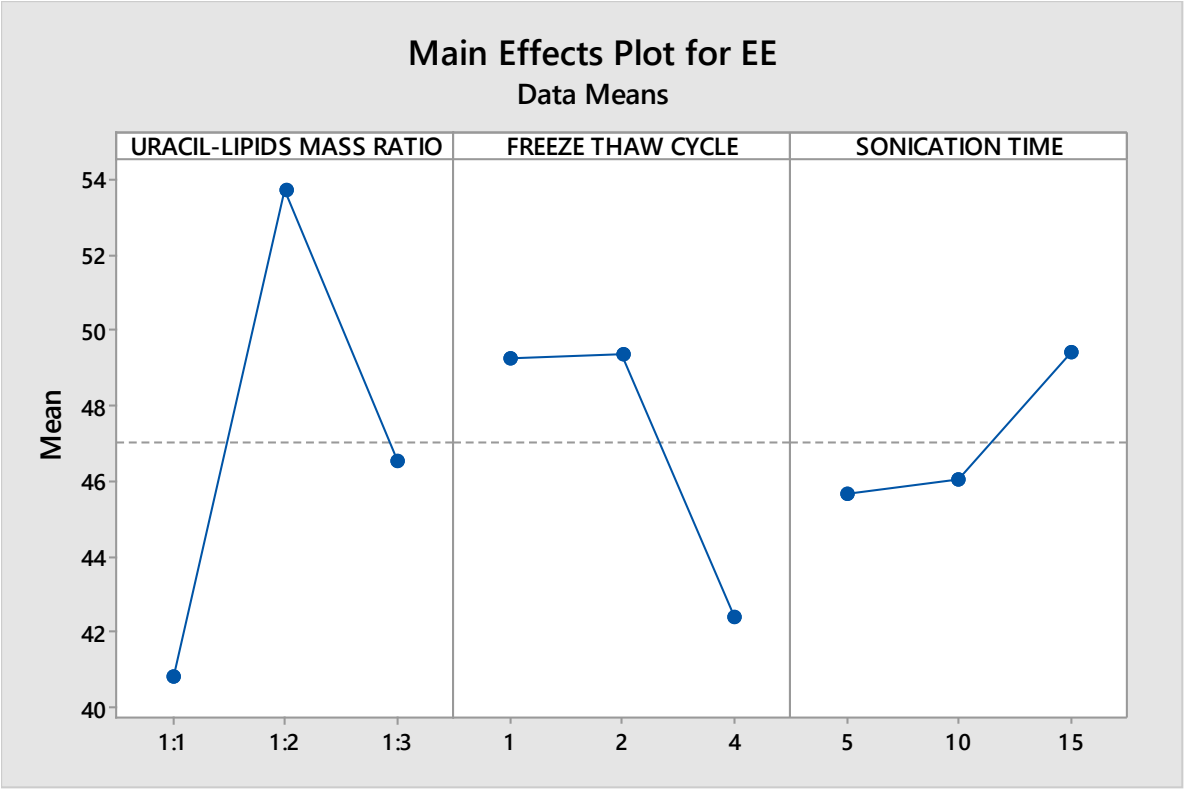

Figure 2.7 a. Main effects plot of drug-lipids mass ratio, number of freeze-thaw cycles and sonication time

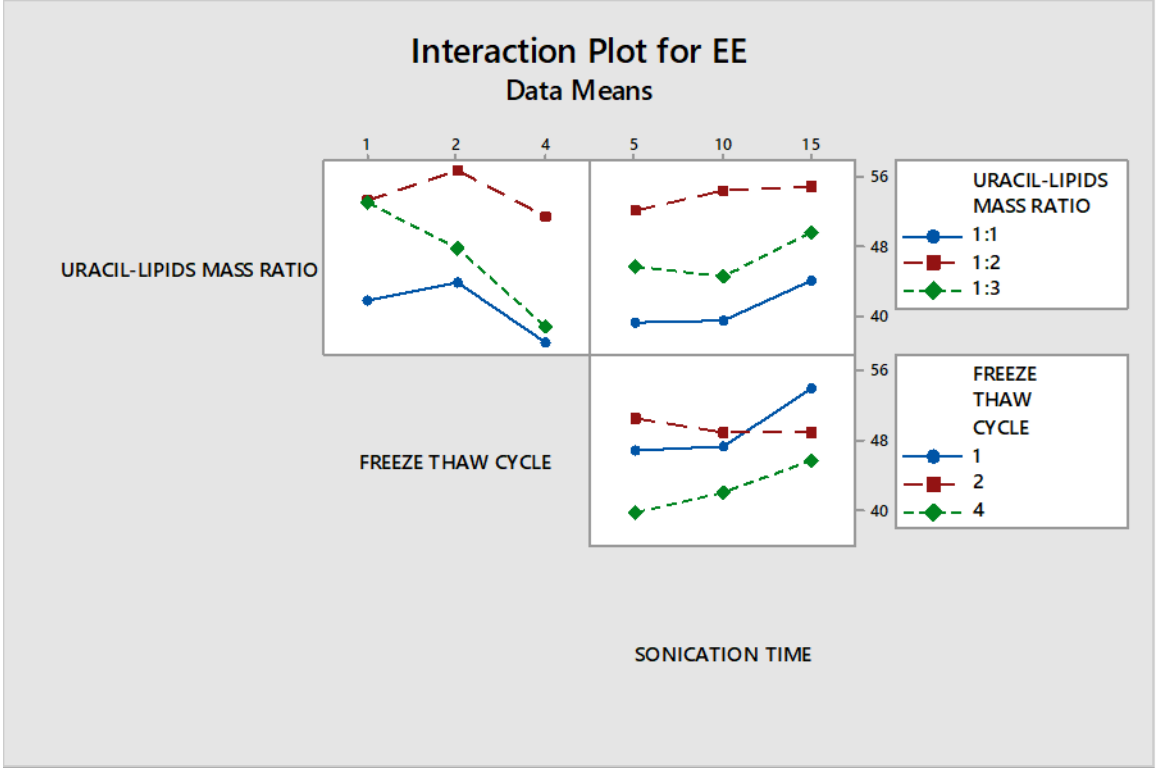

Figure 2.7 b. Interaction plot of drug-lipids mass ratio, number of freeze-thaw cycles, and sonication time.

Table 2.6. The encapsulation efficiency of uracil loaded liposomes with their average particle sizes, zeta potentials, and PDI

Formulation code	**PS ± SD (nm)**	**PDI ± SD**	**ZP ± SD**	**%EE ± SD**
F1	731 ± 10	0.335 ± 0.04	-42 ± 1	42 ± 3
F2	657 ± 7	0.226 ± 0.01	-40 ± 1	40 ± 2
F3	602 ± 10	0.312 ± 0.05	-32 ± 1	44 ± 1
F4	869 ± 16	0.483 ± 0.02	-43 ± 1	45 ± 2
F5	786 ± 9	0.226 ± 0.03	-25 ± 1	44 ± 5
F6	744 ± 8	0.244 ± 0.03	-35 ± 1	43 ± 1
F7	815 ± 9	0.309 ± 0.09	-44 ± 4	31 ± 2
F8	770 ± 7	0.376 ± 0.05	-45 ± 2	34 ± 4
F9	710 ± 13	0.316 ± 0.02	-40 ± 1	46 ± 4
F10	787 ± 1	0.446 ± 0.01	-46 ± 2	47 ± 2
F11	674 ± 13	0.414 ± 0.01	-65 ± 1	52 ± 9
F12	623 ± 12	0.269 ± 0.17	-64 ± 1	61 ± 3
F13	587 ± 7	0.333 ± 0.06	-65 ± 1	60 ± 7
F14	**784 ± 15**	**0.371 ± 0.04**	**-74 ± 2**	**61 ± 4**
F15	545 ± 5	0.203 ± 0.01	-66 ± 1	49 ± 1
F16	752 ± 17	0.443 ± 0.04	-54 ± 1	50 ± 5
F17	823 ± 15	0.287 ± 0.01	-54 ± 1	50 ± 7
F18	738 ± 19	0.254 ± 0.01	-62 ± 1	55 ± 7
F19	700 ± 13	0.333 ± 0.03	-72 ± 2	54 ± 5
F20	668 ± 13	0.380 ± 0.01	-61 ± 1	52 ± 4
F21	650 ± 15	0.418 ± 0.05	-67 ± 1	50 ± 1
F22	722 ± 8	0.245 ± 0.01	-53 ± 2	50 ± 1
F23	617 ± 11	0.247 ± 0.03	-73 ± 4	44 ± 2
F24	661 ± 10	0.328 ± 0.07	-70 ± 3	57 ± 1
F25	676 ± 13	0.314 ± 0.02	-58 ± 2	41 ± 4
F26	705 ± 14	0.399 ± 0.06	-73 ± 2	44 ± 1
F27	774 ± 19	0.320 ± 0.02	-65 ± 2	39 ± 1

3.2.2. Particle size and zeta potential analysis

Table 2.4 showed the particle sizes and zeta potentials of uracil loaded liposomes. The obtained zeta potential values (from -25 mV to -73 mV) helps in the liposomes stability during storage and uptake in the cells (Pattni *et al.* 2015). The particle size and Zeta potentials of the empty liposomes and uracil encapsulated liposomes did not show much difference when compared. The PDI values of 0.24 for the uracil loaded liposomes showed a well-distributed and homogenous liposomal formulation.

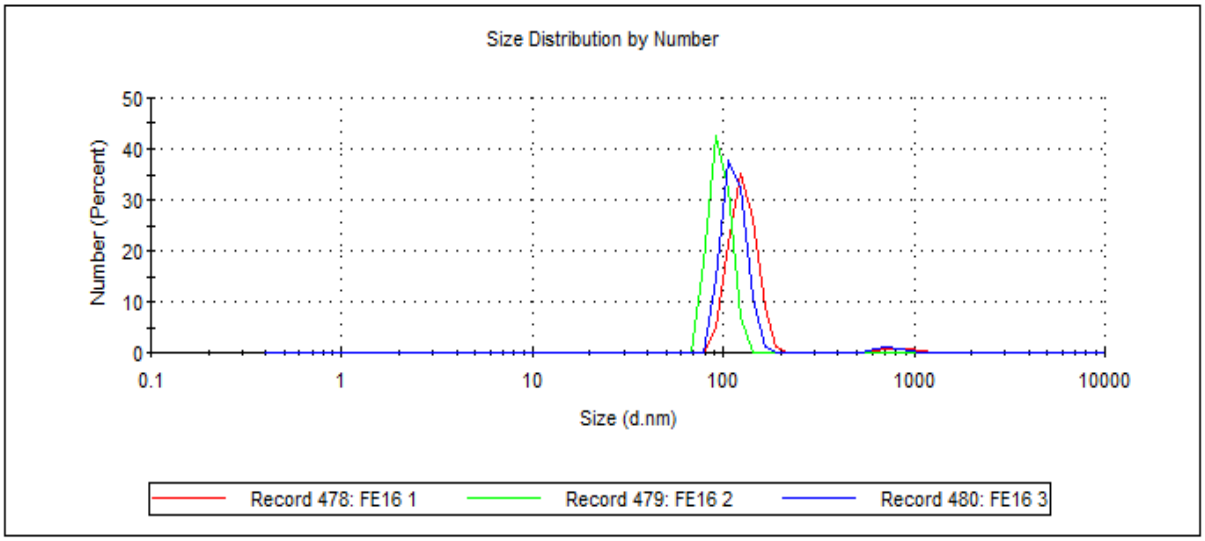

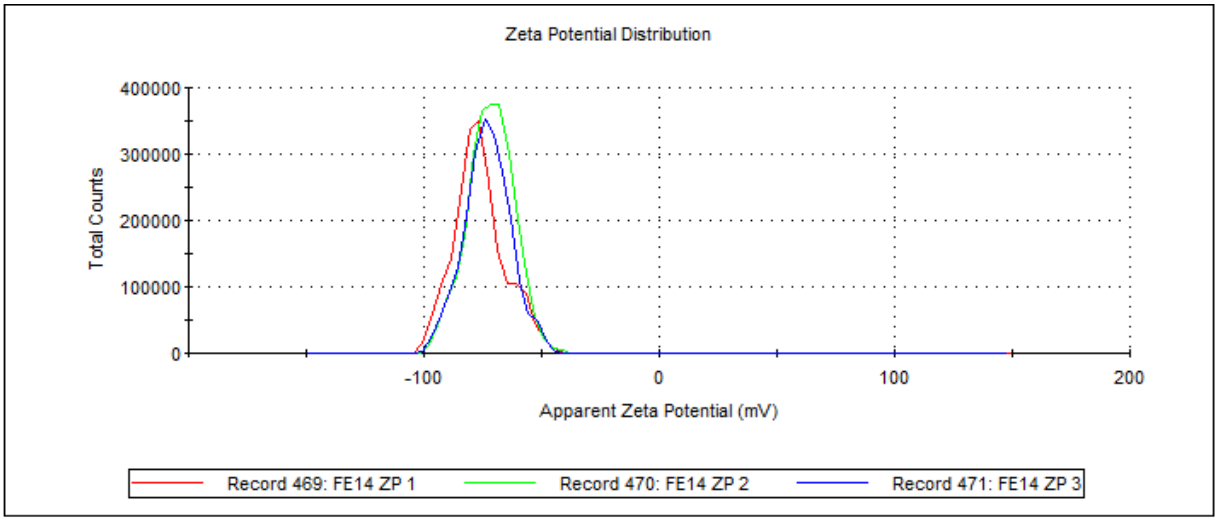

Figure 2.8. Particle size and zeta potential distribution of uracil loaded liposomes.

3.2.3. Morphology analysis

The TEM images showed the presence of spherical shape particles within the nanosized range, confirming the formation of liposomes. There was no aggregation of the liposomes formed as a result of the strong repulsive forces existing in the colloidal dispersion through the presence of high negatively charged zeta potential.

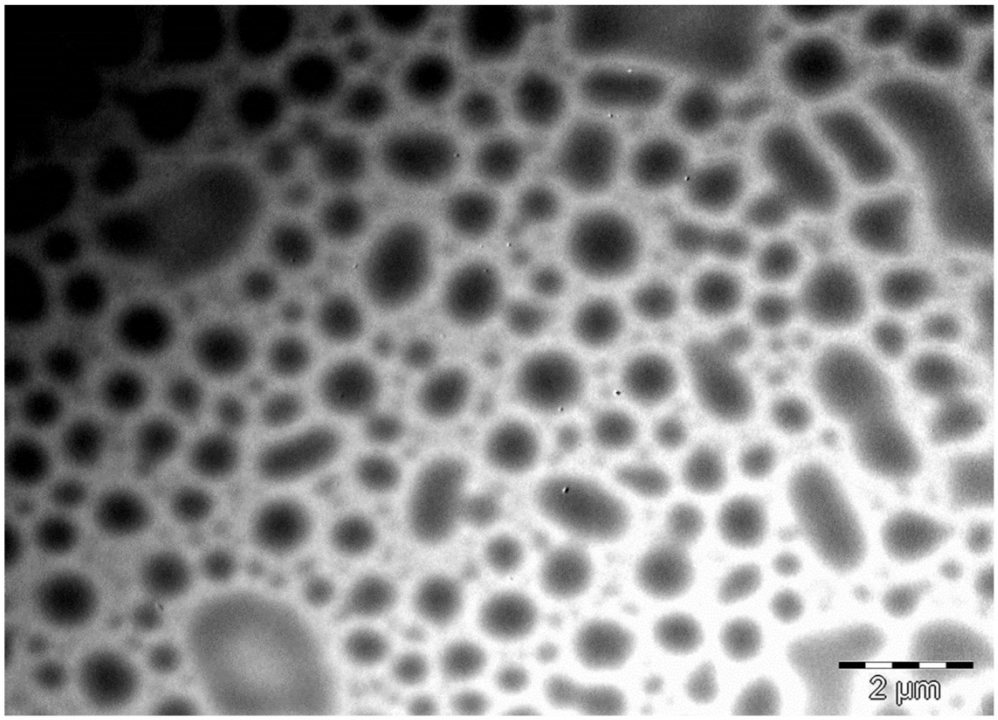

Figure 2.9. TEM image of uracil loaded liposomes.

3.2.4. Differential scanning calorimetry

DSC studies were done to analyze the thermal performance of the prodrug entrapped in the liposome while comparing it to the pure uracil and empty liposomes. **Figure 2.10** presents the DSC of the pure uracil prodrug, the empty liposome, and the uracil encapsulated liposome (FE9). The pure uracil prodrug revealed a sharp endothermic peak around 350°C corresponding to the melting point. However, this peak broadened and shifted to about 300°C in the uracil encapsulated liposome, suggesting that the uracil might be existing in amorphous form in the liposomes (Pattni *et al.* 2015).

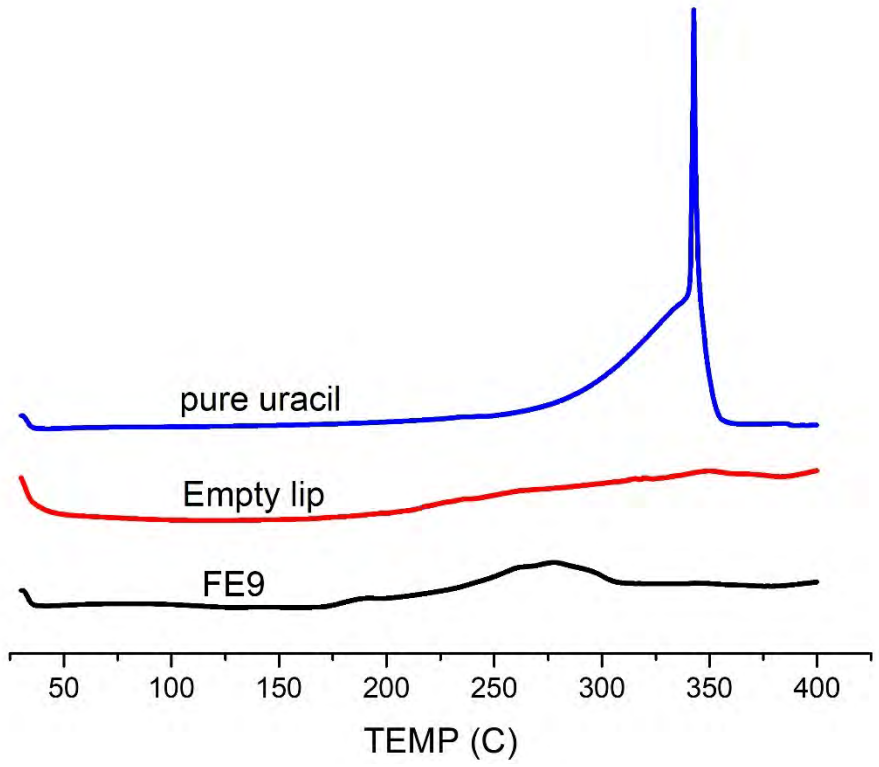

Figure 2.10. DSC plots of pure uracil drug, empty liposomes, and uracil loaded liposomes (FE9).

3.2.5. Fourier transform infrared

FTIR analysis was performed to verify the presence and intactness of the functional groups of uracil in liposomal formulations. **Figure 2.11** shows the FTIR spectra of pure uracil prodrug, empty liposomes, and uracil loaded liposomes. The characteristic band at 1661 cm^{-1} in the FTIR spectrum of pure uracil is the vibration of C=O functional group, the band at 3160 cm^{-1} corresponds to N-H free stretching, the band at 1400 cm^{-1} is that of C-N stretch, the vibration band at 1250 cm^{-1} is that of C-H in plane while the band at 1100 cm^{-1} is that of C-O single bond. The spectra reveal no significant interaction between the empty liposomes and the uracil encapsulated liposomes (Li *et al.* 2010).

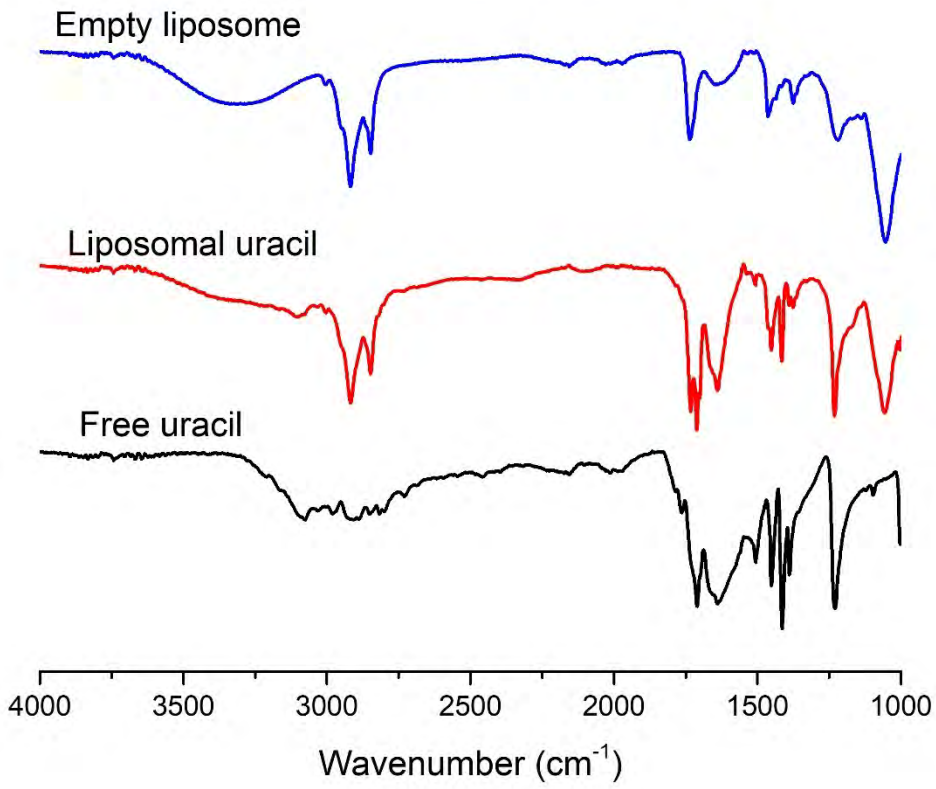

Figure 2.11. FTIR spectra of pure uracil prodrug, uracil encapsulated liposome, and empty liposome.

3.3. Characterization of 5-FU loaded liposomes

3.3.1. Encapsulation Efficiency

The encapsulation efficiency of drug-loaded liposomes is an important characteristic for the effectiveness of the method used for encapsulation. In this study, the formulation with the lipids to drug mass ratio of 2:1 (100 mg lipid components and 50 mg of 5-FU) gave the highest encapsulation efficiency of 62 ± 2%. This agrees with some reports in the literature on the %EE of 5-FU loaded nanoparticles. Fan *et al*. reported a %EE of 55 ± 1% on 5-FU encapsulated lecithin nanoparticles (Fan *et al.* 2014). Yassin *et al.* also reported a %EE of 59% on 5-FU loaded solid lipid nanoparticles (Yassin *et al.* 2010). However, Lopes *et al*. recorded 31% EE of 5-FU on liposomes made of synthetic phospholipids and attributed it to the concentration of 5-FU used in the entrapment process (Lopes *et al.* 2012). This high %EE may also be attributed

to the presence of carbohydrates, a hydrophilic compound in the soy lecithin liposomes, which can stabilize the 5-FU. As a hydrophilic drug, 5-FU is assumed to be entrapped in the aqueous core of the liposomal formulation(Nkanga *et al.* 2017). The average percentage encapsulation efficiency (%EE) of the liposomal 5-FU is showed in **Table 2.5.**

Table 2.7. The percentage Encapsulation efficiency of Liposomal 5-FU and Zeta potential of the liposomal 5-FU formulations (FE)

Formulation code	**ZP ± SD (mV)**	**%EE ± SD**
FE 1	-52 ± 1	53 ± 1
FE 2	-56 ± 1	62 ± 2
FE 3	-58 ± 1	51 ± 1
FE 4	-44 ± 2	54 ± 3
FE 5	-46 ± 2	54 ± 3

The parameters used in achieving this percentage encapsulation efficiency are lipids to drug ratio of 2:1, hydration time of 60 mins, sonication time of 30 mins, and voltex time of 15 mins. These parameters were chosen after the optimization using uracil. All the formulation codes are of the same parameters.

3.3.2. Particle size and Zeta Potential

As a result of tumor-related blood vessels' leaky nature, nano drug carriers and biomacromolecules readily move across the capillary endothelium and move into the interstitial space. Depending on the type of cancer, the size of the space between the cells of the endothelium lining the tumor capillaries falls within the range of 100 to 780 nm while that of the normal endothelium is within the range of 5 – 10 nm (Deshpande *et al.* 2013). The size distribution of the particles from the TEM image showed a Gaussian distribution peak at about

120 nm (**Figure 2.12 C**), correlating with the particle size distribution by number derived from the evaluation of the same sample by DLS (**Figure 2.12 A**). The obtained Zeta potential values (-44 mV to -58 mV) as shown in **Figure 2.13** are encouraging in enhancing the formulations' storage stability (Honary and Zahir 2013). It also plays a key role in cell binding and internalization. Both the empty liposome and the liposomal 5-FU were within the same nanosized range. This suggests that the entrapment of 5-FU did not affect the size and surface charge of the formulations.

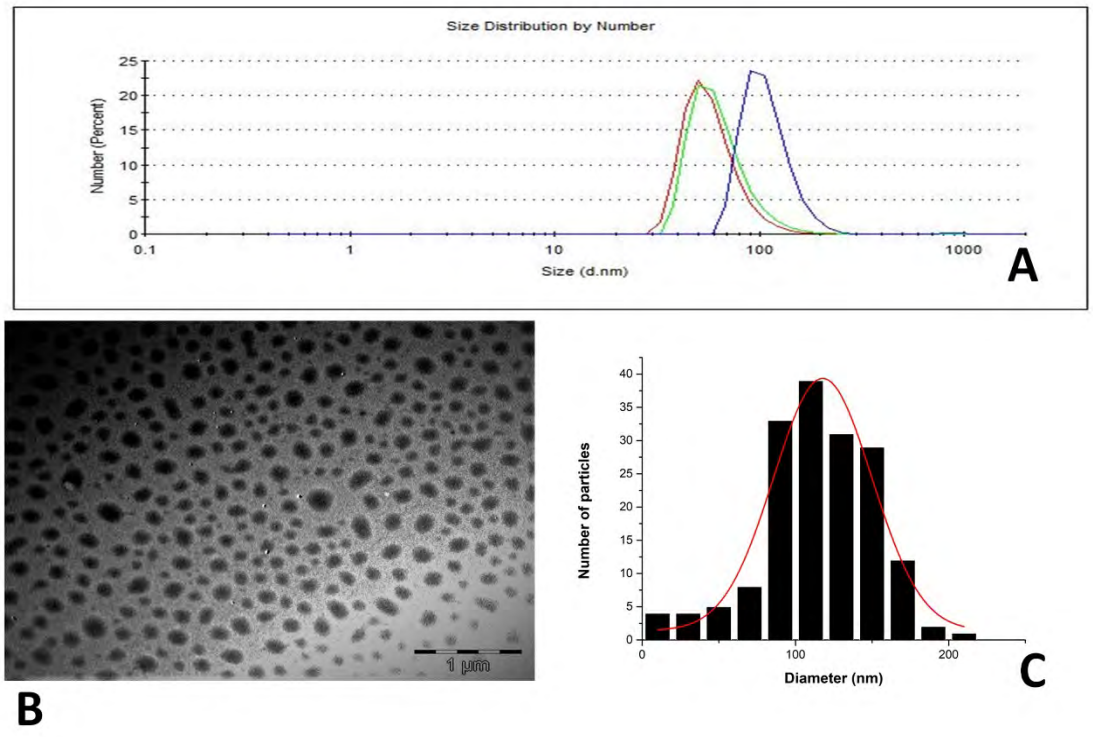

Figure 2.12. DLS size distribution by number (A), TEM image (B), and size distribution histogram generated using ImageJ from the TEM image (C).

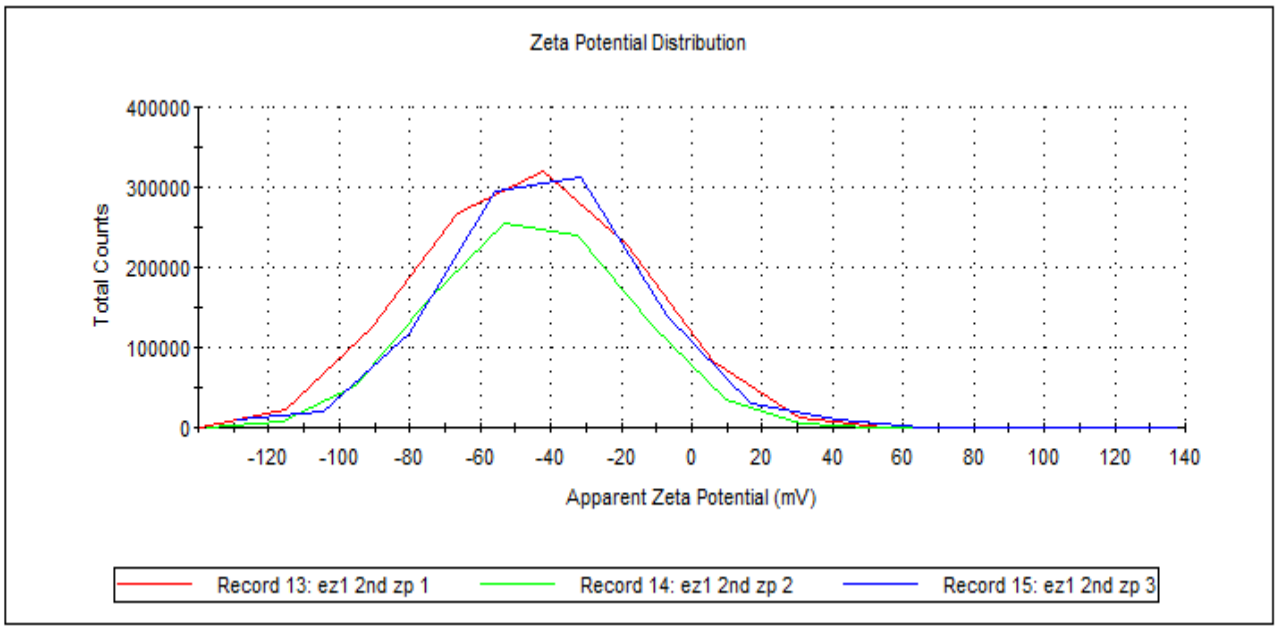

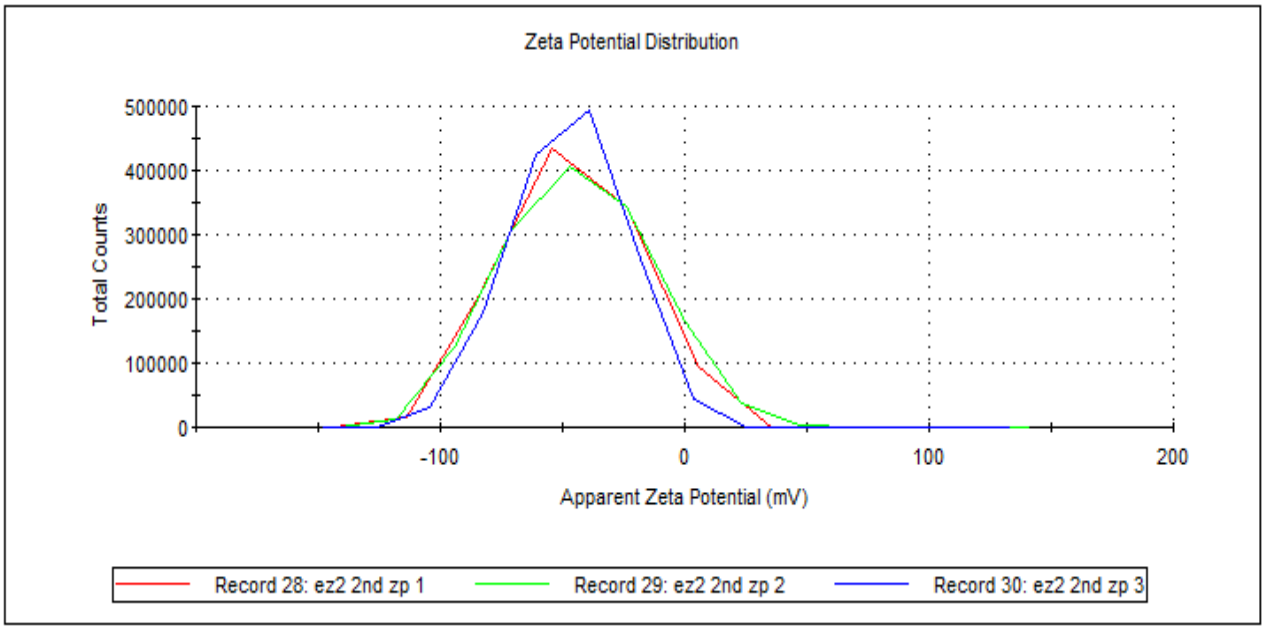

Figure 2.13. Zeta potential distributions of 5-FU encapsulated liposomes

3.3.3. Particle morphology

The TEM Image of all the 5-FU encapsulated liposomes revealed spherical natures associated with liposome nanocarriers (**Figure 2.12 B**). There was no aggregation or fusion as a result of the high negative zeta potential recorded (Honary and Zahir 2013). The strong repulsive forces

that prevented this aggregation correlated with the DLS measurement.

3.3.4. Thermogravimetric analysis (TGA)

There was a clear difference between the thermal behavior of the 5-FU loaded liposome, free 5-FU, and empty liposomes analyzed (**Figure 2.14**). The extrapolated onset temperature signifies the temperature at which the weight loss started. The extrapolated onset temperature of 5-FU is 286.9 °C, which corresponds to what has been reported in the literature (Gupta *et al.* 2015). The weight loss curve shows that it occurs in a single step, with about 90% decomposition of the drug from 280 ° C to 365 °C. Drug loaded liposomal formulation revealed TGA extrapolated onset temperature at 280 °C to 410 °C. The TGA thermogram of empty liposome also showed a gradual and steady weight loss between the temperature of 300 to 450 °C resulting in the burning of the soy lecithin.

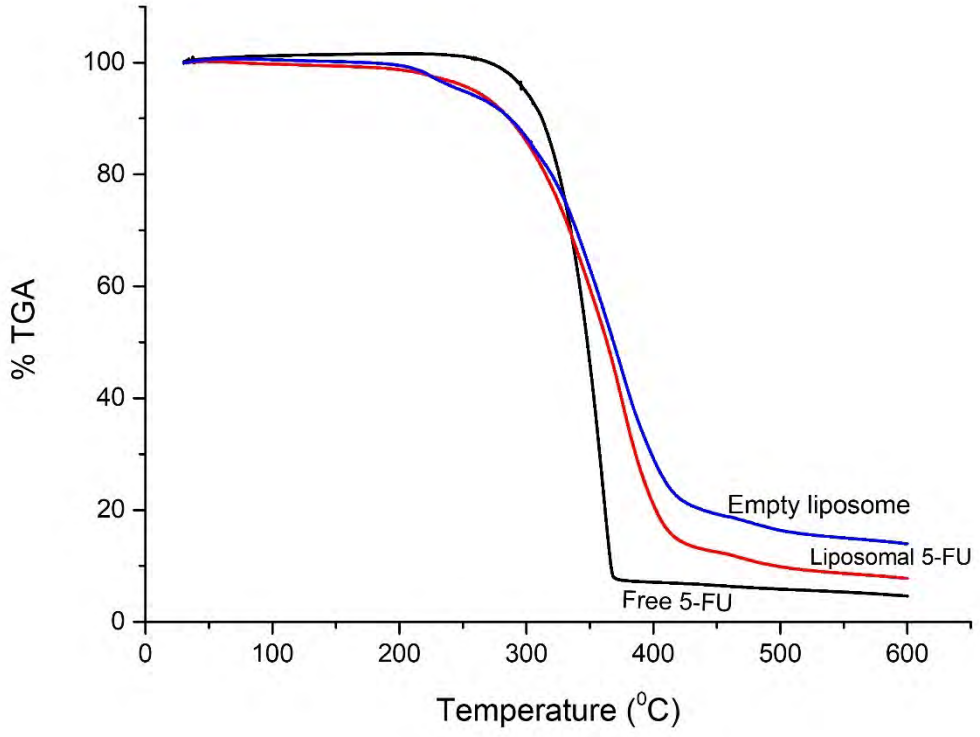

Figure 2.14. TGA thermograms of free 5-FU, liposomal 5-FU, and empty liposome.

3.3.5. Differential scanning calorimetry (DSC)

The DSC thermogram of free 5-FU showed a sharp melting endothermic peak at about 287°C, corresponding to the TGA data and close to the melting point of the compound (283°C). The

amorphous nature of the drug, when encapsulated, made it impossible to notice the endothermic peak in the liposomal 5-FU. The melting peak at 287°C was followed by decomposition, as reported in the literature (Gupta *et al.* 2015).

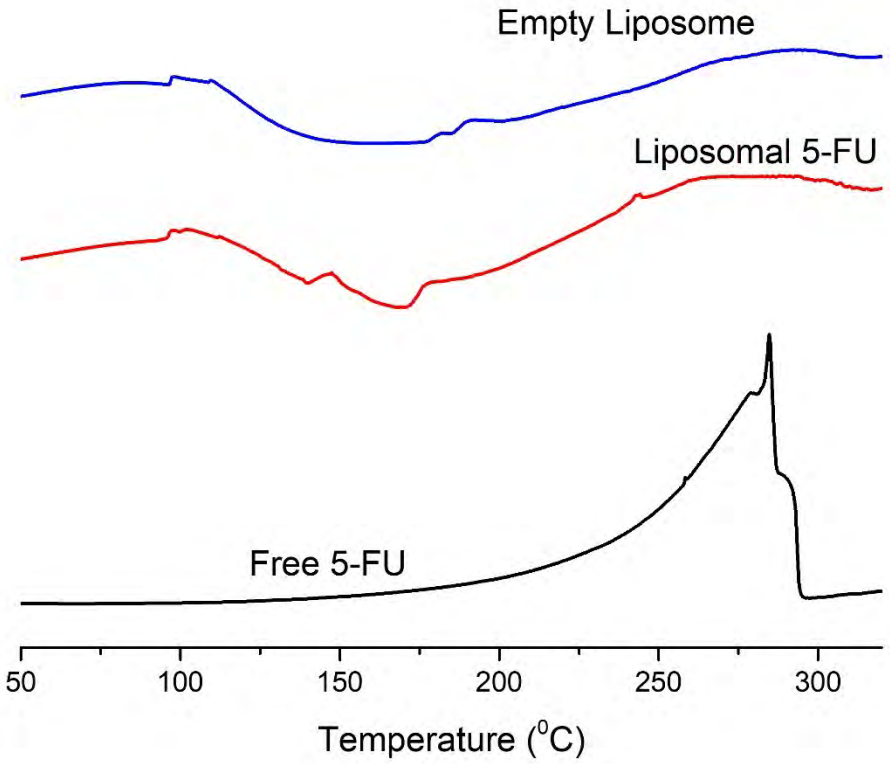

Figure 2.15. DSC thermogram of free 5-FU, empty liposome, and liposomal 5-FU.

3.3.6. X-ray diffraction (XRD)

The X-ray diffraction patterns of free 5-FU, liposomal 5-FU, and empty liposomes are shown in **Figure 2.16**. The XRD pattern of free 5-FU showed a sharp and intense peak at 2Θ = 29° and smaller peaks at 2Θ = 16° and 33°, confirming its crystalline nature as also reported in the literature (Wang *et al.* 2012). The peak at 29° could be seen also in the diffractogram of liposomal 5-FU, although at a lower intensity, suggesting that the drug was successfully encapsulated in the carrier. These data support the earlier DSC results that there was a change in the physical structure of 5-FU in liposomes, probably in a more amorphous state due to the lower intensity of the peak. However, no peak was observed in the empty liposome.

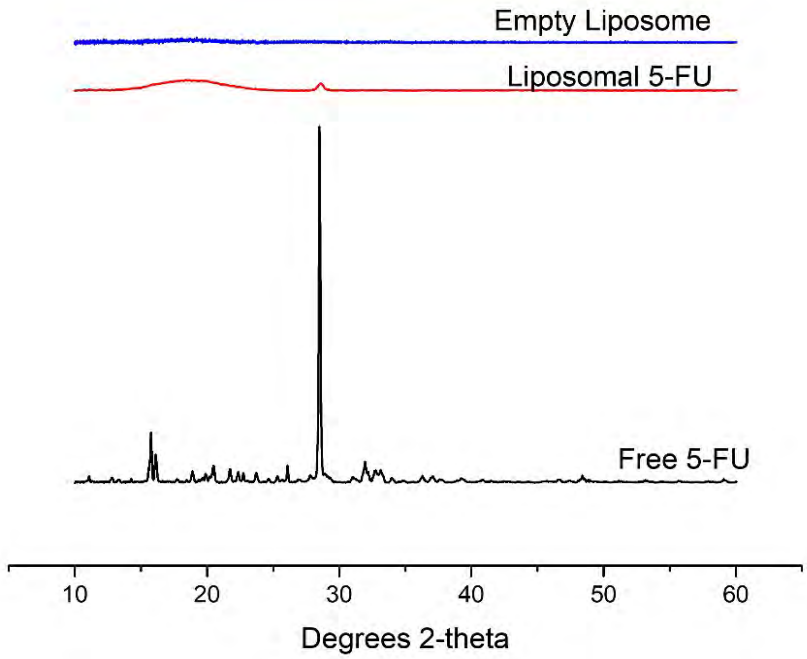

Figure 2.16. DSC diffractogram of free 5-FU, empty liposome, and liposomal 5-FU.

3.3.7. Fourier-transform infrared spectroscopy

As shown in **figure 2.17**, the characteristic peak at about 1660 cm^{-1} in the spectrum of free 5-FU is the stretching vibration of C=O group and corresponds to what has been reported in the literature (Li *et al.* 2010). The peaks at 1230 cm^{-1} and 1735 cm^{-1} in the empty liposome can be related to the stretching vibration of the P=O in the phosphate group and the C=O in the ester groups of the polar head of the phospholipids in interactions with other components of the liposomal formulations, respectively. Both peaks were lower in the spectra of the liposomal 5-FU as a result of the restriction in motion of the P=O and C=O that interacts with the molecules in the 5-FU. The characteristic peak at 1660 cm^{-1} in the free 5-FU corresponding to the C=O stretching vibration shifted to about 1637 cm^{-1} and overlapped with the phospholipids' amino groups. The spectra went further to prove that the drug was successfully encapsulated into the nanoparticle.

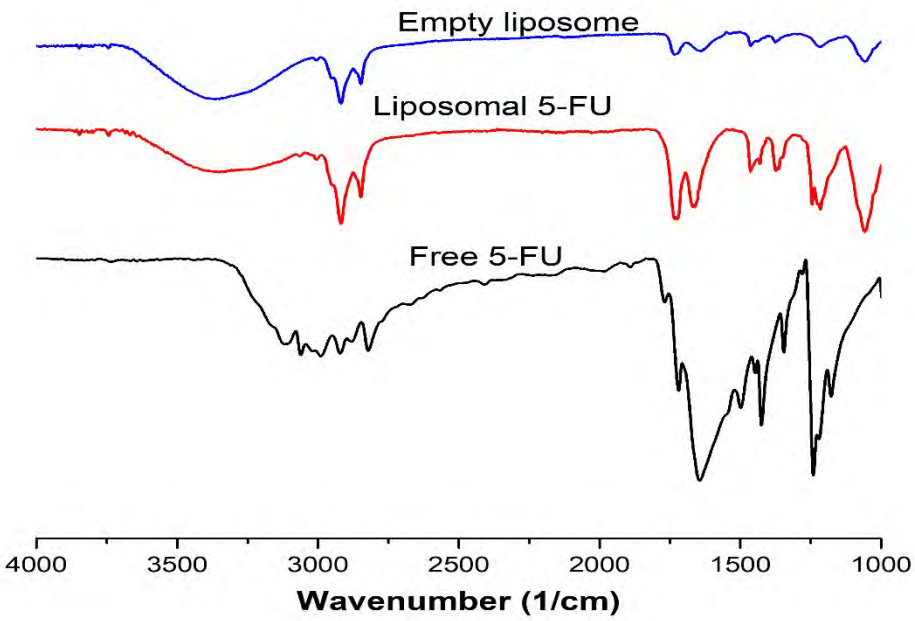

Figure 2.17. FT-IR spectra of free 5-FU, liposomal 5-FU, and empty liposome.

3.3.8. Energy-dispersive X-ray spectroscopy

Figure 2.18 shows the elemental surface compositions of the free 5-FU, 5-FU encapsulated liposome, and empty liposome. Phosphorus, a significant element in the phospholipids' hydrophilic heads, was present in the surface of the liposomal formulations. Other elements (C and O), which are components of the phospholipids, were also present in the liposomal formulations. For the free 5-FU, C, N, O, and F were observed on the surface. However, some of these elements, like N and F, were not noticed in the liposomal 5-FU. This suggests that the 5-FU as a hydrophilic drug was encapsulated inside the nanocarrier's aqueous core, and none was found on the surface (Nkanga *et al.* 2018).

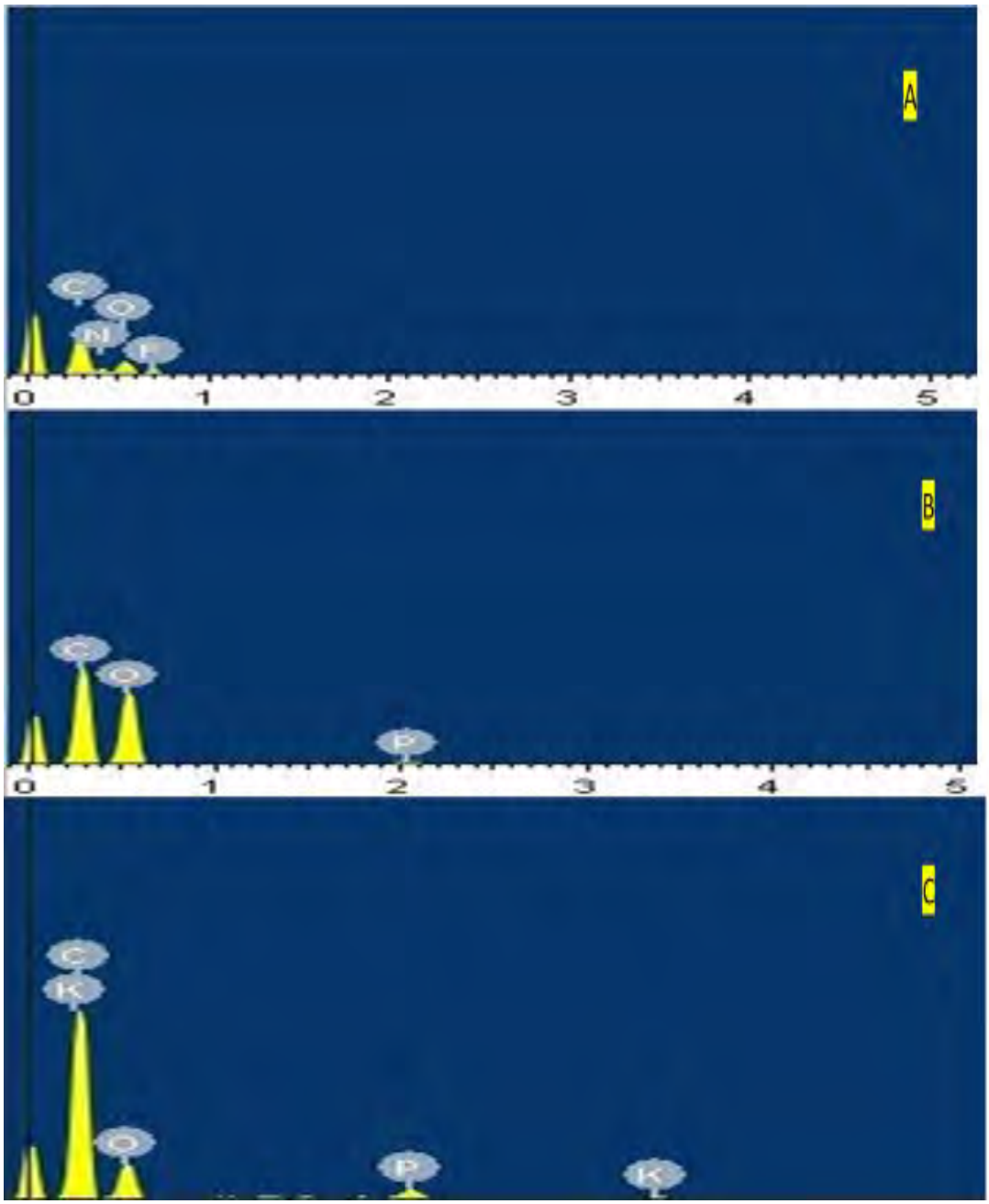

Figure 2.18. EDX spectra showing the elemental surface compositions of free 5-FU (A), liposomal 5-FU (B), and empty liposome (C).

3.3.9. Proton nuclear magnetic resonance (^{1}HNMR)

The intermolecular and intramolecular interaction existing within liposomes can be evaluated using NMR spectroscopy (Timoszyk 2017). ^{1}HNMR was used to compare the profile of free 5-FU, liposomal 5-FU, and empty liposomes in this study. As observed in **figure 2.19**, there was a variation in the split chemical shift of free 5-FU from 7.60 and 7.56 ppm, which broadened

and shifted to 7.58 and 7.55 ppm. These chemical shifts may be attributed to the encapsulation of the hydrophilic drug molecules at the polar interfacial side of the nanocarrier, while the split signal suggests the presence of at least two states of 5-FU explained by their different location in the territory (Lopes *et al.* 2012). The signal at 7.60 ppm was assumed to be the existence of the 5-FU molecules absorbed at the membrane water interface, while that of 7.56 ppm was assumed to represent some level of penetration into the liposome membrane. The signal broadened in the liposomal 5-FU suggests the existence of nuclear exchange processes between the 5-FU molecules in the different locations of the carrier. This result agrees with published data in the literature on 5-FU binding and mobility in fluid lipid bilayer membrane of liposomes (Yoshii and Okamura 2009).

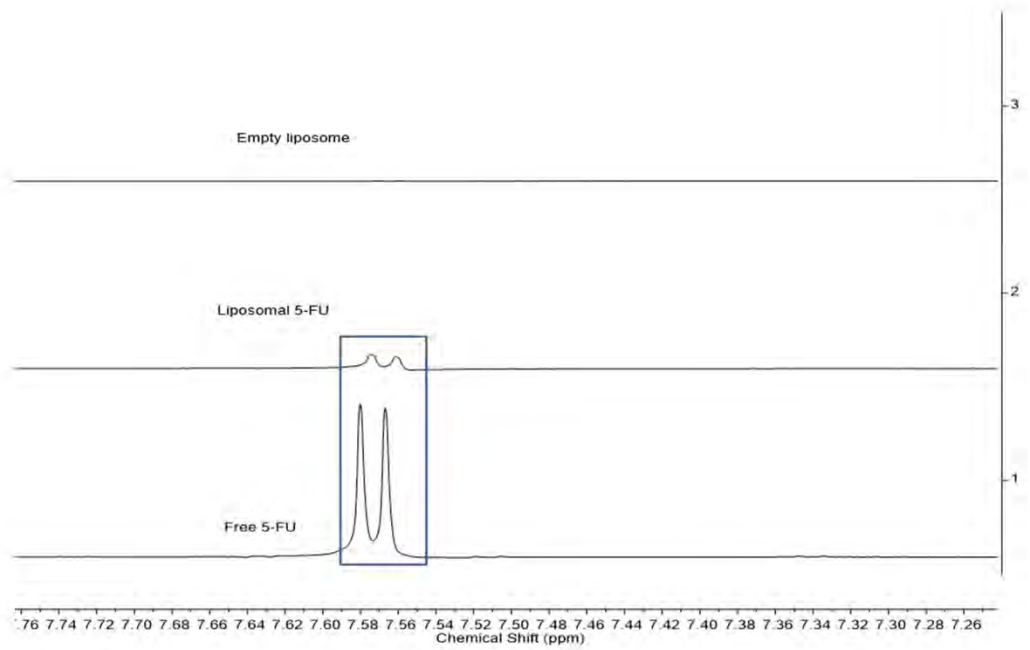

Figure 2.19. Partial ^{1}HNMR of free 5-FU, liposomal 5-FU, and empty liposome.

3.3.10. *In vitro* release study

Table 2.6. Show the data obtained from drug content evaluation and *in vitro* release study conducted using the dialysis tubing membrane under physiological conditions of 37 ° C and pH 7.4 phosphate buffer.

Table 2.8. Data from *In vitro* release study of liposomal 5-FU and free 5-FU.

Time (hours)	Liposomal 5-FU	Free 5-FU
0	0	0
0.5	29	54
1	38	62
1.5	45	64
2	51	67
3	53	72
4	58	74
5	62	79
7	66	85
9	69	89
12	71	94

The *in vitro* release profiles of 5-FU from liposomes and free 5-FU were plotted to elucidate the release behavior of the drug. As can be seen in **figure 2.20**, The cumulative percent of 5-FU release from the liposomes in the first 2 h was approximately 51%, whereas that of free 5-FU was about 67% Encapsulation of 5-FU in crude soy lecithin liposome expectedly reduced both the drug release rate and the cumulative amount released. The burst effect over the first 2 hours and slower phase of release is evident. These findings are in agreement with what has been reported in the literature for the release profile of 5-FU in a liposomal dispersion (Mahmoud *et al.* 2005). Above all, the total amount of 5-FU released in the liposomal dispersion was about 70% in 12 hours, while it was about 95% from the free 5-FU in the same 12 hours. This proves that the release profile of free 5-FU was faster than that in the liposomal 5-FU;

therefore, crude soy lecithin liposomal 5-FU may be explored as an effective nanocarrier for controlled release of therapeutics into colorectal cancer sites.

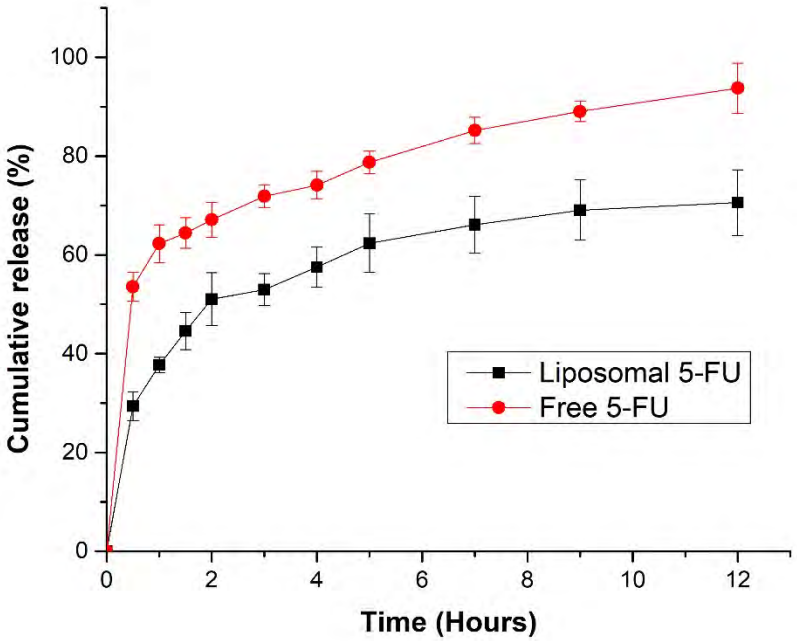

Figure 2.20. *In vitro* release profiles of liposomal 5-FU (square) and free 5-FU (circle).

3.3.11. Conclusion

This chapter's principal objective was to formulate and characterize crude soy lecithin liposome encapsulating 5-fluorouracil (a first-line chemotherapeutic drug in treating colorectal cancer). 5-FU was successfully encapsulated into the natural phospholipid components with a percentage encapsulation efficiency of 62 %. The mean particle sizes and zeta potential fall within the nanosized range associated with nanocarriers used in drug delivery. The TEM images also revealed spherical shaped particles while the physicochemical characterizations reviewed the intramolecular interactions that existed between the nanocarrier and the therapeutics. The *in vitro* release profile also proved the crude soy lecithin liposome's effectiveness on the drug as the liposomal 5-FU exhibited a more controlled and sustained release than the free 5-FU. This work, to the best of our knowledge, was the first to encapsulate 5-fluorouracil in crude soy lecithin liposome using the thin film hydration techniques, and our result showed that liposomes

produced from natural crude soy lecithin have the potential as biocompatible, and effective drug delivery system for the management of colorectal cancer. This research will go a long way in improving the limitations and challenges encountered in administering the drug in its free form like the gastrointestinal and bone marrow toxicity.

CHAPTER THREE

ULTRASOUND TRIGGERED RELEASE OF 5-FLUOROURACIL FROM ECHOGENIC LIPOSOMES

3.1 INTRODUCTION

Ultrasound-triggered drug delivery is a potential tool for effectively managing many health conditions. Ultrasound enhances the delivery of therapeutics across cell membranes by the permeability of cell membranes through two mechanisms. The first is by the formation of microbubbles close to the cells, and the second is by the formation of pores in the cell membranes by cavitation (Joshi and Joshi 2019). Ultrasound can also result to local heating of the cell and the drug carrier. An objective of advanced drug delivery system is to target the therapeutic agent to the desired diseased cells and release the drug in a desired therapeutic manner. The challenges persist in controlling the release kinetics at the target site. Ultrasound is outstanding among other materials used for triggering because it allows for control of the drug release site and its profile simply by application of an external stimulus (Frenkel 2008).

For effective triggered drug delivery, the ultrasound parameters like frequency, intensity/amplitude, exposure time, and mechanical index needs to be optimized. The frequency range for ultrasound used in drug delivery is in the range of kHz to MHz. The frequency is lower in therapeutic purposes but higher in diagnostic applications. A lower ultrasound frequency results in deeper tissue penetration due to less attenuation resulting in higher therapeutic outcomes (Coussios *et al.* 2007). Lower frequency ultrasound is much safer because it can be applied for much longer time without damage to the tissue or the drug, it can also be applied to sensitive areas including soft tissue. High-intensity ultrasound can damage the tissue by introducing excessive heat. The mechanical index provides a direct measure of cavitation; a high mechanical index leads to high cavitation activity (Barnett *et al.* 2000). The type and location of tissue been treated, the type of drug carrier, and the ultrasound intensity/amplitude will determine the exposure time chosen. The time should also be optimized according to the time it takes to arrive at inertial or stable cavitation and sonoporation while avoiding thermal effects (Mitragotri 2005).

Echogenic liposomes are designed to exhibit physicochemical properties that impart sonosensitivity. They have a size range of 40 nm to 6 µm (Kopechek *et al.* 2011). Researchers have loaded drugs, genes, therapeutic gases, and stem cells into echogenic liposomes made of different compositions of expensive synthetic lipids (Shaw *et al.* 2009, Britton *et al.* 2010, Buchanan *et al.* 2010). No report, to the best of our knowledge, has used crude soy lecithin, a cheap and readily available mixture of phospholipids, to formulate an echogenic liposome and encapsulate 5-FU. This chapter aims to develop an echogenic liposome entrapping argon, a biocompatible gas in the bilayers while encapsulating 5-fluorouracil, a chemotherapeutic drug

in the aqueous core, and evaluate its sensitivity and effects of ultrasound parameters on the release profile of the drug.

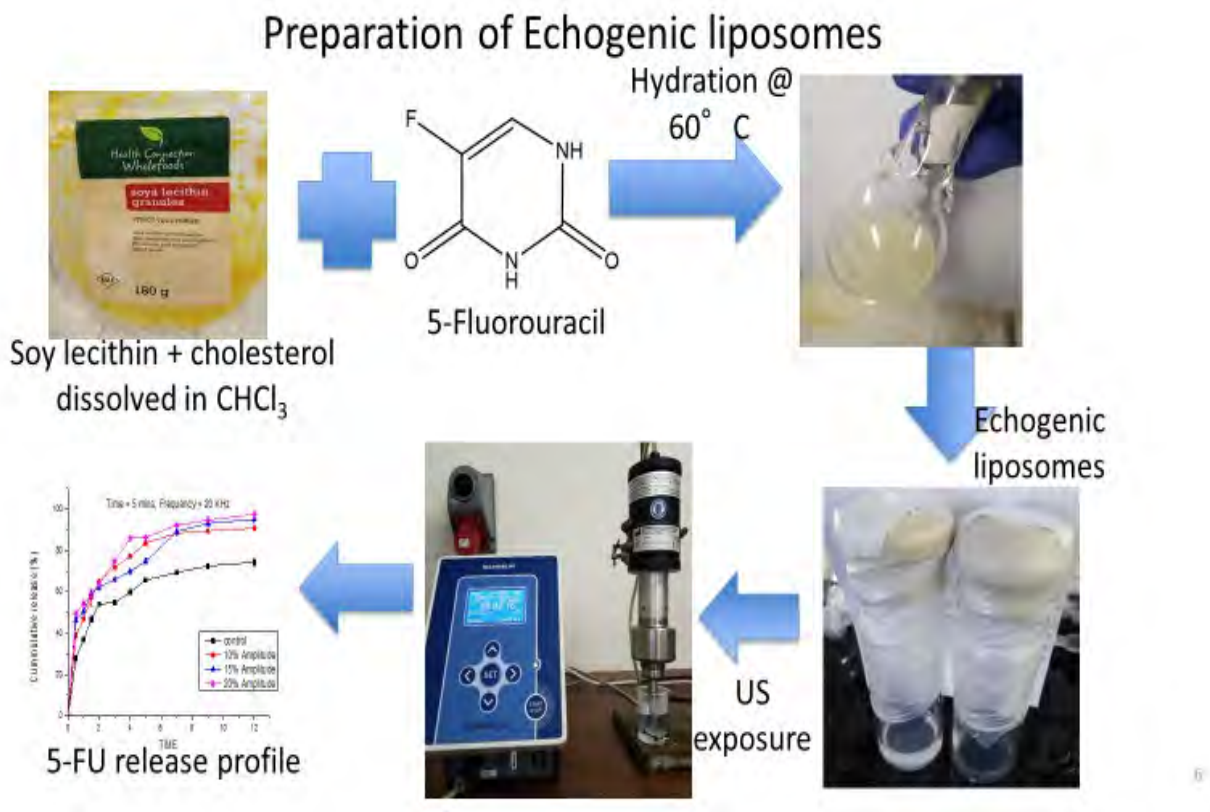

Figure 3.1. Flowchart illustrating the formulation of echogenic liposomes.

3.2. Experimental

3.2.1. Materials and method

Crude soybean lecithin used in this research was from Health Connection Wholefoods (USA). Cholesterol used was from Carlo Erba/Divisione Chemica (Italy). 5-Fluorouracil, D-mannitol, mono and dibasic sodium phosphate, methanol, acetonitrile (HPLC grade), and chloroform were purchased from Sigma Aldrich (Germany). Argon gas used was from Afrox gas (South Africa) and was 99.9% purity. All these chemicals were used as procured without any purification.

The following equipment was used; Rotary evaporator (Buchi R-205 Switzerland), Bath

sonicator (909-digital spellbound), Dynamic light scattering (Zetasizer nanoZEN Malvern instrument), Centrifuge (MSE–Mistral 1000), HP1100 Agilent LC-MSD high-performance liquid chromatography (HPLC), A Zeiss Libra-120 KV Transmission electron microscopy (TEM), Freeze dryer LABCONCO FreeZone® 6 Liter Benchtop Freeze Dry System (USA), Sonopuls HD 4200 low-frequency ultrasound (Bandelin Germany).

3.2.2. Preparation of echogenic liposomes (ELIP)

The best-optimized formulation for the production of liposomes encapsulating 5-FU was maintained for the formulation of echogenic liposomes. A conventional thin-film hydration method was also used. Phospholipid compositions of 75 mg crude soy lecithin and 25 mg cholesterol were weighted in a clean 25 mL round bottom flask and dissolved in 1 mL of chloroform. The organic solvent was dried in a rotatory evaporator set at 60 °C under pressure of 30 mm Hg and 200 rpm for 5 min. The thin film formed in the round bottom flask was removed from the rotary evaporator and stored overnight in a desiccator at room temperature of 25 °C for the complete drying. According to the method described by Huang *et al.* with some modifications as regards to lipids and drug composition (Huang *et al.* 2008), 50 mg of the drug was dissolved in a solution containing 0.36 mol/L D-mannitol as D-mannitol facilitates achievement of ensuring physiological osmolarity and entrapment of Ar and 5-FU. The suspension was hydrated for 60 min under continuous stirring at 400 rpm and heating at 60 °C. The suspension was further sonicated for 30 min and Voltex for 5 min, then transferred into a 50 mL high-pressure resistance glass vial capped with Suba-seal rubber septa. The argon gas was introduced into the vial through the septum with a 10 mL syringe having a 27G×1/2" needle. The septa were tested for leakage under high pressure for 6 h, and no leak was detected. The high-pressured liposomal formulation was incubated at room temperature for 30 min and then frozen by cooling at -196 °C in liquid nitrogen for 15 min. As soon as the formulation was removed from the cooling system, the pressure was released by removing the septum. The depressurized frozen formulation was thawed by exposure to room temperature of 25 °C for 20 min.

The liposomal formulation entrapping gas and drug was transferred into a 50 mL centrifuge tube and centrifuged for 20 min using MSE Mistral-1000 low-speed centrifuge set at RCF of 1020 g. The pellets (unencapsulated 5-FU) were separated, and the supernatants were further transferred into 1.5 mL Eppendorf tubes and centrifuged using Eppendorf 5414 micro high-

speed centrifuge set at RCF of 15600 g. The supernatants were separated and discarded, while the liposomes in the pellets were rinsed three times with 1 mL of HPLC grade water to wash off the unencapsulated 5-FU. The 5-FU entrapped liposomal formulations were then freeze-dried for 48 hours and stored at 4 °C for further characterizations.

3.3. Characterization of echogenic liposomes

3.3.1. Determination of encapsulation efficiency of echogenic liposomes

The validated HPLC method for the standard 5-FU solution was used to quantify the amount of 5-FU in the echogenic liposomes' supernatant. A 1/100 dilution was made using the eluent, a mixture of methanol and water (both HPLC grade) at the ratio of 80:20. The solutions were filtered with a 0.22 µm PVDF Millipore filter. The amount of drug incorporated into the nanocarrier was determined quantitatively using the validated HPLC method. . The percentage encapsulation efficiency (%EE) was determined as per the equation

$$\% \text{ EE} = \frac{Mass\ of\ encapsulated\ 5\text{-}FU}{Total\ mass\ of\ 5\text{-}FU\ used} \times 100 \quad \text{…. Equation 3.1}$$

3.3.2. Particle size, polydispersity index, and Zeta potential

The freeze-dried formulated echogenic liposomes were characterized for size, polydispersity index, and Zeta potential by re-dispersing 2 mg in HPLC grade water and analyzed with the use of ZEN-360 MAL1043132 Nano Malvern instrument at a scattering angle of 173°. The particle size distribution was confirmed by analyzing TEM images with ImageJ software.

3.3.3. Morphology analysis

The shape of the formulated echogenic liposomes was evaluated using the transmission electron microscopy instrument Zeiss Libra 120 KV. The re-dispersed liposomes used in particle size analysis were dropped in the copper grid and allowed to dry for 24 hours. The excess liquids were absorbed with filter paper.

3.3.4. Ultrasound triggered release

The effects of ultrasound stimulation on the release profile of 5-FU from echogenic liposomes were evaluated using the below method. A 20 mg sample of the freeze-dried echogenic liposome (encapsulating 5-FU) was dissolved in 2 mL HPLC grade water and allowed to incubate for 60 minutes. The suspension was gently shaken by hand for homogenization. A 0.5 mL aliquot of the suspension was placed in a 5 mL volumetric flask, and acetonitrile was added to make up the mark. The suspension was sonicated for 30 min at 60 °C to destroy the liposome structure and filtered with a 0.22 µm Millipore syringe filter. The solution was analyzed for drug content using the validated HPLC method to determine the concentration of the 5-FU.

A 0.5 mL of the suspension was transferred into the dialysis tubing membrane (Membra-Cell MD10 14X100 CLR, Sigma-Aldrich) for the ultrasound-triggered release studies. The dialysis bag containing the dissolved echogenic liposomes was inserted into a 50 mL glass beaker containing 30 mL of PBS buffer pH 7.4. The beaker was placed in a temperature-regulated water bath and the temperature monitored at 37°C all through the duration of the experiment to avoid hyperthermia-induced drug release (Hosokawa *et al.* 2003). A 20 kHz low-frequency ultrasonic processor (Sonopuls HD 4200, Bandelin, Germany) was used. The 13 mm ultrasonic probe was immersed in the glass beaker containing the sample. The triggering was conducted in a continuous mode at varying amplitudes and exposure time (Abed *et al.* 2018). The sample was immediately removed from the release medium after the ultrasound irradiation, and the released drug was evaluated from the medium using the already validated HPLC method. According to the above procedure, a fresh sample was prepared to assess the effects of ultrasound exposure on the drug percentage cumulative release. The sample in the dialysis bag was placed in a glass vial containing 30 mL of the release medium, exposed to ultrasound irradiation of various parameters. After the ultrasound stimulation, the sample was maintained at 37 ° C and 100 rpm. An aliquot of 5 mL of the sample was withdrawn after 0.5, 1, 1.5, 2, 3, 4, 5, 7, 9, and 12 hours and replaced with the same volume. With respect to the ultrasound parameters selected, a total of 7 groups were investigated, including the control group, which was non-echogenic liposomes, and was not exposed to ultrasound irradiation as with the other 6 groups. The remaining liposomes were triggered for 5 minutes or 10 minutes at amplitudes of 10 %, 15 %, and 20 %. The released 5-FU was quantified using the validated HPLC method.

3.3.5. Stability studies

The Freeze-dried echogenic liposomal formulations were stored at 4°C, and their stability was monitored for four weeks. A 2 mg of the samples were dissolved in 1 mL phosphate buffer pH 7.4. Aggregation and fusion were studied through the variations in Zeta potential for day 7, day 14, day 21, and day 28 with the use of DLS.

3.4. RESULTS AND DISCUSSIONS

3.4.1. Encapsulation efficiency

The percentage encapsulation efficiency of all the formulated echogenic liposomes is presented in **Table 3.1**. As expected, the average value of %EE were within 60 % and agreed with data obtained for the liposomal 5-FU. Most hydrophilic drugs encapsulated in liposomes prepared by the thin-film hydration method exhibit low % EE (Costa *et al.* 2014). This % EE may be attributed to the presence of carbohydrates, a hydrophilic compound in the soy lecithin liposomes, which can stabilize the 5-FU molecule. The gas that was fused after the hydration of the lipid can be assumed to be entrapped in between the bilayers while the drug was encapsulated in the aqueous core of the echogenic liposome (Huang *et al.* 2008). This recorded % EE showed that the echogenic liposomes could get to colorectal cancer cells and release their payloads when triggered with ultrasound.

3.4.2. Particle size, polydispersity index, and Zeta Potential

The size distribution of the echogenic liposomal formulations from the TEM image showed a Gaussian distribution peak at about 160 nm **(Figure 3.2 B),** correlating with the particle size distribution by number derived from the same evaluation sample by DLS **(Figure 3.2 A).** These particle sizes are attractive because they can cross the leaky vasculature and deliver the drugs to the colorectal cancer cells when triggered with ultrasound. The zeta potentials are within the range of – 50 to -61 mV (**Figure 3.3**). These ZP figures are attractive for long term stability and storage of the formulation at the shelf. It also helps in preventing aggregation and fusion of the echogenic liposomes (Pattni *et al.* 2015).

Table 3.1. Zeta potentials and Encapsulation efficiency (%EE) of formulated echogenic liposomes (ELIP).

Formulation code	**ZP ± SD (mV)**	**%EE ± SD**
ELIP 1	-62 ± 1	58 ± 1
ELIP 2	-63 ± 2	51 ± 7
ELIP 3	-59 ± 3	44 ± 8
ELIP 4	-52 ± 2	41 ± 7
ELIP 5	-53 ± 2	36 ± 3

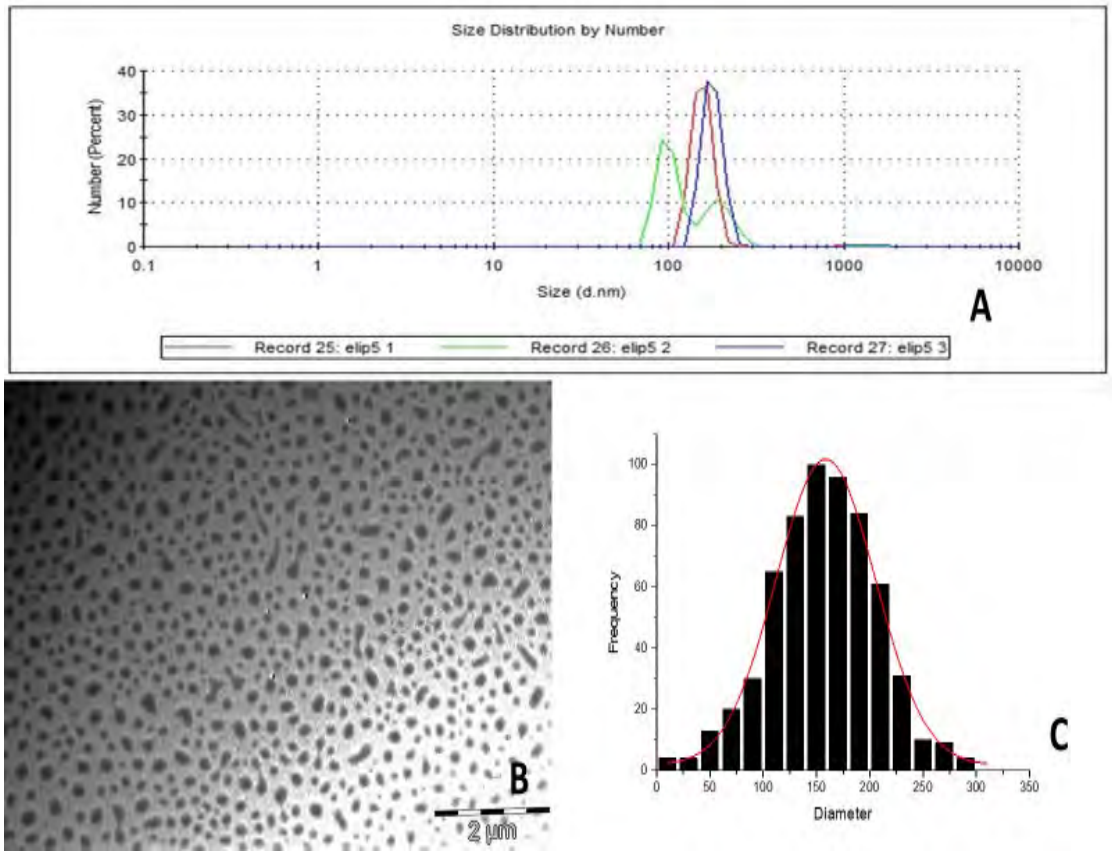

Figure 3.2. DLS size distribution by number (A), TEM image (B), and size distribution histogram generated using ImageJ from TEM image (C).

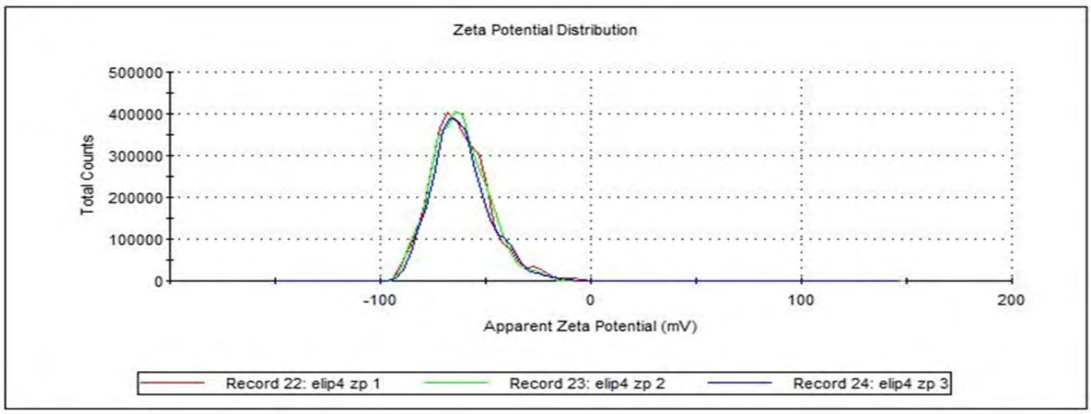

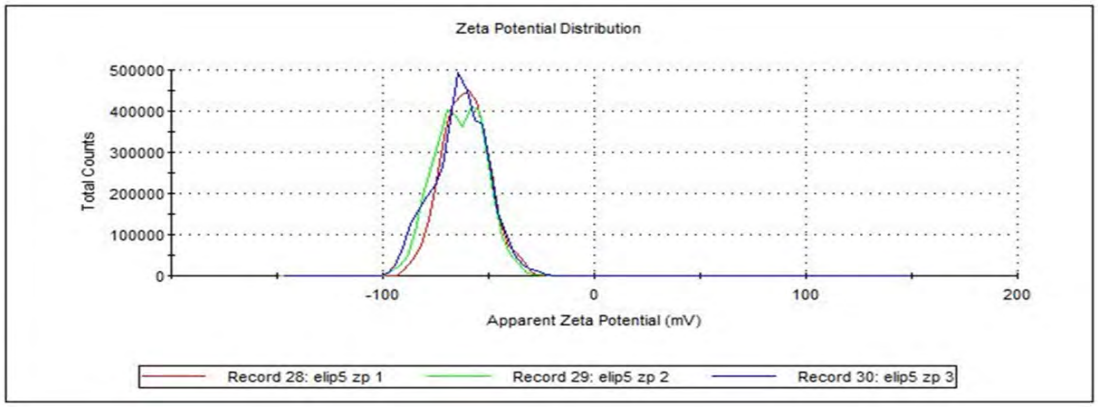

Figure 3.3. Zeta potential distribution by number of echogenic liposomes

3.4.3. Morphology analysis

The TEM images of the formulated echogenic liposomes are shown in **Figure 3.2 B.** All the formulations depicted the spherical shaped and dispersed components identical to liposomes. The particles were not aggregated due to the strong repulsive forces based on the higher negative zeta potentials observed from the DLS analysis.

3.3.4. Ultrasound-triggered release

3.3.4.1 Effects of Ultrasound Amplitude and Exposure time on Drug Release Profile

Drug release from liposomes is affected by applied ultrasound (Schroeder *et al.* 2007). Three different amplitudes 10 %, 15 %, and 20 % were investigated and the 5-FU released increased in proportion to the increase in applied amplitude, which could be as a result of the introduction of transient cavitation in the liquid release medium (**Figure 3.4**). This cavitation might have occurred near the liposomal membrane or through small cavitation nuclei in the liposome aqueous core. The liposomal formulations were irradiated for an exposure time of 5 minutes and 10 minutes. It was inferred that the higher the ultrasound amplitude and the longer the exposure time, the greater the amount of energy density transferred to the nanocarrier, which directly altered the quantity of 5-FU release. These data show that a good amount of this drug can be released from the liposomal formulation on exposure to low-frequency ultrasound in a short time. This could result in the availability of a higher concentration of the compound in the

colorectal cancer cells when triggered, thereby resulting in prolonged circulation time with reduced off-target toxicity.

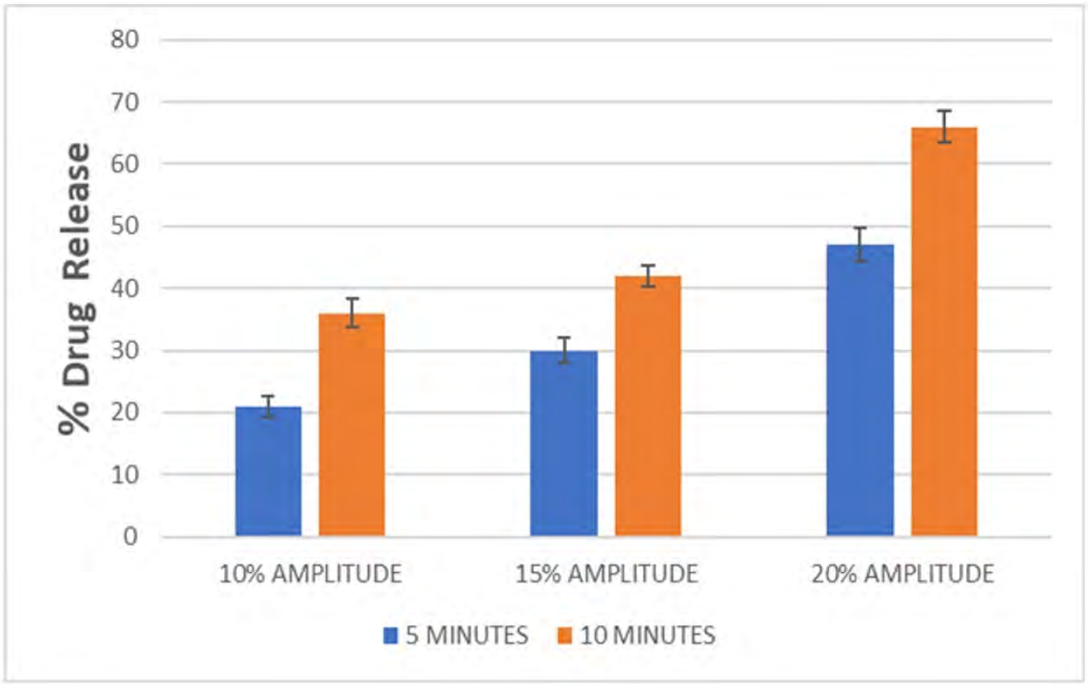

Figure 3.4. Percentage drug release from echogenic liposome exposed to ultrasound irradiation of different amplitudes and exposure time.

Figures 3.5 also showed the cumulative release rate of the drug on exposure to ultrasound, including the control. The cumulative release was above 95 % for all the ultrasound parameters considered but was about 70 % for the control. This showed that the percentage of drug release from the echogenic liposomes increased significantly when previously triggered with ultrasound before monitoring it under continuous stirring for 12 hours. The formulation triggered with a 20 % amplitude reached 99 % release after 5 hours, confirming that the higher the amplitude and exposure time, the greater the percentage release. The hypothesis is that it could be as a result of higher energy that went into the liposome, permeabilizing it and creating more pores. It was assumed that the drug was released from the pores formed as a result of transient cavitation that occurs on ultrasound irradiation, and there was an exponential burst release after 2 hours, then followed by a gradual release phase. All the echogenic liposomes

displayed a several-fold increase in the extent of drug release compared to the control that served as reference. The complete mechanism behind ultrasound-triggered drug release from liposomes has not been fully explained in the literature. This, to an extent, might be due to some limitations in the methods of determining reversible changes in the bilayers of phospholipids that only occur during ultrasound irradiation. These results correlate with what was reported by Abed *et al.* when they applied 3 MHz ultrasound to magnetic polylactic co-glycolic acid nanoparticles encapsulating 5-FU; they reported that an increase in the percentage of drug released is directly proportional to the exposure time and intensity/amplitude (Z. Abed *et al.* 2016). Schroeder *et al.* also obtained a similar result when they controlled the release of doxorubicin, methylprednisolone hemisuccinate, and cisplatin co-loaded in liposome using 20 kHz low-frequency ultrasound; they obtained about 80 % release on 3 minutes exposure and they concluded that the percentage of drug release was a function of amplitude and exposure time. They also suggested that exposure of liposomes to ultrasound induced reversible pore-like defects in the membrane which allows drugs to be released (Schroeder *et al.* 2007). T.J Evjen *et al.* exposed synthetic-based echogenic liposomes encapsulating a drug to 40 kHz US at 20 % amplitude and observed that 95 % of the drug was released on the exposure time of 6 minutes (Evjen *et al.* 2011). As displayed in the ultrasound system, the amount of energy delivered into the medium on ultrasound irradiation by the piezoelectric effect was higher on prolonged time exposure. In the experiment, for 5 minutes of exposure time and 20 % amplitude, 39.428 KJ of energy was delivered to the medium, while 75.315 KJ of energy was delivered to the medium on 10 minutes irradiation and 64 % of the drug was released. It can be concluded that the longer the exposure time, the higher the amount of energy imparted to the medium, causing more perturbation into the nanoparticle membrane and accelerating its rate of drug release.

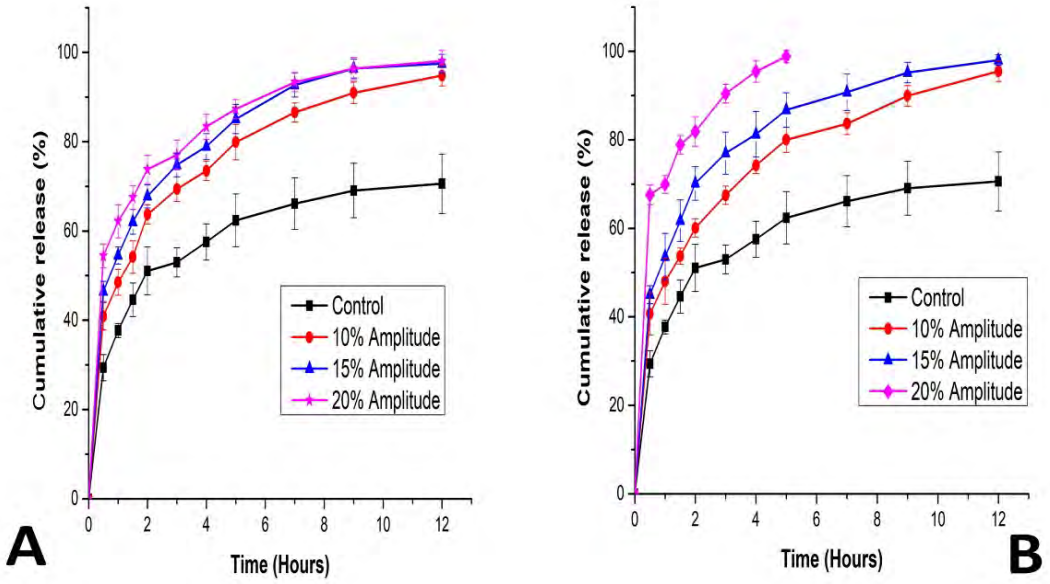

Figure 3.5. 5-FU release from echogenic liposomes exposed to ultrasound of different amplitudes for 5 min (**A**), and 10 min (**B**). 5-FU liposomes (FE) not exposed to ultrasound served as control

3.3.4.2. Effects of gas entrapment on the sensitivity of liposome to ultrasound.

The effect of gas entrapment on the percentage release of the drug from the nanocarrier was further investigated. It was noticed that for the echogenic liposome, 38 ± 4 % of the drug was released on exposure to 10 % amplitude of ultrasound for 10 min, while 16 ± 2 % was released for the non-echogenic liposome (without a gas). This is a significant increase showing the impact of gas entrapment in the carrier's sensitivity to ultrasound triggering resulting to higher quantity of the therapeutic being released. The non-echogenic liposome (without gas) could release such a small percentage because of mechanical effects imparted on the carrier by the ultrasound and as a result of the atmospheric air that was inadvertently entrapped in the bilayer during formulation (Huang *et al.* 2002).

Ultrasound-induced diffusion of gas is evaluated by the composition of the liposomes, the parameters of the ultrasound and the properties of the entrapped gas (Huang 2008). The hypothesis is that ultrasound can cause oscillation comportment of liposomes and push the argon gas to be diffused from the echogenic liposome at a low amplitude. To evaluate the mechanism of argon release from the echogenic liposomes by the application of ultrasound, direct measurement of the amount of argon encapsulated in the liposomes and the amount that diffused out after ultrasound application must be investigated in future research.

3.3.5. Stability studies

Zeta potential of nanoparticles has been proven to affect both their stability, release rate, circulation in the bloodstream, and their absorption into body membranes (Honary and Zahir 2013).

As shown in **Figure 3.6**, all the echogenic liposomes studied for stability maintained their zeta potential within the range of – 47 to – 64 mV from the first day to the 28th day. This confirmed that the nanocarriers were stable for the period under storage at 4°C as no fusion or aggregation was observed. The addition of D-mannitol in the formulation, which serves as a cryoprotectant, and the presence of carbohydrates in the phospholipid mixtures have been shown to contribute to the stability of the echogenic liposomal formulations. The stable ZP further proved the nanocarrier's appropriateness for triggered and control release of the therapeutic agent. It correlates with the study where chitosan proved that its interaction with negatively charged drugs, when entrapped into films, affected the drug release behaviors and the physicochemical characteristics of the drug and the polymer (Puttipipatkhachorn *et al.* 2001).

This result also agreed with the result obtained by Bapolisi *et al.* when they carried out stability studies on crude soy lecithin liposomes entrapping rifampicin and human serum albumin. They discovered that the zeta potential of the formulations was stable for the 28 days study and attributed it to the presence of about 8 % carbohydrates in the crude soy lecithin used in the formation of the liposome, which could serve as cryoprotectant (Bapolisi *et al.* 2020)

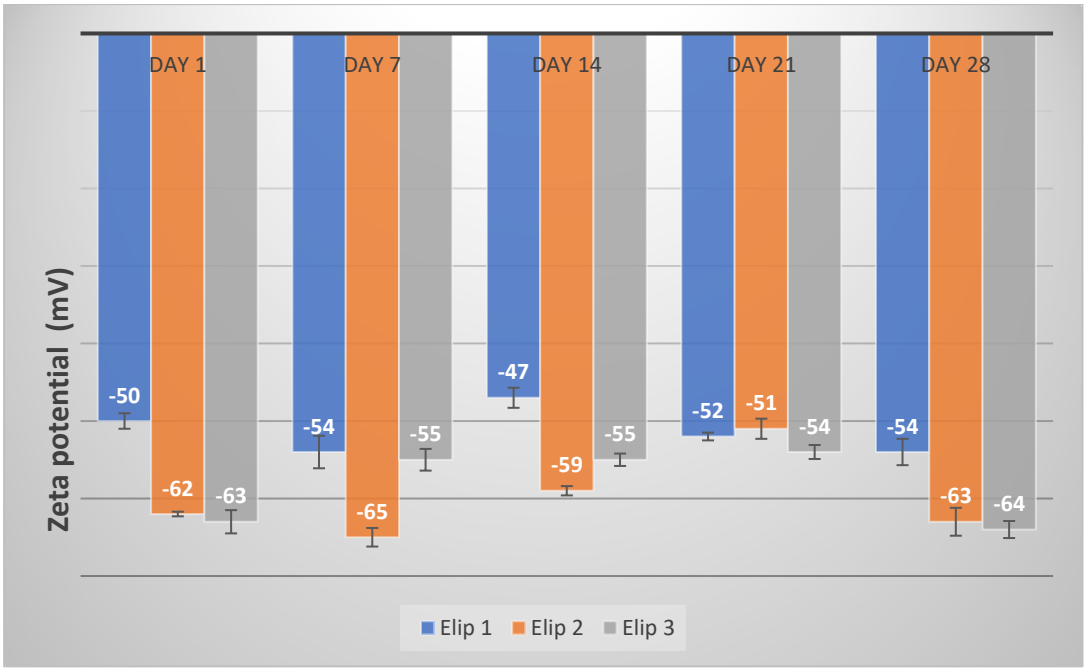

Figure 3.6. DLS result showing the stability study of echogenic liposomes by zeta potential.

3.5. Concluding remarks

This chapter aimed to formulate echogenic liposomes co-encapsulating argon gas and 5-FU in the lipid bilayer and aqueous core respectively using crude soybean lecithin, characterize them and trigger the release of the drug with ultrasound. The formulations showed a percent encapsulation efficiency (% EE) of 58 ± 1%, and all the formulations were shown to be spherical and within the nano-size range. The zeta potential of these formulations (-63 ± 2 mV) is high enough for long storage stability without aggregation and for the drug's triggered and controlled release.

These nanocarriers' exposure to 20 kHz low-frequency ultrasound revealed that a more significant percentage of the drug was released under higher amplitude and longer exposure time. On exposure to 10% amplitude for 5 min, 22% of the drug was released, while 34% was

released when the time was increased to 10 min under the same amplitude. For 20% amplitude and 5 min, 45% of the drug was released, and it also increased to 64% as the time was increased to 10 min. This agrees with what has been reported in the literature that higher amplitude and longer exposure time increased the percentage release of drugs in echogenic liposomes when triggered with ultrasound (Abed *et al.* 2018).

The cumulative release profile studied under phosphate buffer pH 7.4 also revealed that the higher the amplitude and the longer the exposure time, the greater the drug percentage release. All the formulations exposed to ultrasound were released up to 95 % in 12 h, while the control that was not exposed to ultrasound was released up to 70 %.

However, the total mechanism behind the ultrasound-mediated disruption of liposomes bilayers remains to be clarified, but the reality that less energy is needed to achieve drug release from echogenic liposomes compared to the control could be of good clinical importance because it will help in reducing damage to healthy cells and tissues during treatment. The release of this chemotherapeutic agent from the liposome by exposure to low-frequency ultrasound within the selected amplitude and exposure time may help in the development of concepts on the potential use of low-frequency ultrasound to trigger and control the release of drugs from liposomes. It should, however, be noted that for clinical applications, a focused ultrasound transducer with high frequency is required to enhance focusing ability (Evjen *et al.* 2011).

Though this formulation was meant to be applied to a colorectal cancer cell in an *in/ex vivo* experiment to determine its efficacy in slowing down the growth of the cancer cell, and to evaluate the release rate of the 5-FU with and without ultrasound triggering, this could not be achieved however because of limited resources caused by the outbreak of COVID-19. This serves as limitation of this research and the future plan.

4. GENERAL CONCLUSION

The main aim of this research was to design, formulate, and evaluate an echogenic liposome co-encapsulating argon gas and 5-fluorouracil, a first-line chemotherapeutic regimen in the treatment of colorectal cancer. Both were entrapped in the lipid bilayer and the aqueous core respectively by the thin-film hydration method using crude soybean lecithin. The formulation was also exposed to 20 kHz low-frequency ultrasound, which triggered the release of the therapeutic agent under various amplitudes and exposure time, and their release profile was examined.

The average particle size of the echogenic liposomes was in the nano-size of about 160 nm. The higher negative zeta potential (-62 ± 1 mV) is also good for the nanocarrier's long shelf stability without aggregation. Encapsulation efficiency (% EE) of 56 ± 1 % was achieved, and this will enhance the possibility of delivering the drug to the tumor cell in a controlled and sustained manner.

Argon and 5-fluoruracil were successfully co-encapsulated in the echogenic liposomes which made it possible to study the effect of ultrasound stimulation on the nanocarrier release profile which showed that the higher the amplitude and the longer the exposure time, the greater the percentage of drug released. The cumulative release profile conducted under the application of ultrasound and compared to the release profile without application of ultrasound also reviewed a higher percentage release of up to 99 % percent when ultrasound was applied and 70 % without ultrasound. This novel and facile method for producing echogenic liposomes for ultrasound triggered drug delivery may lead to further investigation into the practical *in vivo* systems of drug delivery related to colorectal cancer.

This present study detailed the possibility of using two non-expensive, naturally occurring and readily available components, crude soil lecithin and argon in the production of echogenic liposomes in place of synthetic phospholipids and expensive perfluorocarbon gases. This may encourage other researchers to investigate the possibility of using other natural occurring lipid components and medical gases like crude rice lecithin and helium respectively in large scale production of echogenic liposome for triggerable drug delivery. The release of this chemotherapeutic agent from the liposome by exposure to low-frequency ultrasound within the

selected amplitude and exposure time may help develop concepts on the potential use of low-frequency ultrasound to trigger and control the release of drugs from liposomes.

The presence of D-mannitol which served as a cryoprotectant for the freeze-dried echogenic liposomes greatly improved its shelf stability which is a drawback to the wider applications of the liposomes.. The presence of this D-mannitol during freezing was also vital for the formulation of the gas-containing liposome. The solution lead to lipid fusion resulting to the formation of gas bubble in the lipid bilayer (Huang *et al.* 2001). The use of D-mannitol both increased the gas encapsulation efficiency and ultrasound sensitivity (Antimisiaris 2017).

To the best of our knowledge, this is the first work detailing the co-encapsulation of argon and 5-FU in crude soy lecithin liposome and triggering the release of the drug with ultrasound. Because of the inexpensive nature and availability of these phospholipids compared to their synthetic and some natural phospholipid components, this work might help optimize and further investigate large-scale production of these novel echogenic liposomal formulation towards the management of colorectal cancer and other types of diseases.

The presence of this gas in the liposomes was confirmed by exposing the same amount of the echogenic liposome (with a gas) and conventional liposome (without a gas) in the ultrasound system, the echogenic liposome exhibited higher echogenicity and greater drug release than the conventional liposome. Moreover, further research is needed to evaluate the exact amount of the gas entrapped in the nanoparticle. Ultrasound-triggered 5-FU release from the echogenic liposomes needs to be investigated through *in vivo* experiments for targeted chemotherapy to a colorectal cancer cell in a mice model. Future plans in particular include:

1. To estimate the exact amount of argon gas encapsulated in the echogenic liposomes before exposure to ultrasound by using improved gas chromatographic method.
2. To evaluate the exact quantity of the argon gas that was released after exposure to ultrasound by improved gas chromatographic method (An and Joye 1997).
3. To evaluate the efficacy of the echogenic liposomes in an *in/ex vivo* experiment using a colorectal cancer cell.
4. Modification of the formation with some ligands that enhance “theranostic” effects and investigation of their in *vivo* imaging capabilities.
5. To investigate the echogenic properties of other bioactive gases like helium, xenon using other readily available phospholipid like crude rice lecithin.

REFERENCES

Abed, Z., Beik, J., Khoee, S., Khoei, S., Shakeri-Zadeh, A., & Shiran, M.B., 2016. Effects of Ultrasound Irradiation on the Release Profile of 5-fluorouracil from Magnetic Polylactic co-glycolic Acid Nanocapsules. *J. Biol. Chem.*, 6 (3), 183–194.

Abed, Z., Khoei, S., Ghalandari, B., Beik, J., Shakeri-Zadeh, A., Ghaznavi, H., and Shiran, M.-B., 2018. The Measurement and Mathematical Analysis of 5-Fu Release from Magnetic Polymeric Nanocapsules, following the Application of Ultrasound. *Anti-Cancer Agents in Medicinal Chemistry*, 18 (3), 438–449.

Achim, M., Precup, C., Gonganăuniţu, D., Barbu-Tudoran, L., Porfire, A.S., Scurtu, R., and Ciuce, C., 2009. Thermosensitive liposomes containing doxorubicin. Preparation and in vitro evaluation. *Farmacia*, 57 (6), 703–710.

Adriana, R.M., Leticia, M. de A., Maria, I.R.M., and Leonor, A. de S.-S., 2014. Importance of lecithin for encapsulation processes. *African Journal of Food Science*, 8 (4), 176–183.

Afadzi, M., Strand, S., Nilssen, E.A., Masoy, S.E., Johansen, T., Hansen, R., Angelsen, B., and De L. Davies, C., 2013. Mechanisms of the ultrasound-mediated intracellular delivery of liposomes and dextrans. *IEEE Transactions on Ultrasonics, Ferroelectrics, and Frequency Control*, 60 (1), 21–33.

Ahmed, S.E., Martins, A.M., and Husseini, G.A., 2014. The use of ultrasound to release chemotherapeutic drugs from micelles and liposomes. *Journal of Drug Targeting*, 2330 (1), 1–27.

Akaza, H., 2019. International agency for research on cancer (IARC). *Japanese Journal of Cancer and Chemotherapy*, 46 (1), 34–35.

Akbarzadeh, A., Rezaei-Sadabady, R., Davaran, S., Joo, S.W., Zarghami, N., Hanifehpour, Y., Samiei, M., Kouhi, M., and Nejati-Koshki, K., 2013. Liposome: Classification, preparation, and applications. *Nanoscale Research Letters*, 8 (1), 1.

Alving, C.R., Schneider, I., Swartz, G.M., and Steck, E.A., 1979. Sporozoite-induced malaria: Therapeutic effects of glycolipids in liposomes. *Science*, 205 (4411), 1142–1144.

An, S. and Joye, S.B., 1997. An improved chromatographic method to measure nitrogen, oxygen, argon and methane in gas or liquid samples. *Marine Chemistry*, 59 (1–2), 63–70.

André, T., De Gramont, A., Vernerey, D., Chibaudel, B., Bonnetain, F., Tijeras-Raballand, A., Scriva, A., Hickish, T., Tabernero, J., Van Laethem, J.L., Banzi, M., Maartense, E., Shmueli, E., Carlsson, G.U., Scheithauer, W., Papamichael, D., Möehler, M., Landolfi, S., Demetter, P., Colote, S., Tournigand, C., Louvet, C., Duval, A., Fléjou, J.F., and De Gramont, A., 2015. Adjuvant fluorouracil, leucovorin, and oxaliplatin in stage II to III colon cancer: Updated 10-year survival and outcomes according to BRAF mutation and mismatch repair status of the MOSAIC study. *Journal of Clinical Oncology*, 33 (35), 4176–4187.

Antimisiaris, S.G., 2017. Preparation of DRV liposomes. *Methods in Molecular Biology*, 1522, 23–47.

Anwekar, H., Patel, S., and Singhai, A.K., 2011. Liposome-as drug carriers. *Int. J. of Pharm. & Life Sci. (IJPLS)*, 2 (7), 945–951.

Aryal, M., Vykhodtseva, N., Zhang, Y.Z., Park, J., and McDannold, N., 2013. Multiple treatments with liposomal doxorubicin and ultrasound-induced disruption of blood-tumor and blood-brain barriers improve outcomes in a rat glioma model. *Journal of Controlled Release*, 169 (1–2), 103–111.

Ayyappan, J., Umapathi, P., and Darlin Quine, S., 2011. Development and validation of a stability indicating high-performance liquid chromatography (HPLC) method for the estimation of isoniazid and its related substances in fixed dose combination of isoniazid and ethambutol hydrochloride tablets. *African Journal of Pharmacy and Pharmacology*, 5 (12), 1513–1521.

Balon, N., Kriem, B., Dousset, E., Weiss, M., and Rostain, J.C., 2002. Opposing effects of narcotic gases and pressure on the striatal dopamine release in rats. *Brain Research*, 947 (2), 218–224.

Banerjee, R., 2001. Liposomes: Applications in medicine. *Journal of Biomaterials Applications*, 16 (1), 3–21.

Bangham, A.D., Standish, M.M., and Watkins, J.C., 1965. Diffusion of Univalent Ions across the Lamellae of Swollen Phospholipids. *Journal of Molecular Biology*, 13 (1), 238–252, IN26–IN27.

Bapolisi, A.M., Nkanga, C.I., Walker, R.B., and Krause, R.W.M., 2020. Simultaneous liposomal encapsulation of antibiotics and proteins: Co-loading and characterization of

rifampicin and Human Serum Albumin in soy-liposomes. *Journal of Drug Delivery Science and Technology*, 58 (May), 101751.

Barnett, S.B., Ter Haar, G.R., Ziskin, M.C., Rott, H.D., Duck, F.A., and Maeda, K., 2000. International recommendations and guidelines for the safe use of diagnostic ultrasound in medicine. *Ultrasound in Medicine and Biology*, 26 (3), 355–366.

Barry, B.W., 2001. Novel mechanisms and devices to enable successful transdermal drug delivery. *European Journal of Pharmaceutical Sciences*, 14 (2), 101–114.

Bartsch, H. and Nair, J., 2006. Chronic inflammation and oxidative stress in the genesis and perpetuation of cancer: Role of lipid peroxidation, DNA damage, and repair. *Langenbeck's Archives of Surgery*, 391 (5), 499–510.

Bray, F., Ferlay, J., Soerjomataram, I., Siegel, R.L., Torre, L.A., and Jemal, A., 2018. Global cancer statistics 2018: GLOBOCAN estimates of incidence and mortality worldwide for 36 cancers in 185 countries. *CA: A Cancer Journal for Clinicians*, 68 (6), 394–424.

Britton, G.L., Kim, H., Kee, P.H., Aronowski, J., Holland, C.K., McPherson, D.D., and Huang, S.L., 2010. In vivo therapeutic gas delivery for neuroprotection with echogenic liposomes. *Circulation*, 122 (16), 1578–1587.

Buchanan, K.D., Huang, S.L., Kim, H., McPherson, D.D., and MacDonald, R.C., 2010. Encapsulation of NF-κB decoy oligonucleotides within echogenic liposomes and ultrasound-triggered release. *Journal of Controlled Release*, 141 (2), 193–198.

Carlson, R.W., Larsen, J.K., McClure, J., Fitzgerald, C.L., Venook, A.P., Benson, A.B., and Anderson, B.O., 2014. International adaptations of NCCN clinical practice guidelines in oncology. *JNCCN Journal of the National Comprehensive Cancer Network*, 12 (5), 643–648.

Carugo, D., Bottaro, E., Owen, J., Stride, E., and Nastruzzi, C., 2016. Liposome production by microfluidics: Potential and limiting factors. *Scientific Reports*, 6, 1–15.

Chauhan, A., 2014. Powder XRD Technique and its Applications in Science and Technology. *Journal of Analytical & Bioanalytical Techniques*, 5 (6), 129-137.

Costa, A.P., Xu, X., and Burgess, D.J., 2014. Freeze-anneal-thaw cycling of unilamellar liposomes: Effect on encapsulation efficiency. *Pharmaceutical Research*, 31 (1), 97–103.

Coussios, C.C., Farny, C.H., ter Haar, G., and Roy, R.A., 2007. Role of acoustic cavitation in the delivery and monitoring of cancer treatment by high-intensity focused ultrasound (HIFU). *International Journal of Hyperthermia*, 23 (2), 105–120.

Dermime, S., 2013. Cancer Diagnosis, Treatment and Therapy. *Journal of Carcinogenesis & Mutagenesis*, S14, 7–8.

Deshpande, P.P., Biswas, S., and Torchilin, V.P., 2013. Current trends in the use of liposomes for tumor targeting. *Nanomedicine*, 8 (9), 1509-1528.

Diasio, R.B. and Harris, B.E., 1989. Clinical Pharmacology of 5-Fluorouracil. *Clinical Pharmacokinetics*, 16 (4), 215-237.

Dinh, T.T.N., Thompson, L.D., Galyean, M.L., Brooks, J.C., Patterson, K.Y., and Boylan, L.M., 2011. Cholesterol content and methods for cholesterol determination in meat and poultry. *Comprehensive Reviews in Food Science and Food Safety*, 10 (15), 269-289.

Domańska, U., Klofutar, C., and Paljk, Š., 1994. Solubility of cholesterol in selected organic solvents. *Fluid Phase Equilibria*, 97 (C), 191–200.

Draper, D.O., Castel, J.C., and Castel, D., 1995. Rate of temperature increase in human muscle during 1 MHz and 3 MHz continuous ultrasound. *Journal of Orthopaedic and Sports Physical Therapy*, 22 (4), 142–150.

Durowoju, I.B., Bhandal, K.S., Hu, J., Carpick, B., and Kirkitadze, M., 2017. Differential scanning calorimetry — A method for assessing the thermal stability and conformation of protein antigen. *Journal of Visualized Experiments*, 2017 (121), 391–395.

Evjen, T.J., Nilssen, E.A., Barnert, S., Schubert, R., Brandl, M., and Fossheim, S.L., 2011. Ultrasound-mediated destabilization and drug release from liposomes comprising dioleoylphosphatidylethanolamine. *European Journal of Pharmaceutical Sciences*, 42 (4), 380–386.

Fan, Y.L., Fan, B.Y., Li, Q., Di, H.X., Meng, X.Y., and Ling, N., 2014. Preparation of 5-fluorouracil-loaded nanoparticles and study of interaction with gastric cancer cells. *Asian Pacific Journal of Cancer Prevention*, 15 (18), 7611–7615.

Fleige, E., Quadir, M.A., and Haag, R., 2012. Stimuli-responsive polymeric nanocarriers for the controlled transport of active compounds: Concepts and applications. *Advanced Drug Delivery Reviews*, 64 (9), 866-884.

Fleming, M., Ravula, S., Tatishchev, S.F., and Wang, H.L., 2012. Colorectal carcinoma: Pathologic aspects. *Journal of Gastrointestinal Oncology*, 3 (3), 153-173.

Frenkel, V., 2008. Ultrasound mediated delivery of drugs and genes to solid tumors. *Advanced Drug Delivery Reviews*, 60 (10), 1193-1208.

Giron, D., 2002. Applications of thermal analysis and coupled techniques in pharmaceutical industry. *In*: *Journal of Thermal Analysis and Calorimetry*. 335–357.

Gregoriadis, G., 1983. Liposomes as drug carriers. *Pharmacy International*, 4 (2), 33–37.

Gregoriadis, G., da Silva, H., and Florence, A.T., 1990. A procedure for the efficient entrapment of drugs in dehydration-rehydration liposomes (DRVs). *International Journal of Pharmaceutics*, 65 (3), 235–242.

Gujral, R.S. and Haque, S.M., 2009. Development and validation of a new HPLC method for the determination of gabapentin. *International Journal of Biomedical Science*, 5 (1), 63–69.

Gupta, A., Tiwari, G., Tiwari, R., Srivastava, R., and Rai, A.K., 2015. Enteric coated HPMC capsules plugged with 5-FU loaded microsponges: A potential approach for treatment of colon cancer. *Brazilian Journal of Pharmaceutical Sciences*, 51 (3), 591–606.

Hajdu, S.I., 2011. A note from history: Landmarks in history of cancer, part 2. *Cancer*, 117 (12), 1097–1102.

Hajdu, S.I., 2012. A note from history: Landmarks in history of cancer, part 4. *Cancer*, 118 (20), 4914–4928.

Halazonetis, T.D., Gorgoulis, V.G., and Bartek, J., 2008. An oncogene-induced DNA damage model for cancer development. *Science*, 319 (5868), 1352–1355.

Honary, S. and Zahir, F., 2013. Effect of zeta potential on the properties of nano-drug delivery systems - A review (Part 1). *Tropical Journal of Pharmaceutical Research*, 12 (2), 255–264.

Hosokawa, T., Sami, M., Kato, Y., and Hayakawa, E., 2003. Alteration in the temperature-dependent content release property of thermosensitive liposomes in plasma. *Chemical and Pharmaceutical Bulletin*, 51 (11), 1227–1232.

Hu, X., Zhang, Y., Xie, Z., Jing, X., Bellotti, A., and Gu, Z., 2017. Stimuli-Responsive

Polymersomes for Biomedical Applications. *Biomacromolecules*, 18 (3), 649–673.

Huang, S.L., 2008. Liposomes in ultrasonic drug and gene delivery. *Advanced Drug Delivery Reviews*, 60 (10), 1167–1176.

Huang, S.L., Hamilton, A.J., Nagaraj, A., Tiukinhoy, S.D., Klegerman, M.E., McPherson, D.D., and Macdonald, R.C., 2001. Improving ultrasound reflectivity and stability of echogenic liposomal dispersions for use as targeted ultrasound contrast agents. *Journal of Pharmaceutical Sciences*, 90 (12), 1917–1926.

Huang, S.L., Hamilton, A.J., Pozharski, E., Nagaraj, A., Klegerman, M.E., McPherson, D.D., and MacDonald, R.C., 2002. Physical correlates of the ultrasonic reflectivity of lipid dispersions suitable as diagnostic contrast agents. *Ultrasound in Medicine and Biology*, 28 (3), 339–348.

Huang, S.L., Kee, P.H., Kim, H., Moody, M.R., Chrzanowski, S.M., MacDonald, R.C., and McPherson, D.D., 2009. Nitric Oxide-Loaded Echogenic Liposomes for Nitric Oxide Delivery and Inhibition of Intimal Hyperplasia. *Journal of the American College of Cardiology*, 54 (7), 652–659.

Huang, S.L. and MacDonald, R.C., 2004. Acoustically active liposomes for drug encapsulation and ultrasound-triggered release. *Biochimica et Biophysica Acta - Biomembranes*, 1665 (1–2), 134–141.

Huang, S.L., McPherson, D.D., and MacDonald, R.C., 2008. A Method to Co-Encapsulate Gas and Drugs in Liposomes for Ultrasound-Controlled Drug Delivery. *Ultrasound in Medicine and Biology*, 34 (8), 1272–1280.

Huang, Z., Li, X., Zhang, T., Song, Y., She, Z., Li, J., and Deng, Y., 2014. Progress involving new techniques for liposome preparation. *Asian Journal of Pharmaceutical Sciences*, 9 (4), 176-182.

Huwyler, J., Drewe, J., and Krähenbühl, S., 2008. Tumor targeting using liposomal antineoplastic drugs. *International Journal of Nanomedicine*, 3 (1), 21-29.

Hynynen, K., McDannold, N., Vykhodtseva, N., Raymond, S., Weissleder, R., Jolesz, F.A., and Sheikov, N., 2006. Focal disruption of the blood-brain barrier due to 260-kHz ultrasound bursts: A method for molecular imaging and targeted drug delivery. *Journal of Neurosurgery*, 105 (3), 445–454.

Joshi, B. and Joshi, A., 2019. *Ultrasound-based drug delivery systems*. Bioelectronics and Medical Devices: From Materials to Devices - Fabrication, Applications and Reliability. Elsevier Ltd, 241-260.

Karami, N., Moghimipour, E., and Salimi, A., 2018. Liposomes as a novel drug delivery system: Fundamental and pharmaceutical application. *Asian Journal of Pharmaceutics*, 12 (1), S31–S41.

Karan, S., Choudhury, H., Chakra, B.K., and Chatterjee, T.K., 2019. Polymeric microsphere formulation for colon targeted delivery of 5-fluorouracil using biocompatible natural gum katira. *Asian Pacific Journal of Cancer Prevention*, 20 (7), 2181–2194.

Kauscher, U., Holme, M.N., Björnmalm, M., and Stevens, M.M., 2019. Physical stimuli-responsive vesicles in drug delivery : Beyond liposomes and polymersomes, 138, 259–275.

Ken-ichi Fujita and Yasutsuna Sasaki, 2007. Pharmacogenomics in Drug-Metabolizing Enzymes Catalyzing Anticancer Drugs for Personalized Cancer Chemotherapy. *Current Drug Metabolism*, 8 (6), 554–562.

Kopechek, J.A., Haworth, K.J., Raymond, J.L., Douglas Mast, T., Perrin, S.R., Klegerman, M.E., Huang, S., Porter, T.M., McPherson, D.D., and Holland, C.K., 2011. Acoustic characterization of echogenic liposomes: Frequency-dependent attenuation and backscatter. *The Journal of the Acoustical Society of America*, 130 (5), 3472–3481.

Laouini, A., Jaafar-Maalej, C., Limayem-Blouza, I., Sfar, S., Charcosset, C., and Fessi, H., 2012. Preparation, Characterization and Applications of Liposomes: State of the Art. *Journal of Colloid Science and Biotechnology*, 1 (2), 147–168.

Le, N.T.T., Cao, V. Du, Nguyen, T.N.Q., Le, T.T.H., Tran, T.T., and Thi, T.T.H., 2019. Soy lecithin-derived liposomal delivery systems: Surface modification and current applications. *International Journal of Molecular Sciences*, 20 (19), 108-119.

Leighton, T.G., 2007. What is ultrasound? *Progress in Biophysics and Molecular Biology*, 93 (1-3), 3-83.

Lentacker, I., Geers, B., Demeester, J., De Smedt, S.C., and Sanders, N.N., 2010. Design and evaluation of doxorubicin-containing microbubbles for ultrasound-triggered doxorubicin delivery: Cytotoxicity and mechanisms involved. *Molecular Therapy*, 18 (1), 101–108.

Levin, B., Lieberman, D.A., McFarland, B., Smith, R.A., Brooks, D., Andrews, K.S., Dash, C., Giardiello, F.M., Glick, S., Levin, T.R., Pickhardt, P., Rex, D.K., Thorson, A., and Winawer, S.J., 2008. Screening and Surveillance for the Early Detection of Colorectal Cancer and Adenomatous Polyps, 2008: A Joint Guideline from the American Cancer Society, the US Multi-Society Task Force on Colorectal Cancer, and the American College of Radiology. *CA: A Cancer Journal for Clinicians*, 58 (3), 130–160.

Li, J., Wang, X., Zhang, T., Wang, C., and Huang, Z., 2016. A review on phospholipids and their main applications in drug delivery systems ScienceDirect A review on phospholipids and their main applications in drug delivery systems. *Asian Journal of Pharmaceutical Sciences*, 10 (2), 81–98.

Li, P., Wang, Y., Peng, Z., She, M.F., and Kong, L., 2010. Physichemical property and morphology of 5-fluorouracil loaded chitosan nanoparticles. *ICONN 2010 - Proceedings of the 2010 International Conference on Nanoscience and Nanotechnology*, 248–250.

Lin, H.Y. and Thomas, J.L., 2003. PEG-lipids and oligo (ethylene glycol) surfactants enhance the ultrasonic permeabilizability of liposomes. *Langmuir*, 19 (4), 1098–1105.

Longley, D.B., Harkin, D.P., and Johnston, P.G., 2003. 5-Fluorouracil: Mechanisms of action and clinical strategies. *Nature Reviews Cancer*, 3 (5), 330-338.

Lopes, S., Simeonova, M., Gameiro, P., Rangel, M., and Ivanova, G., 2012. Interaction of 5-fluorouracil loaded nanoparticles with 1,2-dimyristoyl- sn -glycero-3-phosphocholine liposomes used as a cellular membrane model. *Journal of Physical Chemistry B*, 116 (1), 667–675.

López-Pinto, J.M., González-Rodríguez, M.L., and Rabasco, A.M., 2005. Effect of cholesterol and ethanol on dermal delivery from DPPC liposomes. *International Journal of Pharmaceutics*, 298 (1), 1–12.

Mahmoud, M., Labiba, N., Khalil, E.K., and Khalafallah, N., 2005. Release stability of 5-fluorouracil liposomal concentrates, gels and lyophilized powder. *Acta Poloniae Pharmaceutica - Drug Research*, 62 (5), 381–391.

Maring, J.G., Schouten, L., Greijdanus, B., De Vries, E.G.E., and Uges, D.R.A., 2005. A simple and sensitive fully validated HPLC-UV method for the determination of 5-fluorouracil and its metabolite 5,6-dihydrofluorouracil in plasma. *Therapeutic Drug Monitoring*, 27 (1), 25–30.

Masato, K., Shinji, U., Naoto, T., and Yasutaka, O., 2012. Validation of analytical procedures by high − performance liquid chromatography for pharmaceutical analysis. *Chromatography*, 33 (2), 65–73.

Mitragotri, S., 2005. Healing sound: The use of ultrasound in drug delivery and other therapeutic applications. *Nature Reviews Drug Discovery*, 4 (3), 255–260.

Mitragotri, S. and Kost, J., 2004. Low-frequency sonophoresis: A review. *Advanced Drug Delivery Reviews*, 56 (5), 589–601.

Miura, K., Kinouchi, M., Ishida, K., Fujibuchi, W., Naitoh, T., Ogawa, H., Ando, T., Yazaki, N., Watanabe, K., Haneda, S., Shibata, C., and Sasaki, I., 2010. 5-FU metabolism in cancer and orally-administrable 5-FU drugs. *Cancers*, 2 (3), 1717–1730.

Moosavian, S.A., Abnous, K., Akhtari, J., Arabi, L., Gholamzade Dewin, A., and Jafari, M., 2018. 5TR1 aptamer-PEGylated liposomal doxorubicin enhances cellular uptake and suppresses tumour growth by targeting MUC1 on the surface of cancer cells. *Artificial Cells, Nanomedicine and Biotechnology*, 46 (8), 2054–2065.

Mozafari, M.R., Javanmard, R., and Raji, M., 2017. Tocosome: Novel drug delivery system containing phospholipids and tocopheryl phosphates. *International Journal of Pharmaceutics*, 528 (1–2), 381–382.

Muggia, F.M., 2001. Liposomal encapsulated anthracyclines: new therapeutic horizons. *Current oncology reports*, 3 (2), 156–162.

Mura, P., Faucci, M.T., Manderioli, A., Bramanti, G., and Ceccarelli, L., 1998. Compatibility study between ibuproxam and pharmaceutical excipients using differential scanning calorimetry, hot-stage microscopy and scanning electron microscopy. *Journal of Pharmaceutical and Biomedical Analysis*, 18 (1–2), 151–163.

Nakayama, G., Tanaka, C., and Kodera, Y., 2013. Current Options for the Diagnosis, Staging and Therapeutic Management of Colorectal Cancer. *Gastrointestinal Tumors*, 1 (1), 25–32.

Ning, S., Karen, M., Robert, M.A., Anthony, H.H., and George, M.H., 1994. Hyperthermia Induces Doxorubicin Release From Long Circulating Liposomes And Enhances Their Anti-tumor Efficacy. *Int. J. Radiation Oncology Biol. Phys*, 29 (I), 125–132.

Nkanga, C., Werner, R., Siwe, X., and Bryan, R., 2017. Preparation and characterization of

isoniazid-loaded crude soybean lecithin liposomes. *International Journal of Pharmaceutics*, 526 (1–2), 466–473.

Nkanga, C.I., Noundou, X.S., Walker, R.B., and Krause, R.W.M., 2019. Co-encapsulation of Rifampicin and Isoniazid in Crude Soybean Lecithin Liposomes. *South African Journal of Chemistry*, 72 (May), 80–87.

Nkanga, C.I., Walker, R.B., and Krause, R.W., 2018. pH-Dependent release of isoniazid from isonicotinic acid (4-hydroxy-benzylidene)-hydrazide loaded liposomes. *Journal of Drug Delivery Science and Technology*, 45 (March), 264–271.

Nowrangi, D.S., Tang, J., and Zhang, J.H., 2014. Argon gas: A potential neuroprotectant and promising medical therapy. *Medical Gas Research*, 4 (1), 1–8.

Ohlsson, G., Tabaei, S.R., Beech, J., Kvassman, J., Johanson, U., Kjellbom, P., Tegenfeldt, J.O., and Höök, F., 2012. Solute transport on the sub 100 ms scale across the lipid bilayer membrane of individual proteoliposomes. *Lab on a Chip*, 12 (22), 4635–4643.

Ou, J., Peng, Y., Yang, W., Zhang, Y., Hao, J., Li, F., Chen, Y., Zhao, Y., Xie, X., Wu, S., Zha, L., Luo, X., Xie, G., Wang, L., Sun, W., Zhou, Q., Li, J., and Liang, H., 2019. ABHD5 blunts the sensitivity of colorectal cancer to fluorouracil via promoting autophagic uracil yield. *Nature Communications*, 10 (1), 1–14.

Papahadjopoulos, D., Allen, T.M., Gabizon, A., Mayhew, E., Matthay, K., Huang, S.K., Lee, K.D., Woodle, M.C., Lasic, D.D., Redemann, C., and Martin, F.J., 1991. Sterically stabilized liposomes: Improvements in pharmacokinetics and antitumor therapeutic efficacy. *Proceedings of the National Academy of Sciences of the United States of America*, 88 (24), 11460–11464.

Pardini, B., Kumar, R., Naccarati, A., Novotny, J., Prasad, R.B., Forsti, A., Hemminki, K., Vodicka, P., and Lorenzo Bermejo, J., 2011. 5-Fluorouracil-based chemotherapy for colorectal cancer and MTHFR/MTRR genotypes. *British Journal of Clinical Pharmacology*, 72 (1), 162–163.

Pattni, B.S., Chupin, V. V., and Torchilin, V.P., 2015. New Developments in Liposomal Drug Delivery. *Chemical Reviews*, 115 (19), 10938–10966.

Pitot, C. and Dragan, P., 1991. Facts the mechanisms of carcinogenesis. *Faseb*, 5, 2280–2286.

Pitt, W.G., Husseini, G., and Staples, B.J., 2004. Ultrasonic drug delivery - A general review.

Expert Opinion on Drug Delivery, 1 (1), 37-56.

Podell, S., Burrascano, C., Gaal, M., Golec, B., Maniquis, J., and Mehlhaff, P., 1999. Physical and biochemical stability of Optison®, an injectable ultrasound contrast agent. *Biotechnology and Applied Biochemistry*, 30 (3), 213–223.

Provder, T., 1997. Challenges in particle size distribution measurement past, present and for the 21st century. *Progress in Organic Coatings*, 32 (1–4), 143–153.

Puttipipatkhachorn, S., Nunthanid, J., Yamamoto, K., and Peck, G.E., 2001. Drug physical state and drug-polymer interaction on drug release from chitosan matrix films. *Journal of Controlled Release*, 75 (1–2), 143–153.

Radhakrishnan, K., Haworth, K.J., Huang, S.L., Klegerman, M.E., McPherson, D.D., and Holland, C.K., 2012. Stability of Echogenic Liposomes as a Blood Pool Ultrasound Contrast Agent in a Physiologic Flow Phantom. *Ultrasound in Medicine and Biology*, 38 (11), 1970–1981.

Reich, O., Mseddi, A., Zaak, D., Trottmann, M., Hungerhuber, E., and Schneede, P., 2004. Use of argon plasma coagulation in endourology: In vitro experiments. *Urology*, 63 (2), 387–391.

Rizzitelli, S., Giustetto, P., Boffa, C., Delli Castelli, D., Cutrin, J.C., Aime, S., and Terreno, E., 2014. In vivo MRI visualization of release from liposomes triggered by local application of pulsed low-intensity non-focused ultrasound. *Nanomedicine: Nanotechnology, Biology, and Medicine*, 10 (5), e901–e904.

Samad, A., Sultana, Y., and Aqil, M., 2007. Liposomal Drug Delivery Systems: An Update Review. *Current Drug Delivery*, 4 (4), 297–305.

Schmoll, H.J., Van cutsem, E., Stein, A., Valentini, V., Glimelius, B., Haustermans, K., Nordlinger, B., Van de Velde, C.J., Balmana, J., Regula, J., Nagtegaal, I.D., Beets-Tan, R.G., Arnold, D., Ciardiello, F., Hoff, P., Kerr, D., Köhne, C.H., Labianca, R., Price, T., Scheithauer, W., Sobrero, A., Tabernero, J., Aderka, D., Barroso, S., Bodoky, G., Douillard, J.Y., El ghazaly, H., Gallardo, J., Garin, A., Glynne-jones, R., Jordan, K., Meshcheryakov, A., Papamichail, D., Pfeiffer, P., Souglakos, I., Turhal, S., and Cervantes, A., 2012. Esmo consensus guidelines for management of patients with colon and rectal cancer. A personalized approach to clinical decision making. *Annals of Oncology*, 23 (10), 2479–2516.

Schroeder, A., Avnir, Y., Weisman, S., Najajreh, Y., Gabizon, A., Talmon, Y., Kost, J., and Barenholz, Y., 2007. Controlling liposomal drug release with low frequency ultrasound: Mechanism and feasibility. *Langmuir*, 23 (7), 4019–4025.

Schroeder, A., Kost, J., and Barenholz, Y., 2009. Ultrasound, liposomes, and drug delivery: principles for using ultrasound to control the release of drugs from liposomes. *Chemistry and Physics of Lipids*, 162 (1-2), 1-16.

Sharma, A. and Sharma, U.S., 1997. Liposomes in drug delivery: Progress and limitations. *International Journal of Pharmaceutics*, 1 (2), 6–16.

Sharma Vijay, K., Mishra, D.N., Sharma, A.K., and Srivastava, B., 2010. Liposomes: Present prospective and future challenges. *International Journal of Current Pharmaceutical Review and Research*, 1 (2), 6–16.

Shaw, G.J., Meunier, J.M., Huang, S.L., Lindsell, C.J., McPherson, D.D., and Holland, C.K., 2009. Ultrasound-enhanced thrombolysis with tPA-loaded echogenic liposomes. *Thrombosis Research*, 124 (3), 306–310.

Siegel, R., DeSantis, C., and Jemal, A., 2014. Colorectal cancer statistics, 2014. *CA: A Cancer Journal for Clinicians*, 64 (2), 104–117.

Sierra, H., Cordova, M., Chen, C.S.J., and Rajadhyaksha, M., 2015. Confocal imaging-guided laser ablation of basal cell carcinomas: An ex vivo study. *Journal of Investigative Dermatology*, 135 (2), 612–615.

Singh, C., Koduri, L.V.S.K., Singh, A., and Suresh, S., 2015. Novel potential for optimization of antitubercular therapy: Pulmonary delivery of rifampicin lipospheres. *Asian Journal of Pharmaceutical Sciences*, 10 (6), 549–562.

Stratmeyer, M.E. and Christman, C.L., 1983. Biological effects of ultrasound. *Women and Health*, 7 (3–4), 65–82.

Sudhakar, A., 2009. History of Cancer, Ancient and Modern Treatment Methods. *Journal of Cancer Science & Therapy*, 01 (02), i–iv.

Szebeni, J., Winterbourn, C.C., and Carrell, R.W., 1984. Oxidative interactions between haemoglobin and membrane lipid. A liposome model. *Biochemical Journal*, 220 (3), 685–692.

Szoka, F. and Papahadjopoulos, D., 1978. Procedure for preparation of liposomes with large internal aqueous space and high capture by reverse-phase evaporation. *Proceedings of the National Academy of Sciences of the United States of America*, 75 (9), 4194–4198.

Tata, D.B. and Dunn, F., 1992. Interaction of ultrasound and model membrane systems: Analyses and predictions. *Journal of Physical Chemistry*, 96 (8), 3548–3555.

Timoszyk, A., 2017. Application of Nuclear Magnetic Resonance Spectroscopy (NMR) to Study the Properties of Liposomes. *Liposomes*, 3 (10), 345–357.

Ueno, Y., Sonoda, S., Suzuki, R., Yokouchi, M., Kawasoe, Y., Tachibana, K., Maruyama, K., Sakamoto, T., and Komiya, S., 2011. Combination of ultrasound and bubble liposome enhance the effect of doxorubicin and inhibit murine osteosarcoma growth. *Cancer Biology and Therapy*, 12 (4), 270–277.

Unger, E.C., Porter, T., Culp, W., Labell, R., Matsunaga, T., and Zutshi, R., 2004. Therapeutic applications of lipid-coated microbubbles. *Advanced Drug Delivery Reviews*, 56 (9), 1291–1314.

Wang, L., Li, M., and Zhang, N., 2012. Folate-targeted docetaxel-lipid-based-nanosuspensions for active-targeted cancer therapy. *International Journal of Nanomedicine*, 7, 3281–3294.

Wardle, J., Robb, K., Vernon, S., and Waller, J., 2015. Screening for prevention and early diagnosis of cancer. *American Psychologist*, 70 (2), 119–133.

Watabe, A., Yamaguchi, T., Kawanishi, T., Uchida, E., Eguchi, A., Mizuguchi, H., Mayumi, T., Nakanishi, M., and Hayakawa, T., 1999. Target-cell specificity of fusogenic liposomes: Membrane fusion-mediated macromolecule delivery into human blood mononuclear cells. *Biochimica et Biophysica Acta - Biomembranes*, 1416 (1–2), 339–348.

Winer, E., Gralow, J., Diller, L., Karlan, B., Loehrer, P., Pierce, L., Demetri, G., Ganz, P., Kramer, B., Kris, M., Markman, M., Mayer, R., Pfister, D., Raghavan, D., Ramsey, S., Reaman, G., Sandler, H., Sawaya, R., Schuchter, L., Sweetenham, J., Vahdat, L., Schilsky, R.L., and Sweet, D., 2009. Clinical cancer advances 2008: Major research advances in cancer treatment, prevention, and screening-a report from the american society of clinical oncology. *Journal of Clinical Oncology*, 27 (5), 812–826.

Yassin, A.E.B., Khalid Anwer, M.D., Mowafy, H.A., El-Bagory, I.M., Bayomi, M.A., and Alsarra, I.A., 2010. Optimization of 5-fluorouracil solid-lipid nanoparticles: A preliminary study to treat colon cancer. *International Journal of Medical Sciences*, 7 (6), 398–408.

Yoshii, N. and Okamura, E., 2009. Kinetics of membrane binding and dissociation of 5-fluorouracil by pulsed-field-gradient 19F NMR. *Chemical Physics Letters*, 474 (4–6), 357–361.

Yu, B., Lee, R.J., and Lee, L.J., 2009. Microfluidic Methods for Production of Liposomes. *Methods in Enzymology*, 465 (C), 129-141.